

Doctoral Thesis

MicroVectors: Understanding microplastic fragmentation, virus interactions, co-transport and groundwater risks

Submitted in satisfaction of the requirements for the degree of
Doktor der technischen Wissenschaften (Dr. techn.)
of the TU Wien, Faculty of Civil and Environmental Engineering

as a part of the
Vienna Doctoral Programme on Water Resource Systems

by

Ahmad Ameen
Matr.Nr.: 11937883

Supervisors:

Univ. Prof. Dipl.-Ing. Dr.techn. Alfred P. Blaschke
Institute of Hydraulic Engineering and Water Resources Management, TU Wien

Assoc. Prof. PD. Mag. Dr. Alexander K. T. Kirschner
Institute for Hygiene and Applied Immunology, Medical University of Vienna

Examiners:

Prof. Dr. Philippe Ackerer
Strasbourg Institute of Earth and Environment, University of Strasbourg

Univ. Prof. Dipl.-Ing. Dr.techn. Matthias Zessner Spitzenberg
Institute of Water Quality and Resource Management, TU Wien

Vienna, January 2025

Abstract

The world is facing a plastic pollution crisis, suffocating ecosystems, endangering biodiversity, and jeopardizing the health of our planet. Despite increasing awareness, the fact remains that plastic waste continues to flood the environment. Plastics persist indefinitely and degrade into smaller fragments known as microplastics. Microplastics have now infiltrated every corner of the planet, pervading ecosystems, the food chain, and even the human body. Microplastic pollution in rivers has emerged as a pressing environmental challenge. Riverbank filtration (RBF) along major rivers (e.g. River Danube) plays a crucial role in providing drinking water for millions. However, being highly dynamic, RBF systems are susceptible to contamination. Urban runoff and wastewater treatment plants (WWTPs) are well-known contributors to microplastics in rivers. However, commercial and recreational shipping also directly release high amounts of microplastics in rivers through the discharge of paint particles and grey water. Smaller microplastic particles (diameter < 20 μm) are more likely to be transported to aquifers through hyporheic exchange. These microplastics interact with pathogens and undergo further fragmentation, posing serious risks to groundwater contamination. However, the transport behavior of sub-micron-sized microplastics (diameter < 20 μm), particularly their shape and size and their aggregation with pathogens during aquifer passage, remains poorly understood. Therefore, this doctoral dissertation aims to address the critical environmental challenge of microplastic pollution and their potential threats to groundwater systems, with a three-pronged research approach focusing on: first, the development and implementation of (microplastic-rich) fecal pollution from commercial ships and vessels and their detection and monitoring, secondly, the complex interactions and co-transport mechanisms between pathogenic organisms and microplastic particles, and finally, the detailed examination of microplastic transport processes after degradation, within the dynamic environment of different types of riverbank sediments.

In this dissertation, after a brief introduction, the first study investigated how ships contribute to (microplastic-rich) fecal pollution in rivers, a concern often overlooked. We developed a novel, integrated approach combining three elements: theoretical fecal pollution source profiling (PSP) to compare municipal and shipborne sewage, high-resolution field assessments using cultivation-based indicators and qPCR-based source tracking markers, and statistical analyses of pollution levels linked to satellite-based ship tracking (AIS) data. We applied this methodology to a 230 km river section of the Danube in Austria, enabling detailed pollution assessments along and across the river, especially near docking areas. The results showed that despite high local contamination potential, shipborne fecal pollution had minimal overall impact at both local and regional scales, due to effective sewage disposal practices. We successfully traced localized emissions to specific ship types (cruise, passenger, and freight) at

a docking station. This novel methodology can be applied to any river with ship-tracking data, offering a valuable tool for focused monitoring and evidence-based water quality management.

The second study explored the critical role of microplastics in facilitating pathogen transport and survival in the environment. Microplastics, originating from personal care and consumer products (PCCPs), enter sewage systems and can interact with human enteric viruses during wastewater treatment, forming persistent aggregates. The mechanisms governing microplastic-virus interactions and their impact on virus survival and co-transport in riverbank sediments were investigated. Batch experiments were conducted under varying temperature conditions using the PRD1 phage (a surrogate for adenovirus) mixed with microplastics. Furthermore, column experiments examined virus transport in saturated quartz sand. Microplastics were quantified using solid-phase cytometry, while viruses were analyzed via qPCR and culture-based methods.

The third study focused on the rapid degradation of microplastics into fragments and their transport behavior compared to spherical microplastics. Polystyrene microspheres were physically abraded with glass beads to simulate fragmentation. Column experiments were conducted to examine the transport of fragmented microplastics (FMPs ~1 μm in diameter) and spherical microplastics (SMPs ~1, 10, and 20 μm in diameter) through natural gravel (medium and fine) and quartz sand (coarse and medium).

Understanding microplastic transport in riverbank sediments is crucial for evaluating groundwater contamination risks. This dissertation highlights that microplastic size and shape significantly influence transport, with fragmented particles exhibiting higher mobility in sandy aquifers compared to spherical particles. Moreover, microplastics can act as vectors for pathogens. In the presence of microplastics, the co-transport experiments demonstrated enhanced virus transport in quartz sand, raising public health concerns. This dissertation emphasizes that microplastic surface charge makes them ideal particles for fostering pathogen transport in groundwater and their potential role in waterborne viral transmission and environmental contamination.

Kurzfassung

Die Welt befindet sich in einer enormen Zunahme der Verunreinigung unserer Umwelt durch Plastikabfälle, die die Ökosysteme extrem belasten, die biologische Vielfalt gefährdet und die Gesundheit unseres Planeten aufs Spiel setzt. Trotz des wachsenden Bewusstseins bleibt die Tatsache bestehen, dass die Umwelt weiterhin mit Plastikmüll überflutet wird. Kunststoffe bleiben auf unbestimmte Zeit bestehen und zerfallen in kleinere Fragmente, das so genannte Mikroplastik. Mikroplastik ist inzwischen in jeden Winkel der Erde zu finden und durchdringt Ökosysteme, die Nahrungskette und sogar den menschlichen Körper. Die Verschmutzung von Flüssen durch Mikroplastik hat sich zu einem dringenden Umweltproblem entwickelt. Die Flussuferfiltration (RBF) entlang großer Flüsse (z.B. der Donau) spielt eine entscheidende Rolle bei der Trinkwasserversorgung von Millionen Menschen. Da RBF-Systeme sehr dynamisch sind, sind sie anfälliger für Verunreinigungen. Städtische Abwässer und Kläranlagen sind bekannte Verursacher von Mikroplastik in Flüssen. Aber auch die Berufs- und Freizeitschiffahrt bringt durch die Einleitung von Farbpartikeln und Grauwasser große Mengen an Mikroplastik direkt in die Flüsse. Kleinere Mikroplastikpartikel (Durchmesser $< 20 \mu\text{m}$) werden mit größerer Wahrscheinlichkeit durch hyporheischen Austausch in Grundwasserleiter transportiert. Diese Mikroplastikpartikel interagieren mit Krankheitserregern und werden weiter fragmentiert, was ein ernsthaftes Risiko für die Kontamination des Grundwassers darstellt. Das Transportverhalten von Mikroplastik im Submikronbereich (Durchmesser $< 20 \mu\text{m}$), insbesondere seine Form und Größe sowie seine Aggregation mit Krankheitserregern während der Passage im Grundwasserleiter, ist noch kaum erforscht. Daher zielt diese Dissertation darauf ab, die potenzielle Bedrohung für Grundwassersysteme durch eine Mikroplastikverschmutzung besser zu verstehen und damit auch die Möglichkeiten für entsprechende legislative Maßnahmen in Hinsicht auf den Schutz von Grundwasser zu ermöglichen. Dazu wurde ein mehrteiliger Forschungsansatz gewählt, der sich auf Folgendes konzentriert: erstens die Entwicklung und Umsetzung von (mikroplastikreichen) fäkalen Verschmutzungen durch kommerzielle Schiffe und Boote und ihre Erkennung und Überwachung, zweitens die komplexen Wechselwirkungen und Co-Transportmechanismen zwischen pathogenen Organismen und Mikroplastikpartikeln und schließlich die detaillierte Untersuchung von Mikroplastik-Transportprozessen innerhalb des dynamischen Umfelds verschiedener Arten von Flussufersedimenten.

In dieser Dissertation wird nach einer kurzen Einführung erstmals untersucht, wie Schiffe zur (mikroplastikreichen) fäkalen Verschmutzung von Flüssen beitragen, ein Problem, das oft übersehen wird. Wir haben einen neuartigen, integrierten Ansatz entwickelt, der drei Elemente kombiniert: die theoretische Erstellung von Fäkalienverschmutzungsprofilen (PSP) zum Vergleich von kommunalen und schiffsbedingten Abwässern, hochauflösende Felduntersuchungen mit kultivierungsbasierten Indikatoren und qPCR-basierten Markern zur Quellenverfolgung sowie statistische Analysen des Verschmutzungsgrads in Verbindung mit satellitengestützten Schiffsverfolgungsdaten (AIS). Wir haben diese Methodik auf einem 230 km langen Flussabschnitt der Donau in Österreich angewandt, was eine detaillierte Bewertung der Verschmutzung entlang des Flusses und in der Nähe von Anlegestellen ermöglichte. Die

Ergebnisse zeigten, dass trotz des hohen lokalen Verschmutzungspotenzials die fäkale Verschmutzung durch Schiffe sowohl auf lokaler als auch auf regionaler Ebene nur minimale Auswirkungen hat, was auf die effektive Abwasserbehandlung auf Schiffen zurückzuführen ist. Es ist uns gelungen, die lokalisierten Emissionen bestimmten Schiffstypen (Kreuzfahrt-, Passagier- und Frachtschiffen) an einer Anlegestelle zuzuordnen. Diese neuartige Methode kann auf jeden Fluss mit Schiffsverfolgungsdaten angewandt werden und bietet ein wertvolles Instrument für eine gezielte Überwachung und ein evidenzbasiertes Wasserqualitätsmanagement.

Eine weitere Arbeit galt der Untersuchung der kritischen Rolle von Mikroplastik bei der Erleichterung des Transports und des Überlebens von Krankheitserregern in der Umwelt. Mikroplastik, das aus Körperpflege- und Konsumgütern (PCCPs) stammt, gelangt in die Kanalisation und kann während der Abwasserbehandlung mit menschlichen Darmviren interagieren, wobei es persistente Aggregate bildet. Die Mechanismen, die die Wechselwirkungen zwischen Mikroplastik und Viren steuern, und ihre Auswirkungen auf das Überleben und den Co-Transport von Viren in Ufersedimenten wurden untersucht. Es wurden Batch-Experimente unter verschiedenen Temperaturbedingungen mit dem PRD1-Phagen (als Ersatz für pathogene Adenoviren) gemischt mit Mikroplastik durchgeführt. Außerdem wurde in Säulenexperimenten der Virustransport in gesättigtem Quarzsand untersucht. Mikroplastik wurde mittels Festphasenzytometrie quantifiziert, während Viren mittels qPCR und kulturbasierten Methoden analysiert wurden.

Die dritte Studie befasste sich mit dem schnellen Abbau von Mikroplastik in Fragmente und deren Transportverhalten im Vergleich zu kugelförmigem Mikroplastik. Polystyrol-Mikrokugeln wurden mit Glasperlen physikalisch abgerieben, um eine Fragmentierung, wie sie in der Natur passiert, zu simulieren. Es wurden Säulenexperimente durchgeführt, um den Transport von fragmentiertem Mikroplastik (FMP $\sim 1 \mu\text{m}$ Durchmesser) und kugelförmigem Mikroplastik (SMP $\sim 1, 10$ und $20 \mu\text{m}$ Durchmesser) durch natürlichen Kies (mittel und fein) und Quarzsand (grob und mittel) zu untersuchen.

Das Verständnis des Mikroplastiktransports in Flussufersedimenten ist für die Bewertung der Risiken einer Grundwasserkontamination von entscheidender Bedeutung. Diese Dissertation zeigt, dass Größe und Form von Mikroplastik den Transport erheblich beeinflussen, wobei interessanterweise fragmentierte Partikel in sandigen Grundwasserleitern eine höhere Mobilität aufweisen als kugelförmige Partikel. Außerdem kann Mikroplastik als Transportmittel für Krankheitserreger dienen. In Anwesenheit von Mikroplastik zeigten die Co-Transportexperimente einen verstärkten Virustransport in Quarzsand, was Anlass zu Bedenken hinsichtlich der öffentlichen Gesundheit gibt. In dieser Dissertation wird hervorgehoben, dass Mikroplastik aufgrund seiner Oberflächenladung die idealen Partikel ist, um den Transport von Krankheitserregern im Grundwasser zu fördern, und dass sie eine nicht zu unterschätzende Rolle bei der Übertragung von Viren durch Wasser und bei der Umweltverschmutzung spielen.

Acknowledgments

I owe heartfelt thanks to my supervisor, Prof. Alfred Paul Blaschke, for his unwavering guidance, constant availability, and invaluable advice throughout this academic journey. Your support has been a cornerstone in my growth, and I am forever thankful for the trust and encouragement you have shown in me. I am incredibly fortunate to have had the opportunity to learn from someone as kind, dedicated, and wonderfully witty as you. Also, I would also like to express my sincere gratitude to my co-supervisor, Assoc. Prof. Alexander Kirschner, for his constant support, continuous availability, and the insightful discussions.

I could not have done this without my mentor Assist. Prof. Margaret Stevenson. You are the kindest, most humble person I have had the privilege to learn from. You showed me that academic brilliance is not just about sharp minds but also open hearts. In a world where technical competence often steals the spotlight, you reminded me of the power of kindness and accessibility. When I felt lost and confused, you stepped in, patiently helped me shape my ideas, interpret my thoughts, and honestly turn my messy writing into twisted language of academia. You are the best mentor I could have asked for, and I am so grateful for your support.

I am deeply grateful to ICC Water & Health for their incredible support. Prof. Andreas Farnleitner, Prof. Alex Kirschner, Prof. Regina Sommer, and Assist. Prof. Julia Derx, I cannot thank you enough for believing in the potential of microplastic research. Your kindness, guidance and willingness to share your vast knowledge have meant so much to me. I am beyond thankful for the chance to work alongside Sophia Steinbacher and to contribute to the Future Danube Project. Special thanks to Prof. Andreas Farnleitner for sharing his visionary ideas, inspirational conversations, and support and guidance throughout these years.

I am truly grateful to Dr. Patrick Julian Mikuni-Mester (University of Veterinary Medicine Vienna) for the opportunity to work together in a focused and productive way. This experience has been a deeply meaningful one.

I would like to extend my heartfelt thanks to Stefan Jakwerth and Gerhard Lindner for their invaluable support during both the lab and fieldwork.

I am extremely grateful to Prof. Günter Blöschl and all faculty, alumni and student members of the Vienna Doctoral Program on Water Resource Systems. I especially appreciated the annual symposium that gave such nice motivation during my PhD, filled with insightful discussions and unforgettable memories. Special thanks to my colleagues Ali, Anna, Thomas and Yahne for your support throughout my PhD journey.

Finally, my deepest thanks go to my parents, sisters, and family, your support and encouragement have been my foundation. To my precious nieces and nephew, you are the heart of my world. Your love and joyful presence light up my life. I love you all more than words can express, with all the love in my heart.

Table of Contents

Abstract	i
Kurzfassung	iii
Acknowledgments	v
Table of Contents	vii
List of Figures	xi
List of Tables	xii
Abbreviations	xiii
Chapter 1 Introduction	1
Chapter 2 Assessing the impact of inland navigation on the fecal pollution status of large rivers: A novel integrated field approach	7
2.1 Introduction	8
2.2 Materials and methods	10
2.2.1 The selected Danube River reach, transects and docks.....	10
2.2.2 Water quality and fecal pollution	11
2.2.3 Ship data assessment (SDA) using the DoRIS database	13
2.2.4 Pollution source profiling (PSP) for impact scenario estimation.....	14
2.2.5 Statistical analysis and data visualization	15
2.3 Results	17
2.3.1 Establishing AIS-based shipping activities for the selected Danube reaches	17
2.3.2 PSP reveals high local fecal pollution potential from the shipping industry	18
2.3.3 Realizing water quality assessment at high spatial resolution	19
2.3.4 Associations of fecal pollution with ship activity, WWTP discharge and hydrological parameters	25
2.4 Discussion	27
2.4.1 Realization of a novel integrated approach for assessing the impact of inland navigation by an interdisciplinary toolbox.....	27
2.4.2 The local impact of navigation was unexpectedly low but sensitively traceable	29

2.4.3	Regional impacts of navigation were not detectable, but this could change in the future	30
2.4.4	Large rivers are subject to multiple pressures, and water quality varies on longitudinal and cross-sectional scales	31
2.4.5	Increasing use of AIS and RIS in research	32
2.5	Conclusions	32
Chapter 3	Microplastics as vectors for virus transport in saturated porous media	35
3.1	Introduction	36
3.2	Materials and methods	38
3.2.1	Polystyrene microplastics	38
3.2.2	Laboratory preparation of viruses	38
3.2.3	Batch experiments	38
3.2.4	Column experiments	39
3.2.5	Microplastic and virus enumeration	40
3.2.6	Numerical analysis	42
3.3	Results and discussion	43
3.3.1	Influence of microplastics on virus quantification	43
3.3.2	Microplastics reduce virus infectivity	45
3.3.3	Electrostatic interaction facilitating co-transport	47
3.3.4	Microplastics enhance virus transport in porous media	49
3.3.5	Virus removal in porous media	55
3.3.6	Environmental implications	56
3.4	Conclusions	56
Chapter 4	Fate and transport of fragmented and spherical microplastics in saturated gravel and quartz sand	57
4.1	Introduction	57
4.2	Materials and methods	60
4.2.1	Preparations of microplastics	60
4.2.2	Properties of influent water	61
4.2.3	Tracer preparation and analysis	61
4.2.4	Porous media	61
4.2.5	Column experiments	62
4.2.6	Microplastic enumeration	63

4.3	Theoretical considerations.....	64
4.3.1	Filtration efficiency	64
4.3.2	Transport modeling	65
4.4	Results	66
4.4.1	Microplastic fragmentation	66
4.4.2	Microplastic transport in natural gravel and quartz sand	67
4.4.3	Effect of particle shape on microplastic transport.....	70
4.4.4	Filtration efficiency of microplastics	70
4.5	Discussion	72
4.5.1	Role of different aquifer materials in microplastic transport	72
4.5.2	Microplastic shape affects its environmental fate and transport	74
4.5.3	Microplastic response to filtration mechanisms	74
4.5.4	Implications for groundwater management.....	75
4.6	Conclusions	76
Chapter 5	Conclusions.....	77
5.1	Conclusions	77
5.2	Challenges	79
5.3	Recommendations	79
References	81
Appendix A: Supplementary material to Chapter 2	101
Appendix B: Supplementary material to Chapter 3	121
Appendix C: Supplementary material to Chapter 4	131
Appendix D: Contributions of the Author	137

List of Figures

Figure 1 Study area.....	11
Figure 2 Flow chart of ship data assessment.....	14
Figure 3 Seasonal variation in number of ships	17
Figure 4 Comparison of <i>E. coli</i> loads of ships and WWTPs.....	18
Figure 5 Fecal pollution classification	21
Figure 6 Microbial source tracking markers (MST) concentrations	22
Figure 7 Observed <i>E. coli</i> concentrations along River Danube	23
Figure 8 Observed <i>E. coli</i> concentrations across River Danube	24
Figure 9 Correlation of <i>E. coli</i> concentrations with environmental factors	26
Figure 10 Ship numbers and <i>E. coli</i> concentrations at docking station	27
Figure 11 Comparison of DNA extraction methods	44
Figure 12 Virus persistence with and without microplastics	46
Figure 13 Virus concentration in effluent solution.....	50
Figure 14 Observed and modeled breakthrough curves.....	52
Figure 15 Particle size distribution of MPs after fragmentation	66
Figure 16 Breakthrough of SMPs and FMPs in different soils	68
Figure 17 Comparison of 1 µm SMPs and FMPs in coarse quartz sand.....	70
Figure 18 Filtration efficiencies of FMPs and SMPs in various soils.....	72

List of Tables

Table 1: Water quality parameters	20
Table 2: Overview of column experimental parameters.	41
Table 3: Overview of CFT and Hydrus modeled parameters	54
Table 4 Summary of experimental and modeling results.	69

Abbreviations

AIS	automated identification system
CFT	colloid filtration theory
CFU	colony-forming unit
DoRIS	Danube river information services
DNA	deoxyribonucleic acid
ERI	electronic ship reporting
FMPs	fragmented microplastics
LOD	limit of detection
MNP	most probable number
MST	microbial source tracking
MPs	microplastics
PGN	phage genome number
PFU	plaque-forming unit
PS	polystyrene
PSP	pollution source profiling
RNA	ribonucleic acid
qPCR	quantitative polymerase chain reaction
RSTA	reverse ship traffic approximation
SDA	ship data assessment
SMPs	spherical microplastics
TOD	threshold of detection

Plastic pollution has escalated into a global environmental crisis in recent decades, highlighting challenges posed by its end-of-life cycle (Shim and Thomposon, 2015). Plastics are synthetic organic polymers derived from oil and gas (Thompson et al., 2009). Since the introduction of Bakelite, the first modern plastic in 1907, advancements in cost-effective manufacturing techniques have facilitated the mass production of plastics, revolutionizing industries and consumer products worldwide (Cole et al., 2011). In recent years, plastic production has surged to alarming levels, with global output reaching 380 million tons and accounting for 6–8% of total global oil production (Thompson et al., 2009; Walker, 2021; Zhao et al., 2022; Zhu, 2021).

Plastics enter the environment through various pathways, including mismanaged waste, wastewater treatment plants, landfills, agricultural practices, river and atmospheric transport, beach littering, aquaculture, and shipping and fishing activities (Law, 2017; Windsor et al., 2019; Ziajahromi et al., 2017). Once released, plastics continuously degrade into smaller particles (less than 5 mm) known as “microplastics - MPs” (Thompson et al., 2004). Microplastics are commonly classified as primary and secondary MPs. Primary MPs are intentionally manufactured for personal care and cosmetic products (PCCPs), industrial abrasives, and textile fibers (Cole et al., 2011; Fu and Wang, 2019). Secondary MPs formed through the degradation of larger plastic items (bottles, agricultural films, wear of tires, marine paints, synthetic turfs) due to use and exposure to environmental conditions (Cole et al., 2011; Galafassi et al., 2019).

Every year more than 2.3 million tons of plastic waste are carried by rivers to oceans (Eriksen et al., 2023; Lebreton et al., 2017). Rivers act not only as transport pathways but also as zones of accumulation for microplastics (Duis and Coors, 2016; Frei et al., 2019; Lebreton et al., 2017). Commercial ships are often overlooked as significant contributors of microplastics pollution in rivers and oceans. They release microplastics through various sources, including paints and coatings, abrasive materials (used for hull cleaning), cargo spills (plastic pellets), generation of black water (sewage from vessels), gray water (wastewater from laundry, washbasins, showers, and sinks), and ballast water (seawater used to maintain ship stability) (Folbert et al., 2022; Peng et al., 2022; Shim and Thomposon, 2015; Tamburri et al., 2022).

Cruise ships make up less than 1% of the global merchant fleet, yet they produce 25% of aquatic waste, releasing over 1 billion gallons of both treated and untreated wastewater annually (Lee et al., 2018). Mikkola (2020) reported that untreated gray water discharges from cruise ships can lead to the emission of 10–500 g of microplastics per annum per person. A comprehensive microplastic screening study within the Joint Danube Survey 4 revealed the presence of microplastics in the riverine environment, with a maximum concentration of 22.24 µg/mg (Kittner et al., 2022).

In fluvial ecosystems, microplastics do not remain inactive (Ochirbat et al., 2023). Their surfaces often adsorb chemicals, heavy metals, nutrients, pathogens and organic matter which facilitate the formation of microbial biofilms (Shen et al., 2019). This biofilm layer on the microplastic surface creates a conducive environment for pathogens to attach and colonize. Viruses are widespread and abundant components of Earth's microbiomes, influencing host evolution, metabolic processes, and biogeochemical cycles (Li et al., 2024a). Most of the studies have primarily focused on the microplastic interactions with algae, bacteria, protozoa, and fungi (Mammo et al., 2020). A few studies on virions on microplastics have shown that non-enveloped viruses can hitchhike on microplastics and prolong their survival and infectivity by adhering to the microplastic surface in surface water (Lu et al., 2022; Moresco et al., 2022). But microplastic-associated virus transport and infectivity have not been investigated properly in river sediments and porous media.

Rivers can serve as hotspots for microplastic fragmentation due to the continuous movement of water and sediments, which promotes mechanical interactions between microplastics, water, sediments, and riverbeds (Liro et al., 2024; Liro et al., 2023). Such conditions favor their fragmentation into micron-sized microplastics that are more likely to infiltrate to greater depths in sediments (Mancini et al., 2023). Like solutes, the transport of sub-pore-scale microplastics into streambed sediments can be driven by hyporheic exchange (Boos et al., 2021; Frei et al., 2019). The residence time of microplastics in the hyporheic zone can vary widely, from just a few hours to several years (Drummond et al., 2022). Microplastics, as an emerging environmental pollutant, are increasingly discovered in hyporheic zones and groundwater worldwide (Zhang et al., 2025).

Riverbank filtration (RBF) is commonly used for drinking water supply in the world (Derx et al., 2010; Kuehn and Mueller, 2000; Tufenkji et al., 2002; van Driezum et al., 2018). Riverbanks can also capture microplastics from urban and agricultural runoff (Liu et al., 2021b; Werbowski et al., 2021). The concentration of microplastics in the riverbanks of the Yangtze

River has been reported to be 3877 ± 2356 particles/kg (Zhou et al., 2021). This is especially alarming, as RBF is an essential source of drinking water worldwide. Moreover, microplastics have also been detected in groundwater at varying concentrations, ranging from less than 0.7 particles/m³ to 40 particles/L in different aquifers (Mintenig et al., 2019b; Samandra et al., 2022). Given these factors, concerns and interest in the impact of microplastics on human health have surged significantly.

The European Commission's Science Advice for Policy (SAPEA) and the World Health Organization (WHO) report limited data on microplastic toxicity and human exposure, with no direct evidence yet of health risks (SAPEA, 2019; WHO, 2019). However, recent research provides evidence that microplastics can enter the human body via ingestion, inhalation, and skin contact (Liu and You, 2023). Scientific evidence indicates that microplastics are present not only in human tissues that are directly exposed to the external environment, such as the lungs, sputum, alveolar lavage fluid, and feces (Amato-Lourenço et al., 2021; Huang et al., 2022b; Qiu et al., 2023; Yan et al., 2022), but have also been found in the completely enclosed human organs, such as the heart, human bone marrow, placenta, limb joints and testis and semen (Guo et al., 2024; Li et al., 2024c; Weingrill et al., 2023; Yang et al., 2023; Zhao et al., 2023). Growing evidence suggests that microplastics can affect human health, particularly through accumulation in the bloodstream, potentially leading to widespread exposure throughout the body (Leslie et al., 2022). Microplastics in carotid artery plaques have been linked to higher risks of heart attack, stroke, and death (Marfella et al., 2024). Additionally, the presence of microplastics in feces has been associated with inflammatory bowel disease (Yan et al., 2022).

Currently, the European Union (EU) lacks dedicated legislation, regulating microplastic pollution. However, some existing laws indirectly address marine plastic litter and microplastics, which includes the Marine Strategy Framework Directive (MSFD), Waste Directive, Single-Use Plastics (SUP) Directive, and the Directive on Port Reception Facilities (Khan et al., 2024). To safeguard the quality of freshwater ecosystems, the European Commission introduced the Water Framework Directive (WFD), but it has not yet explicitly addressed microplastic pollution. Recently, the EU has adopted a more targeted approach with the Drinking Water Directive (EU 2020/2184), which recognizes microplastics as an emerging concern and mandates regular monitoring of water bodies used for drinking water (European Commission, 2024). However, this directive currently focuses only on MPs larger than 20 μm in size, excluding smaller particles, which are most pertinent to groundwater as the larger microplastics do not infiltrate easily.

This doctoral thesis tackles the pressing and complex issues surrounding microplastic pollution in freshwater ecosystems. As plastic waste levels have skyrocketed worldwide, microplastic pollution (particle size $\leq 20 \mu\text{m}$) has become a pervasive environmental concern for groundwater systems. Commercial ships, though often overlooked, contribute significantly to this pollution, introducing microplastic-associated pathogens. This dissertation attempts to understand the extent of ship pollution and its impact on the Danube River. Since microplastics in the aquatic environment do not stay in isolation, they interact with microbial contaminants (forming biofilms) which can aid in pathogen survival and dissemination in the hyporheic-groundwater zone, posing a potential health risk. The thesis delves into these interactions and examines how microplastics could influence pathogen transport. Furthermore, the fragmentation of microplastics into sub-micron-sized particles ($\leq 20 \mu\text{m}$) can affect their mobility and potential for deeper infiltration into riverbed and aquifer sediments. This dissertation further explores how the shape, size, and fragmentation of microplastics affect their transport in different porous media. Given the current lack of comprehensive legislation on microplastics, particularly in the drinking water domain, this dissertation addresses an essential gap in knowledge, by addressing microplastic transport for particle sizes below $20 \mu\text{m}$, that can provide information for more effective environmental and health protection measures.

Fundamental Science Questions

1. How much pollution do commercial ships add to the river, and how effectively can it be measured? **(Chapter 2)**
2. How do microplastics interact with microbial contaminants in the aquatic environment, and can this affect pathogen transport through saturated sand (streambed sediments)? **(Chapter 3)**
3. How does microplastic fragmentation impact their transport and behavior in various saturated porous media (different sized-streambed sediments)? **(Chapter 4)**

Chapter 2 introduces an innovative approach to assess the impact of ships on the microbial water quality of the River Danube in Austria. A python-code was developed to compute the number of ships, defining different categories (e.g., cruise, freight, passenger) using the DoRIS database (Austrian Danube Rivers Information Services). To implement this approach, first, microbial pollution source profiling was conducted to estimate the pollution impact, comparing two different ship wastewater handling practices. Second, the current status of river microbial fecal pollution was assessed through analysis of standardized fecal indicators (cultivation method) and genetic microbial source tracking markers. Finally, a correlation analysis was performed between observed fecal pollution levels and ship traffic, both along the entire river reach and at specific ship docking stations.

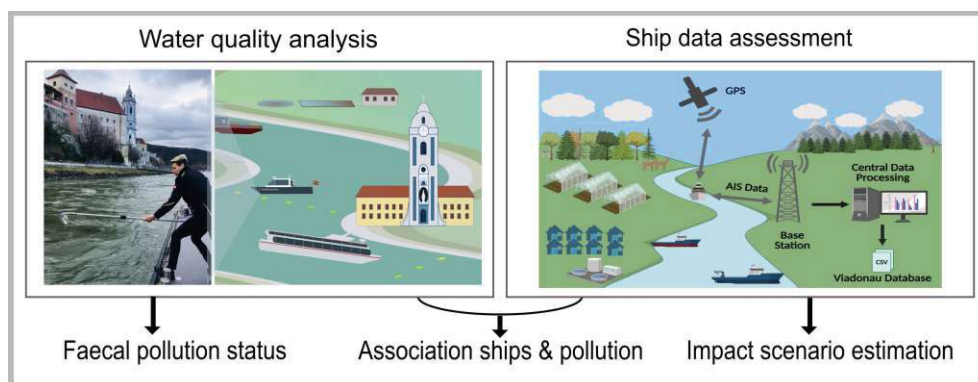
Chapter 3 unveils the crucial role of microplastics in interacting with microbial contaminants, highlighting their impact on virus persistence and dissemination. PRD1 bacteriophages were used as a surrogate for rotavirus/adenovirus. Batch experiments were conducted to investigate virus persistence (with and without microplastics) in drinking water at various temperatures. Additionally, column co-transport experiments in saturated quartz sand were carried out to evaluate how microplastics influence the mobility of the virus. Also, the co-transport scenario was compared to separate transport experiments where viruses and microplastics were injected independently. The enumeration of viruses was performed by qPCR and culture-based methods to differentiate between total and infective viruses.

Chapter 4 examines the influence of microplastic fragmentation, by comparing the transport behavior of irregular-shaped microplastics in saturated porous media. Microspheres present in personal care and cosmetic products (10 and 20 μm) were physically abraded with glass beads to simulate natural fragmentation process. Laboratory column experiments were conducted to investigate how the shape and size of microplastics affect the transport behavior of both fragmented and spherical microplastics in natural gravel and quartz sand.

Chapter 2 Assessing the impact of inland navigation on the fecal pollution status of large rivers: A novel integrated field approach

Abstract

The contribution of ships to the microbial fecal pollution status of water bodies is largely unknown but frequently of high concern. No methodology for comprehensive and target-oriented system analysis was available so far. We developed a novel approach for integrated and multistage impact evaluation. The approach includes, i) theoretical fecal pollution source profiling (PSP, i.e., size and pollution capacity estimation from municipal vs. ship sewage disposal) for impact scenario estimation and hypothesis generation, ii) high-resolution field assessment of fecal pollution levels and chemo-physical water quality at the selected river reaches, using standardized fecal indicators (cultivation-based) and genetic microbial source tracking markers (qPCR-based), and iii) integrated statistical analyses of the observed fecal pollution and the number of ships assessed by satellite-based automated ship tracking (i.e., automated identification system, AIS) at local and regional scales. The new approach was realized at a 230 km long Danube River reach in Austria, enabling detailed understanding of the complex pollution characteristics (i.e., longitudinal/cross-sectional river and upstream/downstream docking area analysis). Fecal impact of navigation was demonstrated to be remarkably low at regional and local scale (despite a high local contamination capacity), indicating predominantly correct disposal practices during the investigated period. Nonetheless, fecal emissions were sensitively traceable, attributable to the ship category (discriminated types: cruise, passenger and freight ships) and individual vessels (docking time analysis) at one docking area by the link with AIS data. The new innovative and sensitive approach is transferable to any water body worldwide with available ship-tracking data, supporting target-oriented monitoring and evidence-based management practices.



2.1 Introduction

Maritime and inland navigation has been an important part of human history, enabling civilizations to explore new lands and establish trade routes (Sanches et al., 2020). Currently, approximately 80–90% of global cargo is transported by ships and ferries using maritime transportation (Schnurr and Walker, 2019). Freight transportation and the transportation of people, especially cruise tourism, have experienced rapid growth within recent decades (Carić and Mackelworth, 2014; Wondirad, 2019). Inland navigation is an important extension for the waterway transportation of goods and persons into intercontinental areas, with the world's busiest rivers being the Yangtze River (cargo traffic volume: 4360 million tons in 2018), the Rhine River (311 million tons in 2019), the Illinois Inland River (90.5 million tons in 2017) and the Danube River (69 million tons in 2019) (Danube Commission, 2021; David et al., 2021; Farazi et al., 2022; Wu et al., 2022b).

Within the European Union, the total inland waterway network has a length of 26000 km with an approximate annual transportation volume of 558 million tons of goods, accounting for 6% of all goods being transported in the EU in 2019 (Viadonau, 2019b). River cruise tourism is very popular, with 1.64 million tourists taking a river cruise in Europe in 2018 (Interreg - Danube Transnational, 2019). The advent of the COVID-19 pandemic led to an abrupt decrease in 2020, though a rise towards the pre-pandemic level has been observed within recent years (Viadonau, 2021, 2022).

Environmental pollution arising from the shipping industry is increasingly in the focus of global research, especially in terms of air emissions and water pollution, such as from wastewater discharges (Cao et al., 2018; Jägerbrand et al., 2019). For maritime navigation, the International Maritime Organization (IMO) adopted the International Convention for the Prevention of Pollution from Ships (MARPOL), which includes regulations concerning the prevention of air pollution as well as pollution from oil, noxious and harmful substances, garbage and sewage (Annex IV) (MARPOL, 1997; Vaneeckhaute and Fazli, 2020). For inland navigation, there are no internationally harmonized regulations concerning pollution arising from ships, though several national or river-specific regulations/roadmaps exist, such as the CCNR roadmap for the Rhine River (CCNR, 2022).

Microbial fecal pollution can have a direct impact on human health if the water resource is used for recreational activities, water withdrawal for drinking water production or irrigation due to the possible presence of pathogens (World Health Organization, 2017, 2021). In urban coastal

areas or at large rivers, fecal pollution primarily arises from municipal wastewater, though ship wastewater discharges may pose an additional impact source. To date, only a minor number of publications have studied the impact of wastewater discharge from ships on ambient waters. A few studies have been published on the impact of maritime cruise ships in vulnerable maritime regions, such as the Bering Sea, the Baltic Sea or the Adriatic Sea (Huhta et al., 2007; Loehr et al., 2006; Perić et al., 2016). Some studies performed calculations of the generated amount of wastewater and/or discharged general chemical pollutants (COD, BOD, SS, TN) based on ship numbers assessed using inland AIS for the Yangtze River or from interviews with watermen at the Danube River in Serbia, but without investigations of the water quality of the river (Chen et al., 2022; Presburger Ulnikovic et al., 2012). Even fewer studies have investigated the microbial fecal water quality of maritime bays/ports and the local number of smaller pleasure boats or sailing ships, frequently reporting a connection of ships and elevated concentration of fecal coliform bacteria (Faust, 1982; Koboević et al., 2022; Sobsey et al., 2003).

The aim of this study was to develop and evaluate a novel integrated field approach for the impact assessment of ships on the microbial fecal pollution status of navigable river reaches by i) fecal impact scenario estimation/comparison using pollution source profiling (*i.e.*, catchment specific analysis of the produced numbers of *E. coli* from potential sources of fecal pollution) including different wastewater handling scenarios from navigation and their comparison municipal wastewater disposal, as a basis for subsequent hypothesis formulation and field analysis, ii) high-resolution longitudinal and cross-sectional microbial and chemical water quality analysis at selected river locations, and iii) statistical analysis covering observed fecal pollution patterns and detailed ship traffic activities for the investigated river locations (covering regional river reach vs. local ship dock impact considerations). The chosen study region was a 230 km river reach of the Danube River in Austria, as a representative large navigable river with high international importance (ICPDR, 2021; Kirschner et al., 2009).

Microbial fecal pollution analysis was based on standardized fecal indicator bacteria enumeration (cultivation-based) and state-of-the-art (qPCR-based) genetic microbial source tracking (Demeter et al., 2023). For precise ship data assessment, raw navigational data from the Donau Riverine Information Service (DoRIS), including inland Automated Identification System (AIS) data, were processed to extract near-real-time ship counts within specific timeframes and areas. The novel approach is suggested to be universally applicable to other large navigable water bodies worldwide if the needed raw navigation data are available.

2.2 Materials and methods

2.2.1 The selected Danube River reach, transects and docks

The investigated river reach stretches from river-km 2111–1873 in the upper region of the Danube River, including the large city of Vienna as well as a highly touristic region for cruise ships in the Wachau Valley in the province of Lower Austria (**Figure 1**).

The catchment of the Danube River reach in Austria has a size of 28.074 km² and the sub-catchment of the investigated Danube reach has an area of 14,126 km² (data assessed from the website of the Hydrographic Service in Austria www.ehyd.gv.at). A total number of approximately 3,370,000 citizens including average daily tourists were registered in the investigated sub-catchment in the year of 2019. This vast catchment area is subject to the influence of the alpine regime, which governs hydrological conditions, resulting in highly variable flow patterns and peak water levels, particularly in early summer (Schiemer et al., 1999). Land use in the sub-catchment in Lower Austria is unevenly distributed, with 40% agricultural land, 40% forest, and 13% grassland (Petschko et al., 2014). The areas south of the Danube and the relatively flat northeast region are predominantly agricultural, while the steeper slopes in the south and southwest are mainly covered by coniferous and deciduous forests (Eder et al., 2011).

The average discharge of the Danube River in this region is approximately 1800 m³/s, and the river width ranges from 217 (Wachau Valley) to 330 m in the flatlands. The 7 sampling transects (A to G) were selected with respect to river morphology, settlements/cities, and highly frequented Danube ship docks to sensitively detect potential fecal emission from navigation (further details are given in the legend of **Figure 1**). As many as 4 additional transects (B+, C+, D+, E+) were chosen for upstream/downstream sampling of ship docking areas (B+/B, C+/C, D+/D, E+/E), resulting in a total of 11 sampled transects. The touristic region of the Wachau Valley lies between sampling site (B) Melk and site (D) Krems.

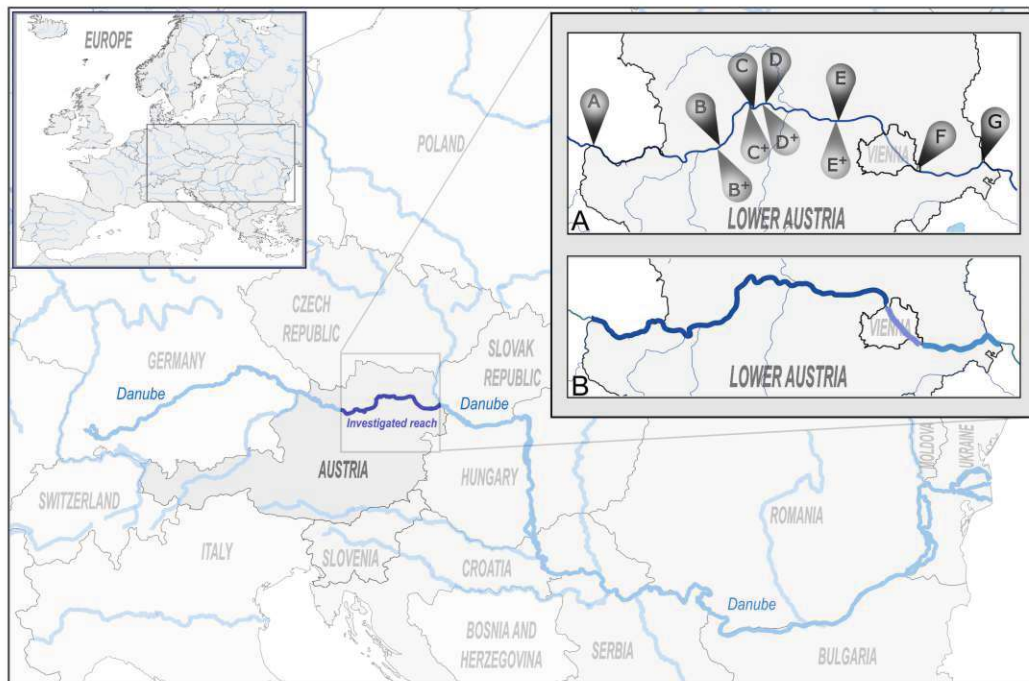


Figure 1 Study area

Overview map of the investigated Danube River reach (dark blue) in the centre of Europe. Upper right map A shows the region of Lower Austria with the sampling locations (A) St Pantaleon - rkm 2108; (B⁺) Melk - upstream ship docks - rkm 2036.6; (B) Melk - downstream ship docks - rkm 2035.5; (C⁺) Dürnstein - upstream ship docks - rkm 2009; (C) Dürnstein - downstream ship docks - rkm 2008; (D⁺) Krems - upstream ship docks - rkm 2003; (D) Krems – downstream ship docks - rkm 2002; (E⁺) Tulln – upstream ship docks: rkm 1964.4; (E) Tulln – downstream ship docks - rkm 1963.4; (F) Wien/Vienna - rkm 1915; (G) Hainburg - rkm 1883. The Wachau Valley spans from (B) – Melk to (D) – Krems. Upper right map B: The investigated Danube River reach and sub-reaches for the theoretical impact estimation, i.e., pollution source profiling (PSP).

2.2.2 Water quality and fecal pollution

2.2.2.1 Sampling at selected transects

To account for possible transversal differences in water composition, each transect consisted of 5 sampling points symmetrically distributed in the cross-profile with orographically left or right: appr. 10–20 m distance from the riverbank, middle: center of river, and middle-left/right: half-distance of outer and center point. Sampling was performed in collaboration with local authorities and the Austrian shipping inspectorate with their official ship, enabling precise navigation to the same sampling locations each time. Due to logistics, sampling at the 11 transects was performed on four different days each month, with a 4-week interval, resulting in a total of 48 different sampling days within the monitoring timeframe from March 2019 to March 2020 (Table A1, Appendix A). Water samples were taken with a sampling rod in approx. 30 cm water depth, stored in the dark in cooling boxes during transportation to the lab, and processed within hours (< 6 h).

2.2.2.2 Chemical and physical water quality parameters

Temperature (°C), pH (-), conductivity (µS/cm) and oxygen (mg/L) were measured directly on the ship using a multimeter device (HQ40D, Hach U.S.) equipped with the corresponding probes. Chemical oxygen demand (COD), total phosphorus (mg/L), total nitrogen (mg/L) and NH₄-nitrogen (mg/L) were analyzed in the laboratory by spectrophotometric methods following the manufacturer's instructions (LCK1414, LCK349, LCK304, Hach U.S.).

2.2.2.3 Fecal indicator bacteria and genetic microbial fecal source tracking markers

All water samples (n = 665) were analyzed for the standard fecal indicator bacterium *E. coli* following ISO 9308-2 (ISO, 2012) using Colilert-18 (IDEXX, Germany). Analysis of genetic microbial fecal source tracking (MST) markers was performed for water samples (n = 100) from three transects (*St. Pantaleon* – A, *Krems* – D and *Hainburg* G). River water samples (500 mL) were filtered through a polycarbonate filter (pore size 0.22 µm, GTTP04700, Merck Millipore) and stored at -80 °C. DNA extraction was performed following a bead-beating and phenol/chloroform protocol (Linke et al., 2021; Mayer et al., 2018; Reischer et al., 2006). DNA was redissolved in 100 µL of 10 mM TRIS at pH 8. Samples were analyzed for human-associated genetic fecal markers HF183/BacR287 (Green et al., 2014) and BacHum (Kildare et al., 2007), as well as for the ruminant-associated marker BacR (Reischer et al., 2006) and the pig-associated marker Pig2Bac (Mieszkin et al., 2009). All qPCR reactions were performed in duplicate with a total reaction volume of 15 µL on a Rotor-Gene Q thermocycler (Qiagen, Hilden, Germany) with each including 2.5 µL sample DNA dilution (1:4). The reaction mixtures and cycling parameters were applied as described previously (Linke et al., 2021; Mayer et al., 2018; Reischer et al., 2013). Quality assessment was performed as described in (Mayer et al., 2018; Reischer et al., 2006; Reischer et al., 2011). All qPCR runs in this study revealed calculated qPCR efficiency between 95–100%, R-square values of the calculated standard curves were ≥ 0.99 and no-template and extraction controls were consistently negative. A previously established threshold of detection (TOD) concept was applied, considering the filtration volume, the DNA extract volume, potential dilutions and the minimal amount of detectable targets per reaction (Reischer et al., 2007; Reischer et al., 2006). It is a robust approximation for the sample limit of detection, covering sampling and sample processing and the efficiency of the qPCR analysis (Demeter et al., 2023). The results of the qPCR analysis were expressed as marker equivalents per 100 mL [$\log_{10} (\text{ME} + 1)/100 \text{ mL}$].

2.2.3 Ship data assessment (SDA) using the DoRIS database

In Europe, standardized River Information Services (RIS) were implemented and harmonized to enable reliable and efficient inland waterway transport via the EU Directive 2005/44/EC (European Parliament, 2005). The Austrian version Donau RIS (DoRIS) is maintained by via Donau GmbH, operating the 23 land-based AIS stations connected to a central database server storing and processing all ship tracking data.

We developed a Python programming language-based script for ship data assessment (SDA) using raw navigational data from the DoRIS database (Via Donau GmbH), including inland AIS data of all ships navigating the Austrian Danube River reach (rkm: 2223–1873) in the 12-month monitoring timeframe (see **Appendix A1** for the script). The resulting database consisted of 101 966 ASCII files (one file per ship per day), including 23 AIS data fields with data records every 15 seconds, resulting in a total of 405 000 000 data records.

The script was designed to extract data based on two input fields: i) a specific date and timeframe and ii) the start and end distance of a specific river area (in river kilometers) (**Figure 2**). The obtained reduced ship datasets for specific areas/timeframes were sorted into three main shipping categories, namely, cruise (with accommodation), passenger (without accommodation), and freight (including working) ships, based on the Electronic Reporting International (ERI) and AIS codes, with small pleasure boats and others not being considered. Three different ship data assessment approaches were performed for subsequent analysis, namely, i) daily shipping activity at different Danube River reaches for pollution source profiling, ii) reverse ship traffic approximation (RSTA) accounting for the flow of the polluted water for association analysis of the general fecal pollution and ships at the entire river reach (regional), and iii) counting of ships in the ship dock areas within the timeframe of sampling for local ship association analysis. For more details on the RIS and the three different ship counting concepts, see **Appendix A2**.

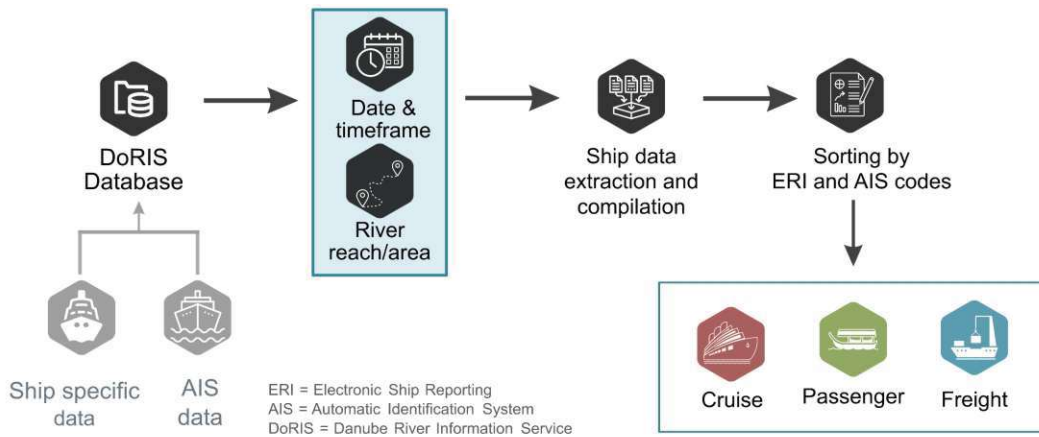


Figure 2 Flow chart of ship data assessment

Scheme of the ship data assessment process: Input data of date/time and river reach for ship data extraction and compilation and subsequent sorting by ERI (Electronic Ship Reporting) and AIS (Automated Identification System) codes for obtaining the number of ships per type in the selected area/timeframe.

2.2.4 Pollution source profiling (PSP) for impact scenario estimation

PSP was designed for the analysis of fecal pollution sources for a specific catchment/river reach to estimate the amount of fecal bacteria emitted from all considered human and animal fecal pollution sources (Derx et al., 2023; Frick et al., 2020; Reischer et al., 2011). Here, we transferred the concept to estimate human fecal pollution based on the daily *E. coli* load, extending it for inland navigation and investigation of different ship wastewater handling scenarios (correct/incorrect) and comparison with municipal wastewater input (see **Appendix A2** for details). PSP was performed for the selected Danube River reach, as well as the sub-reaches: upstream of Vienna, Vienna and downstream of Vienna with high and low season differentiation as performed for ship activity assessment (**Figure 1 panel B** and **Appendix A2** for details).

2.2.4.1 PSP parameters and scenarios

Estimates of fecal emissions from ships and from municipal wastewater treatment plants (WWTP) were based on the number of people contributing to the given source, the amount of *E. coli* shed per person and day, and the reduction in *E. coli* concentrations due to treatment (depending on the investigated scenario and ship type). The amount of *E. coli* shed per person and day was calculated using 10^8 CFU *E. coli* per gram feces and 150 g feces per person and day according to Reischer et al. (2011). For municipal wastewater input calculation, the number of citizens and tourists in the catchment and the three sub catchments were obtained from the government of Lower Austria for the year 2019. A median reduction of \log_{10} 2.3 for biological

wastewater treatment was assumed as reported by Mayer et al. (2016). Summer tourism in Austria (May to September) significantly builds around outdoor recreation activities, with the peak holiday season occurring in July and August (Falk, 2014; Pröbstl-Haider et al., 2021), while in winter (December to February), tourism industry predominantly focuses on ski sports (Steiger and Scott, 2020). These tourism patterns are also related with seasonal variation in ship numbers in Austria. Referring to these patterns, which are also reflected in the annual ship traffic statistics (2019 – 2022, (Viadonau, 2019a, 2021, 2022)), we selected the two months January and February for low season (LS) and July and August for the high season (HS) investigation. Information about the anticipated number of passengers was obtained from the local authorities (Government of Lower Austria expert judgement: Günther Konheisner) with: i) cruise (with accommodation): 185 persons (both seasons), ii) passenger (day trip – without accommodation): high season on weekdays: 250 persons; on weekend: 500 persons; low season weekend/weekday: 20 persons; and iii) freight: 5 persons (both seasons). The treatment of ship wastewater and therefore the reduction in emissions is dependent on the type of ship as well as the assumed scenario of correct or incorrect ship wastewater handling, therefore two different scenarios with i) the correct handling of wastewater (scenario 1) and ii) with incorrect handling of wastewater were assumed for theoretical load calculation (scenario 2) for both seasons:

Scenario 1 - Correct Wastewater Handling Ship Emission: assuming, i) cruise ships with an on-board WWTP, achieving a \log_{10} 1.9 reduction of *E. coli* (referring to the 25th percentile reduction by mechanical biological wastewater treatment according to Mayer et al. (2016), as no specific reduction data for on board WWTPs was available, ii) passenger ships equipped with sewage tanks, assuming no emissions to the waters if correctly handled (*i.e.*, transfer to municipal WWTPs), and iii) freight ships with no wastewater treatment or storage facilities, hence direct emission (no reduction).

Scenario 2 - Maximum Potential Ship Emission: in case of incorrect wastewater handling there is no reduction of any of the emissions from cruise, passenger or freight ships assumed (no treatment, no storage).

2.2.5 Statistical analysis and data visualization

Statistical analysis and data visualization were performed using R and RStudio (R Core Team, 2022; RStudio Team, 2021) with the support of Microsoft Excel (Microsoft Corporation, 2019). For more details on the RStudio packages used, specific functions and additional software used

for graphic design, see **Appendix A3**. For all statistical tests the level of significance was set to $p \leq 0.05$ and in case of multiple testing, correction of probability was applied (Bonferroni or false discovery rate (fdr)).

2.2.5.1 Statistical analysis of the water quality data

Analysis of variance (ANOVA) was used for the analysis of the microbial fecal pollution data *i.e.*, differences in the decadic logarithm of the concentration of *E. coli* at the different transects and sampling points. Post-hoc Tukey test was additionally performed to obtain more information of the specific group differences. Non-parametric spearman rank correlation was used for the investigation of the correlation of *E. coli* concentrations and the other physio-chemical parameters assessed in the water samples. For specific information on the used R functions see **Appendix A3**.

2.2.5.2 Associations of fecal pollution and ship activity: Correlation and regression analysis

For the entire selected river reach association analysis (regional analysis), spearman rank correlation was performed with the *E. coli* concentrations (decadic logarithm) from transects A, B, C, D, E, F, and G and i) environmental/hydrological parameters such as the 3-day sum of precipitation and river/tributary discharge, ii) wastewater treatment plant discharge data, and iii) the number of ships counted with respect to river flow, sampling time and date (see **RSTA Appendix A2, Figure A1**). For *E. coli* concentrations, median values of the cross-section samples were used for correlation analysis, resulting in a total of 84 individual sample sets (11, 11, 13, 13, 12, 12, and 12 for transects A to G, respectively). For detailed information on the environmental parameters, WWTP discharge data and the used functions, see **Appendix A3, Table A2** and **Table A3**.

For the ship dock analysis (local analysis), the change in *E. coli* concentration of samples on the respective side of the ship docks (orographically right river side: B+/B, E+/E; left: C+/C, D+/D) was calculated as the ratio of increase (downstream divided by upstream, see **Figure A4, Appendix A**) or the positive difference (downstream minus upstream) of *E. coli* concentrations (see **Figure 10**) and plotted against the number of ships between the upstream/downstream sampling transects during sampling. Spearman rank correlation as well as a multiple linear regression analysis was performed to assess relations among the number of ships and hydrological parameters (precipitation/rain, river discharge) on the increase on *E. coli* concentrations (dependent variable) at the dock C+/C. For detailed information on the used functions see **Appendix A3**.

2.3 Results

2.3.1 Establishing AIS-based shipping activities for the selected Danube reaches

The inland AIS data-based SDA script was used to analyze the ship traffic volume in the investigated Danube River reach, revealing frequent activity with seasonal differences. Especially for cruise and passenger ships seasonal fluctuations were observed, in line with ship schedules and elsewhere reported seasonal patterns (Viadonau, 2019a, 2021, 2022). The daily median ship number at the entire Danube River reach (river-km: 2111–1873) in the high season (HS, summer months) was 159 ships in total, with approx. 44% of cruise ships ($n = 69$), 5% of passenger ships ($n = 8$) and 46% of freight ships ($n = 73$) (**Figure 3**, left panel) during the analyzed period. In the low season (LS, winter months), the median daily ship number decreased to 114, with the highest drop in cruise ships ($n = 31$), though the daily number of passenger ships ($n = 5$) and freight ships ($n = 73$) remained almost the same.

Sub-reaches of the river reach were analyzed to obtain detailed information, revealing a higher number of cruise ships for the reach in Vienna (HS/LS: $n = 44/6$) and upstream of Vienna (HS/LS: $n = 44/26$) in comparison to the downstream Vienna reach (HS/LS: $n = 27/1$) (**Figure 3**, right panels). No passenger ships were observed in the LS upstream and downstream of Vienna, which is appropriate, as passenger ferries did not operate in winter months. Freight traffic is highest for the Danube reach upstream of Vienna (HS/LS: $n = 50/48$), followed by the reach in Vienna (HS/LS: $n = 35/37$) and the downstream of Vienna reach (HS/LS: $n = 26/24$) (**Figure 3**, right panels).

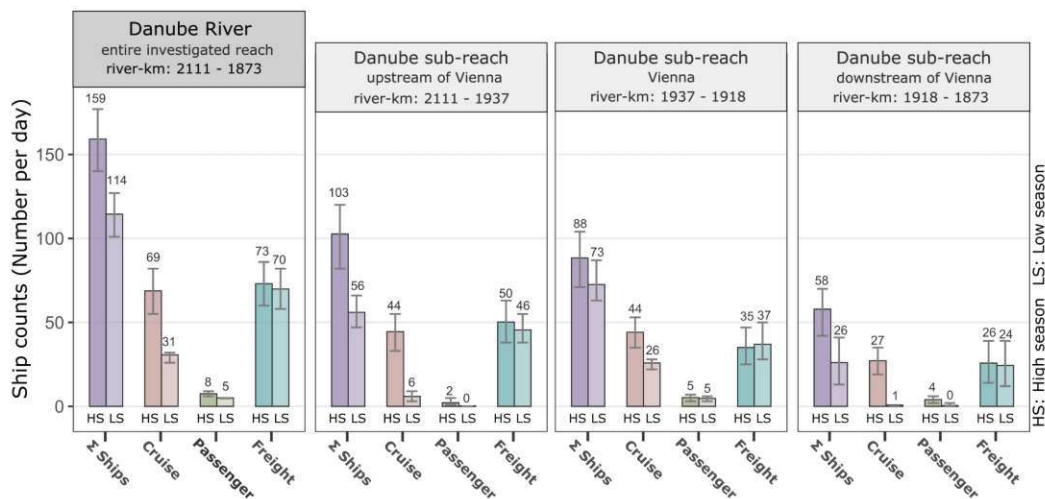


Figure 3 Seasonal variation in number of ships

Bar chart of the daily shipping activity with seasonal (HS: high season; LS: low season) differentiation for all ships (Σ ships) and ships per type (cruise, passenger, and freight) for the river reaches and

investigated period 03/2019–03/2020 i) entire investigated reach of the Danube River in Lower Austria (river-km: 2111–1873), and sub-reaches of the Danube River in Lower Austria: ii) upstream of Vienna (river-km: 2111–1937), iii) in Vienna (river-km: 1937–1918) and iv) downstream of Vienna (river-km: 1918–1873). Median value given; lower/upper error bars: smallest/largest value within 1.5 times interquartile range below/above 25th/75th percentile. HS: high season (summer months, 2019); LS: low season (winter months, 2020).

2.3.2 PSP reveals high local fecal pollution potential from the shipping industry

For the PSP, we estimated the theoretical daily emitted number of *E. coli* from ships, with correct or incorrect ship wastewater handling scenarios, versus the daily emitted number of *E. coli* from municipal WWTPs. The scenario of correct ship wastewater handling for the entire Danube River reach resulted in a theoretical daily fecal load of 12.9 log₁₀ CFU *E. coli* during HS and 12.8 log₁₀ CFU *E. coli* during LS (**Figure 4** left panel, ‘correct handling ship emission’) for the investigated period of 03/2019–03/2020. In the case of incorrect ship wastewater handling, the daily fecal load was considerably higher, with 14.4 log₁₀ (HS) or 13.9 log₁₀ (LS) CFU *E. coli*, which in HS is in the same order of magnitude as the input from mechanically treated municipal wastewater (14.4 log₁₀ CFU *E. coli*) (**Figure 4** left panel, “max. potential ship emission”). The results for sub-reaches gave analogous results: For two of the three sub-reaches, the theoretical daily emitted load in the case of incorrect ship wastewater handling was slightly higher than the input from treated municipal wastewater in the high season (**Figure 4** right panels). In general, the scenario assuming correct ship wastewater handling resulted in a lower input by 1 to 2 orders of magnitude for all sub-reaches compared to incorrect wastewater handling.

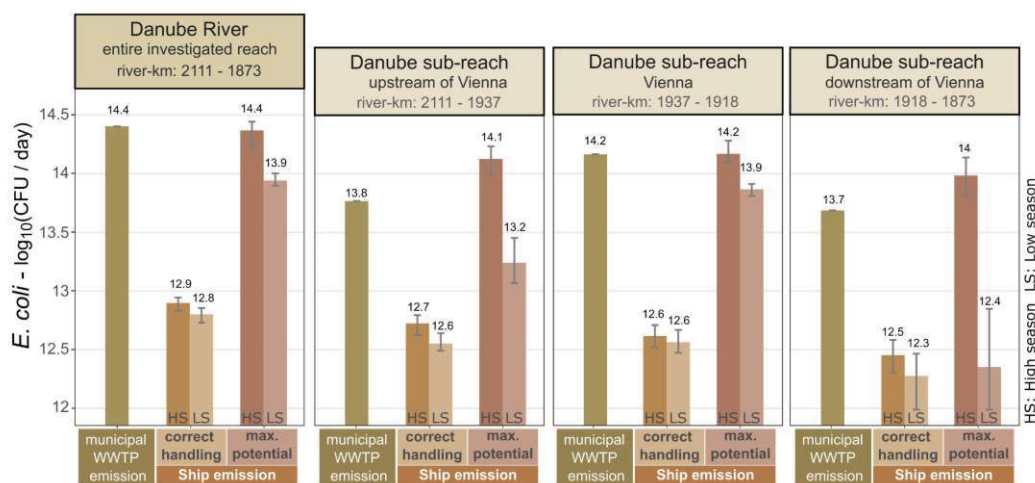


Figure 4 Comparison of *E. coli* loads of ships and WWTPs

Bar chart of the estimated *E. coli* load (log₁₀ CFU per day) discharged into i) the entire reach of the Danube River in Lower Austria (river-km: 2111-1873) and the sub-reaches ii) upstream of Vienna

(river-km: 2111-1937), iii) Vienna (river-km: 1937 to 1918) and iv) downstream of Vienna (river-km: 1918–1873) for emissions from municipal WWTP emission, from ships with correct treatment of ship wastewater (correct handling ship emission) and for ships with incorrect/no ship wastewater treatment giving the maximum potential load/worst-case scenario (max. potential ship emission). Median value given; lower/upper error bars: smallest/largest value within 1.5 times interquartile range below/above 25th/75th percentile. HS: high season (summer months, 2019); LS: low season (winter months, 2020).

Hypothesis formulation based on PSP scenarios: Even under the incorrect wastewater handling scenario from entire navigation activities (*i.e.*, 100% raw wastewater direct emission input to the river reach), the PSP indicates that the pollution capacity from the shipping industry does not exceed municipal fecal wastewater emissions (mechanical biological treatment without disinfection). We assume that the realistic situation ranges somewhere in between the highly unrealistic worst case and the optimum situation of correctly handled emissions, amounting to a few percent (3-6%) in comparison to treated municipal wastewater emissions. Considering the long mixing stretches between the selected transects (A to G, **Figure 1**) and the inherent statistical uncertainty observed in microbiological quantification, we hypothesized that fecal emissions from shipping cannot be detected at the regional scale for the current situation of wastewater disposal at the investigated Danube River reach (*i.e.*, regional-scale fecal pollution hypothesis). In contrast, especially for spatially aggregated ships with incorrect wastewater handling, we hypothesize that navigation sources have the highest fecal pollution capacity locally (*i.e.*, local-scale fecal pollution hypothesis), such as observed downstream of docks (*i.e.*, pairs of B+/B, C+/C, D+/D, E+/E, **Figure 1**). These two hypotheses formed the foundation for the subsequent field investigations and statistical analyses (see section 2.2.5.2 for details on performed statistics).

2.3.3 Realizing water quality assessment at high spatial resolution

2.3.3.1 Overall fecal pollution, classification and chemo-physical parameters

Water quality analysis for the entire selected river reach during 03/2019–03/2020 (n = 665) revealed an overall concentration range of *E. coli* from log₁₀ 0.9 to log₁₀ 3.38 (MPN+1) per 100 mL, with a median concentration of log₁₀ 2.08 (MPN+1) per 100 mL (**Table 1**). The Danube River discharge on the sampling days was distributed over the annual variation within the monitoring year, which was in the same range as the years before (**Figure A2, Appendix A**). Descriptive statistics of the assessed key fecal indicator parameter *E. coli* as well as of the two human-associated fecal MST markers and chemical and physical parameters are given in **Table 1**.

Table 1: Water quality parameters

Descriptive statistics of analyzed water quality parameters: fecal indicator bacteria *E. coli*, human-associated microbial fecal genetic source tracking markers (HF183/BacR287 and BacHum) and chemo-physical parameters. n... number of samples, n > LOD (TOD for MST markers) number of samples with concentrations higher than the limit of detection (LOD) or threshold of detection (TOD), median, arithmetic mean, and range (minimum value to maximum value).

parameter	n	n > LOD*	% > LOD*	median	mean (arithmetic)	Range (min-max)		unit
<i>E. coli</i>	665	665	100	2.08	2.16	0.90	3.38	log ₁₀ (MPN+1) per 100 mL
HF183/BacR287 (human-associated)	100	75	75	3.36	3.49	2.32	4.83	log ₁₀ (ME+1) per 100 mL
BacHum (human-associated)	100	84	84	3.91	3.95	2.78	5.39	log ₁₀ (ME+1) per 100 mL
temperature	665	665	100	11.4	12.2	3.3	21.9	°C
pH	665	665	100	8.2	8.2	6.8	8.7	-
conductivity	665	665	100	312	315	164	494	µS/cm
oxygen	665	665	100	10.7	10.7	8.1	15.0	mg/L
COD	665	414	62.3	6.0	6.9	< 5	21.0	mg/L
nitrogen (total)	665	620	93.2	2.0	2.0	< 1	5.0	mg/L
phosphorus (total)	665	74	11.10	0.06	0.06	< 0.05	0.09	mg/L
ammonium	665	495	74.40	0.03	0.04	< 0.015	0.40	mg/L

*TOD (Threshold of Detection) for MST markers

According to the fecal pollution classification of Kavka et al. (2006), the majority (94%) of water samples ranged within the low and moderate fecal pollution levels. Only 6% of samples showed critical levels of fecal pollution, though no strong or excessive fecal pollution events were observed (**Figure 5** left panel). Spearman rank correlation analysis of *E. coli* and the chemical and physical parameters revealed significant positive correlations between *E. coli* concentration and chemical oxygen demand - COD ($\rho = 0.20$, adjusted $p = 1.6 \times 10^{-5}$), total phosphorous - P total ($\rho = 0.23$, adj.p = 2.8×10^{-7}) and ammonium - $\text{NH}_4\text{-N}$ ($\rho = 0.32$, adj.p = 5.7×10^{-16}) concentrations (**Figure 5** right panel).

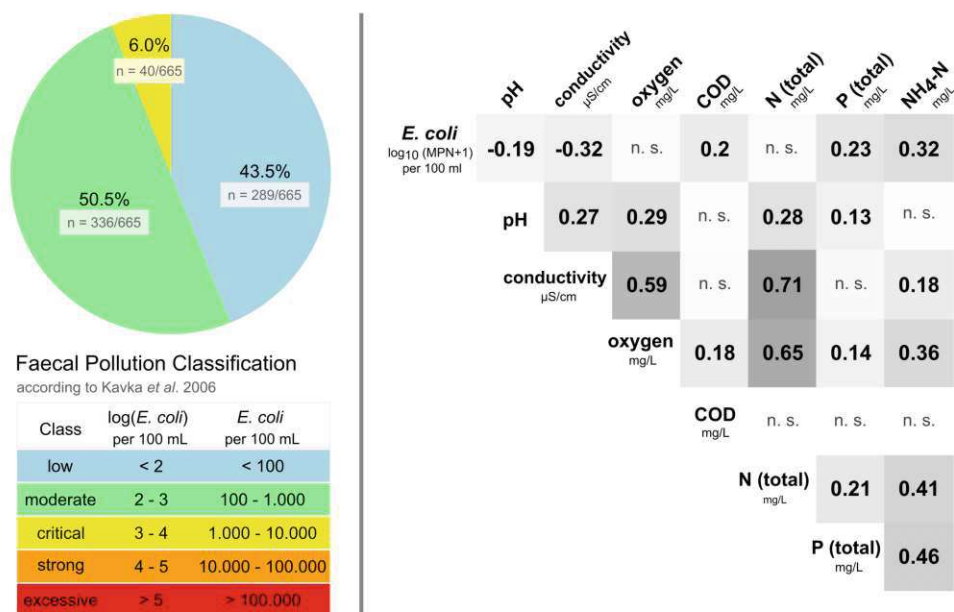


Figure 5 Fecal pollution classification

Left panel: Fecal pollution classification of all water samples (n = 665) based on E. coli concentration according to Kavka et al. (2006). Pie chart giving the proportion of samples as well as number and percentage of samples within each pollution class. Right panel: Spearman rank correlation table of all E. coli concentration values (n = 665) and physical (pH, conductivity) and chemical (chemical oxygen demand (COD), total nitrogen, total phosphorus and ammonium) water quality parameters. Rho values are given only if the p value is below the level of significance (alpha <= 0.05) after p value adjustment using the Bonferroni method. n.s.: not significant.

2.3.3.2 Microbial source tracking uncovers dominating human fecal pollution

Genetic microbial source tracking analysis was performed to further characterize the observed fecal pollution: human (including human wastewater from municipal and ship origin) and suspected animal sources (ruminant and pig/boar) on 100 out of the 665 samples taken in the 12-month sampling timeframe. The results revealed human fecal pollution to be dominant with a positive detection rate of 75%, a median of \log_{10} 3.18 and a range from \log_{10} 2.32 to 4.83 for HF183/BacR287 and 84%, a median of \log_{10} 3.63 and a range from \log_{10} 2.78 to 5.39 (ME+1) per 100 mL for BacHum, respectively (range min to max of positive detects). The animal-associated markers showed a considerably lower occurrence, with only 23% for the ruminant-associated marker BacR and 7% for the pig-associated marker Pig2Bac, both with a median value below the TOD, *i.e.*, not detectable (**Figure 6**). Association with Danube River discharge showed that especially at base flow ($< 1800 \text{ m}^3/\text{s}$), human-associated fecal pollution was dominant, and animal-associated markers were predominantly detected at higher river discharge, where the concentration of human-associated markers was also increased (**Figure 6** right panel).

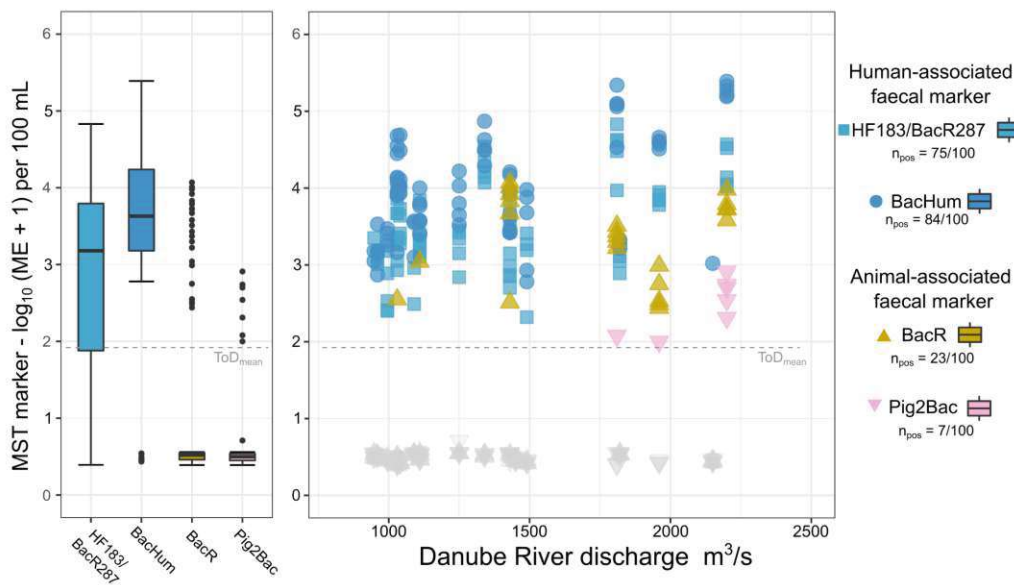


Figure 6 Microbial source tracking markers (MST) concentrations

Left panel: Boxplot of genetic fecal marker concentrations: human-associated HF183/BacR287, BacHum and animal-associated BacR (ruminant) and Pig2Bac (pigs). For nondetects, the sample-specific ½ ToD was taken as the value for plotting; the mean ToD is highlighted with a dotted line. Right panel: Scatterplot of the microbial source tracking marker concentrations (y axis) and the Danube River discharge, n = 100, positive detects: HF183/BacR287 n(pos) = 75, BacHum n(pos) = 84, BacR n(pos) = 23, Pig2Bac n(pos) = 7.

2.3.3.3 Longitudinal fecal pollution analysis at selected river transects

The performed water quality analysis allowed for a detailed investigation of the fecal pollution at the investigated Danube River reach, as of the high resolution of sampling (for the fecal indicator bacteria (FIB) *E. coli* see **Figure A3, Appendix A**). Longitudinal concentrations of *E. coli* at the eleven sampling transects ranged from a median of 1.91 log₁₀ to log 2.29 log₁₀ (MPN+1) per 100 mL (all five cross-profile samples gathered; **Figure 7**). Performed ANOVA revealed that there was no significant difference in the annual median *E. coli* concentrations between the transects ($p = 0.1$, $n = 55 - 65$). Descriptive statistics of all analyzed water quality parameters for each individual transect are given in **Table A4 (Appendix A)**. The fecal pollution dataset at the principal sampling locations A to G (dark blue) was used for the regional river reach association analysis in section 2.3.4.1.

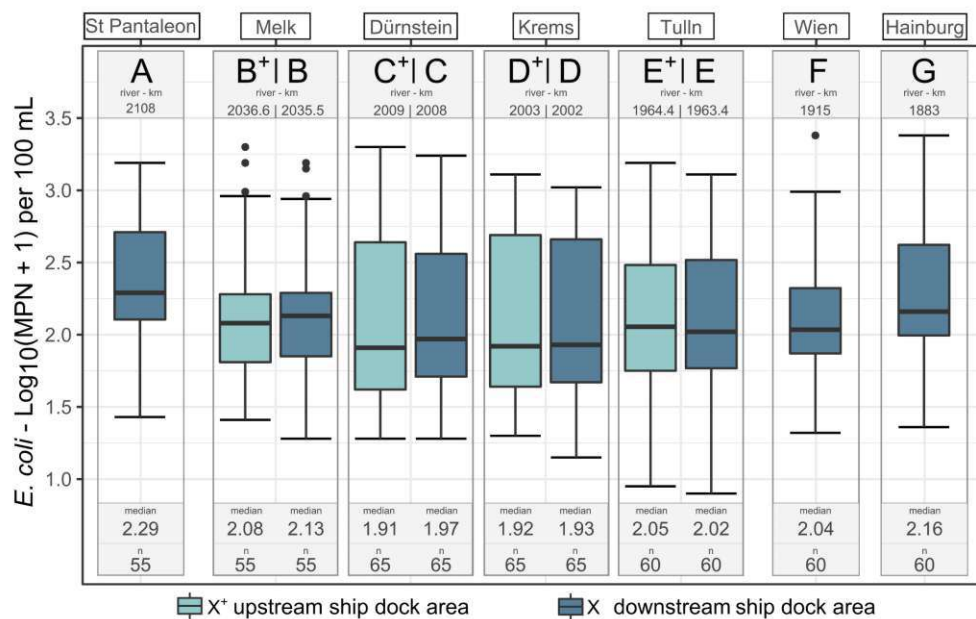


Figure 7 Observed *E. coli* concentrations along River Danube

*Boxplots of the observed *E. coli* concentrations (log₁₀(MPN + 1) per 100 mL) in longitudinal display for all transects A to G for the annual data. n = total number of samples (including all individual samples of each cross-profile at each sampling day). Median values given; lower/upper error bars: smallest/largest value within 1.5 times interquartile range below/above 25th/75th percentile.*

2.3.3.4 Cross-sectional high-resolution fecal pollution analysis

Cross-profile analysis showed strikingly homogeneous *E. coli* concentrations for the majority of the transects (**Figure 8**). Only for transect F (Wien/Vienna) a statistically significant difference of *E. coli* concentrations across the profile, with increased concentrations at the orographic right river side, was obtained (ANOVA, $p < 0.001$, $n = 11 - 13$). A plausible reason

is the inflow of the Danube channel at the right river side, which receives wastewater from the Vienna WWTP 6.5 km upstream of the sampling transect, wastewater from smaller WWTPs as well as combined sewer overflows (CSOs) of the Viennese sewer.

Additionally, an upstream/downstream ship dock comparison of *E. coli* concentrations with respect to the upstream/downstream and river cross-profile position and the sampling date was performed. Only one significant upstream–downstream difference in concentrations of the orographically left sample of the dock C+/C (Dürnstein) was revealed, whereas for the other, no significant differences were obtained. These upstream/downstream pairs were used for investigation of the local ship dock area association analysis in section 2.3.4.2.

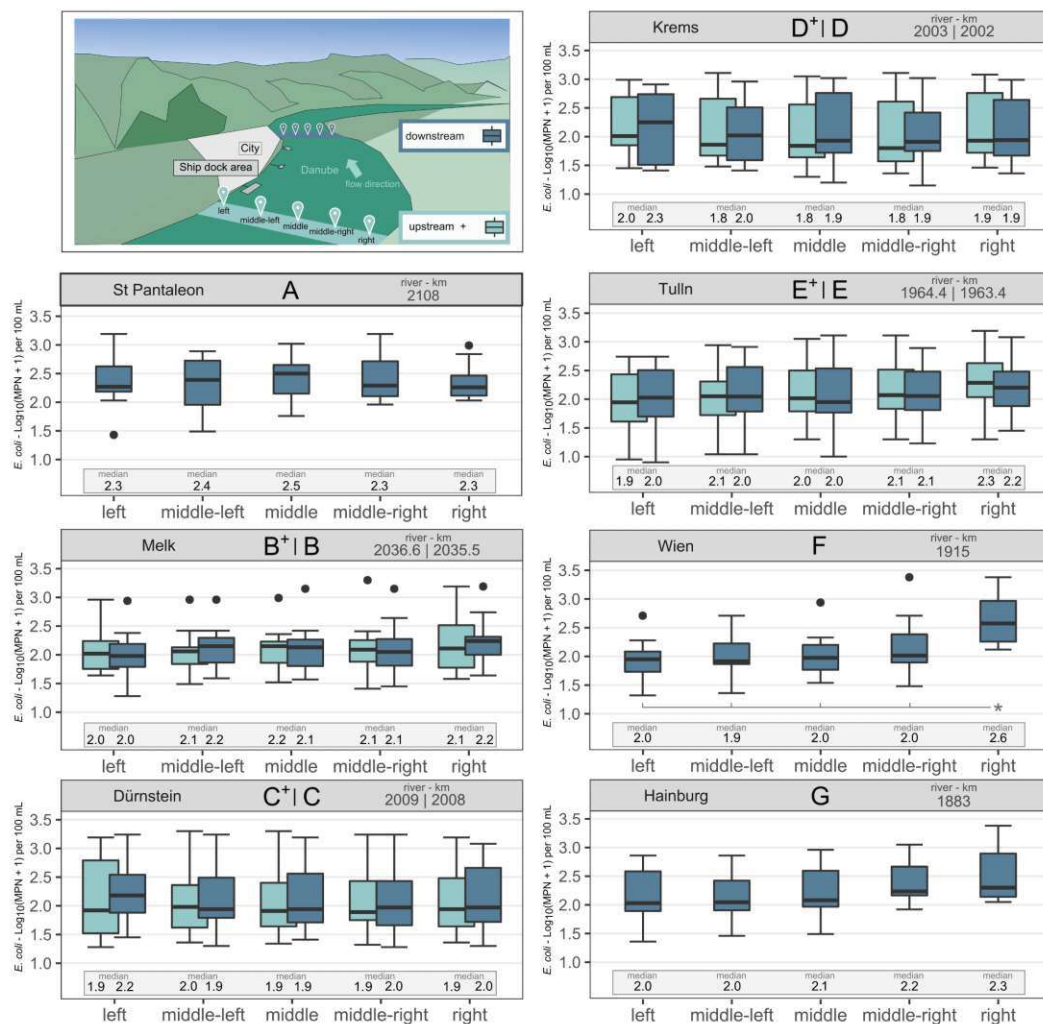


Figure 8 Observed *E. coli* concentrations across River Danube

Boxplots showing the *E. coli* concentration in the cross-profile with upstream downstream samples being paired. Median value given; lower/upper error bars: smallest/largest value within 1.5 times interquartile range below/above 25th/75th percentile. Asterisk * indicates a significant difference of *E.*

coli $\log_{10}(\text{MPN}+1)/100$ mL at the cross-profile position to all the others at the sampling transect assessed by ANOVA and a post-hoc Tukey test ($p < 0.05$, $n = 11 - 13$).

2.3.4 Associations of fecal pollution with ship activity, WWTP discharge and hydrological parameters

2.3.4.1 Correlation analysis at the investigated river reach (regional scale)

To obtain insight into influential factors on the observed fecal pollution on the regional scale (covering the entire investigated river reach), a Spearman rank correlation analysis with hydrological parameters (precipitation, river discharge), municipal WWTP discharges and the number of ships assessed by the RSTA approach was performed. Data from the principal sampling transects (A to G, $n = 84$) were used, as described in section 2.2.5 and **Appendix A2**. Positive significant correlations of *E. coli* concentrations after p-value adjustment using *fd*r were observed for all hydrological parameters: i) 3-day sum of local precipitation ($\rho = 0.33$, $\text{adj.p} = 5 \times 10^{-3}$), ii) Danube River discharge ($\rho = 0.48$, $\text{adj.p} = 1.2 \times 10^{-5}$) and iii) discharge of tributaries with a confluence point < 36 rkm upstream ($\rho = 0.30$, $\text{adj.p} = 1.9 \times 10^{-2}$; **Figure 9** upper panel). For WWTP discharge, no significant correlation with WWTPs situated directly at the Danube, but a significant correlation with WWTPs at tributaries (< 90 rkm, $\rho = 0.30$, $\text{adj.p} = 1.9 \times 10^{-2}$) was obtained. The analysis with the number of ships, including a differentiation of the ship types (cruise, passenger, and freight), showed no significant correlation, irrespective of which metric (1 m/s, 2 m/s river velocity; < 2 h, < 8 h, < 16 h water flow time) was used (**Figure 9** lower panels). Hence, on the regional scale (entire investigated river reach), the number of ships did not have a measurable influence on the *E. coli* concentration in the monitoring timeframe, and fecal pollution was mainly triggered by rainfall and higher river and municipal WWTP discharge.

	Rain		River Discharge		WWTP Discharge	
	Precipitation local	Danube local	Tributary < 36 km	at Danube		at Tributary
	1 m/s	2 m/s		< 36 km	36 - 90 km	< 90 km
<i>E. coli</i> concentration at transect	0.33	0.48	0.3	n. s.	n. s.	0.3

Ships (total) Number in counting area						
	< 2 h river flow time		< 8 h river flow time		< 16 h river flow time	
	1 m/s	2 m/s	1 m/s	2 m/s	1 m/s	2 m/s
<i>E. coli</i> concentration at transect	n. s.	n. s.	n. s.	n. s.	n. s.	n. s.

Cruise Number in counting area						
	< 2 h river flow time		< 8 h river flow time		< 16 h river flow time	
	1 m/s	2 m/s	1 m/s	2 m/s	1 m/s	2 m/s
<i>E. coli</i> concentration at transect	n. s.	n. s.	n. s.	n. s.	n. s.	n. s.

Passenger Number in counting area						
	< 2 h river flow time		< 8 h river flow time		< 16 h river flow time	
	1 m/s	2 m/s	1 m/s	2 m/s	1 m/s	2 m/s
<i>E. coli</i> concentration at transect	n. s.	n. s.	n. s.	n. s.	n. s.	n. s.

Freight Number in counting area						
	< 2 h river flow time		< 8 h river flow time		< 16 h river flow time	
	1 m/s	2 m/s	1 m/s	2 m/s	1 m/s	2 m/s
<i>E. coli</i> concentration at transect	n. s.	n. s.	n. s.	n. s.	n. s.	n. s.

Figure 9 Correlation of *E. coli* concentrations with environmental factors

Spearman rank correlation coefficients (rho) of E. coli concentrations at the transects with meteorological and hydrological parameters (upper panel) and the numbers of ships in the upstream counting area for i) ships (total), ii) cruise liners, iii) passenger ferries and iv) freight vessels considering 1 m/s or 2 m/s river flow velocity and a water flow time < 2 h, < 8 h and < 16 h before sampling (lower panels). Hydrological parameters (upper panel): Sum of precipitation during 3 days before sampling, Danube River discharge, tributary river discharge as well as WWTP discharge at the Danube River for WWTP < 36 rkm, or from 36 – 90 rkm, or WWTP at tributaries up to < 90 rkm upstream of the sampling point on the same day of sampling. n.s. not significant ($p \geq 0.05$) after p-value adjustment using fdr.

2.3.4.2 Correlation analysis at the ship docks (local scale)

In contrast to the regional fecal pollution analysis, we observed a significant correlation of the increase in *E. coli* concentrations and the number of ships in the ship dock area at one of the four investigated docks, namely, Dürnstein (C+/C). The disintegration of ships per type revealed that cruise ships accounted for the high correlation ($\rho = 0.828$ and $p = 0.02$, **Figure 10**), with a maximum difference in *E. coli* (downstream minus upstream) of 233 MPN per 100

mL. Multiple linear regression analysis revealed that precipitation and river discharge were insignificant parameters for the increase in *E. coli* concentrations at dock Dürnstein, but the number of cruise ships was significant ($p = 0.02$). Note that no WWTP discharge point and no confluence point of a river is situated between transects C+ and C. At all the other ship docks (B+/B), (D+/D) and (E+/E), no association with the number of ships and increase in pollution was observed (**Figure A4, Appendix A**).

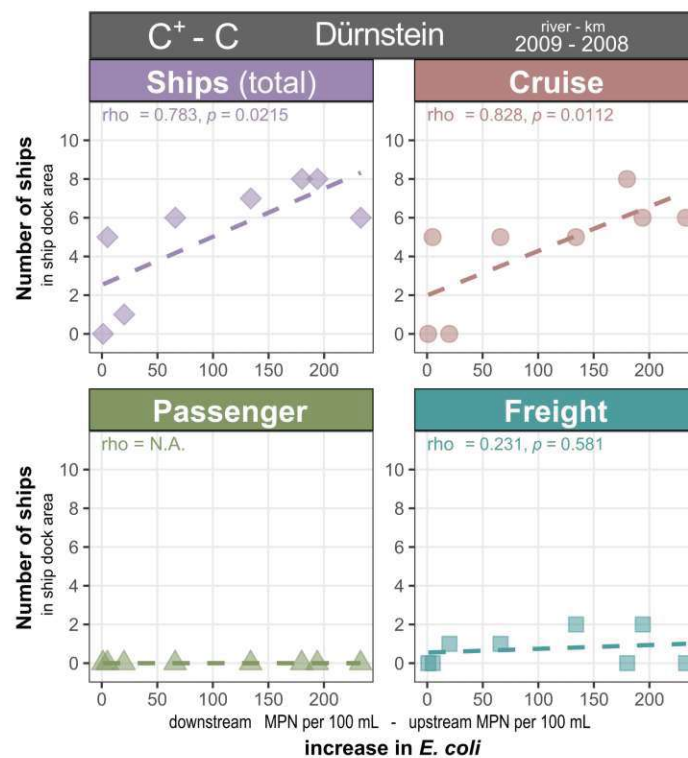


Figure 10 Ship numbers and *E. coli* concentrations at docking station

Scatterplot of the number of ships in the ship dock area and the increase in *E. coli* concentrations of the downstream (C) and upstream (C+) sample pairs at the left river side at the ship dock area of Dürnstein. Spearman rank correlation coefficients ρ and p values are given in the plot. The dotted line gives a fitted linear model.

2.4 Discussion

2.4.1 Realization of a novel integrated approach for assessing the impact of inland navigation by an interdisciplinary toolbox

The impact of inland navigation on the microbial fecal water quality of a large river was assessed using a new, integrated, highly interdisciplinary approach. It is based on three pillars: (1) pollution source profiling (PSP, *i.e.*, estimates of theoretically emitted numbers of *E. coli*)

to assess the theoretical impact of various ship fecal emission scenarios, (2) PSP-targeted longitudinal and transversal water quality analyses combined with tailor-made ship-traffic data extraction, and (3) statistical analysis between pollution source patterns on regional and local scales to test the formulated pollution hypotheses.

The approach combined field-data from A) satellite-based automatic identification system (AIS) used for targeted ship traffic assessment and B) highly resolved water quality analysis based on chemical data and cultivation-based standard fecal indicator enumeration (ISO 9308-2 (ISO, 2012)) in combination with state-of-the-art quantitative genetic microbial source tracking (also referred to as genetic fecal pollution diagnostics, GFPD (Demeter et al., 2023; Steinbacher et al., 2021)).

Internationally, there have been two main approaches to assess the impact of navigation on water quality thus far. In one approach, the studies estimated the pollution potential of vessels by calculating nutrient loads or sewage volumes, often incorporating complex ship traffic data, but without any water quality investigations (Chen et al., 2022; Huhta et al., 2007; Loehr et al., 2006; Parks et al., 2019; Perić et al., 2016; Presburger Ulnikovic et al., 2012). In the other approach, the studies focused rather on the microbiological water quality around ports, without having any ship data (Dheenan et al., 2016; Luna et al., 2019). We found only three studies on the association of the occurrence of ships and microbiological-fecal pollution (Faust, 1982; Koboevi, 2022; Sobsey et al., 2003), all performed at maritime ports.

However, to the best of our knowledge, no study has yet investigated the microbiological water quality of rivers in relation to local and regional ship traffic and no PSP considering all major wastewater sources (including ships) has yet been combined with a multiparametric water quality investigation.

Here, we propose to integrate the state-of-the art of these assessment types into a common framework. The approach is directly transferrable to any other water body (and not limited to lotic/river systems), especially given the increasing global coverage of RIS, including inland AIS (Creemers, 2023; Trivedi et al., 2021). It can also support evidence-based water management decisions of local authorities.

2.4.2 The local impact of navigation was unexpectedly low but sensitively traceable

As hypothesized by the PSP, river sections directly downstream of ports and docks would be crucially affected by wastewater discharges from ships. In our study area, assuming all ships illegally discharge raw wastewater (see **section 2.3.2** and **Figure 4** PSP scenario ‘Maximum Potential Ship Emission’), the total fecal pollution load from navigation would equal the sum of the total municipal wastewater load entering the considered Danube River reach. The local consequences of such a scenario would be serious, given the extremely high concentrations of fecal microorganisms in raw wastewater (log 7 to log 8 MPN/100 mL *E. coli* (Harwood et al., 2019)), demonstrating the local pollution capacity of navigation on beaches, recreation zones and other types of local usages.

Our investigation found only one site, at dock C+/C, where a statistical increase in *E. coli* concentrations was indicated downstream (**Figure 8**). Strikingly, this increase also matched the identified significant correlation with the number of cruise ships extracted from the big-AIS-data near-real-time ship traffic monitoring system (**Figure 10**). Furthermore, using the developed SDA algorithm, we were able to trace back to the individual ships causing this correlation as well as to analyze the average time of the ships in the dock area. In fact, cruise ships spent up to 1 to 3 h at dock C+/C, with seasonal differences, with highest average docking times from May to October and shorter times in the area in the winter months (see **Figure A5, Appendix A**). In contrast, freight ships all over the year only spent approx. 15 minutes in the area, passing the dock C+/C (see **Figure A5, Appendix A**). The used AIS data were “blinded” before being handed over by the authorities for analysis, not intended to identify any specific ship or company involved. However, these results impressively demonstrate the capacity of this suggested approach for analysis and monitoring (including aspects of sensitivity and specificity) by combining “field” water quality data with “post hoc” extraction of AIS stored near-real-time ship trafficking data. It should also be mentioned that the detectability of changes in water quality could even be improved by replacing grab sampling with automated time series sampling, triggered by passing ships (*e.g.*, comparable to event sampling (Stadler et al., 2008)).

Both the minor increase in fecal pollution at dock C/C+ and the lack of increase in pollution at the other three sites indicate that ship wastewater was most likely treated and handled adequately (*e.g.*, ship emissions from correctly managed on-board wastewater treatment) for

the selected Danube reach and time period. Since the investigation was triggered by citizen complaints and considerable media attention, the navigation industry probably had a higher awareness of the importance of correct wastewater handling. Hence, the approach also proved very useful to analyze and highlight the obviously correct realization of the intended management practice. Although a statistically significant but only moderate increase was detected, the formulated local-scale fecal pollution hypothesis had to be clearly rejected, as the potential pollution capacity was not realized at all.

2.4.3 Regional impacts of navigation were not detectable, but this could change in the future

On the regional scale, we hypothesized that the impact of navigation on Danube River fecal pollution patterns would not be discernible under the current state-of-the-art municipal sewage disposal (secondary treatment and no disinfection), irrespective of the assumed type of ship wastewater handling and PSP scenario. Indeed, the recovered results showed no statistically significant increase in the longitudinal development of fecal pollution levels between the selected transects (A to G, **Figure 7**), and no correlation between ship counts in any of the ship classes (and RSTA calculation schemes) versus the *E. coli* concentrations was detectable (**Figure 9**). The regional-scale fecal pollution hypothesis was thus clearly supported by our field data.

However, these proportions may shift in the future, bringing the impact of inland navigation more to the forefront. Proposed changes in European Union law regarding urban wastewater management (EU Regulation 2020/741, 2022) are expected to lead to a reduction in fecal microorganism loads from both treated municipal wastewater and combined sewer overflows in the coming years. If the proposed changes are implemented across the Danube River basin, it is reasonable to assume that the fecal pollution level in the river attributable to municipal wastewater will decrease considerably (e.g., up to 10 000-fold for viral particles (Demeter et al., 2021)), leading to an increase in the relative importance of fecal input from inland navigation.

On the other hand, cruise tourism on the Danube River has great potential to increase (Jászberényi and Miskolczi, 2020). In fact, before the COVID-19 pandemic, during the investigation period, cruise ship tourism on the Danube in Austria grew by 15% in 2019 compared to 2018 (Viadonau, 2019a). Assuming the same trend in the next decades, ship

activity and therefore fecal pollution load from inland navigation could substantially increase. If these two potential changes occurred concurrently, the relationship between municipal wastewater loads and ship discharges could flip, making the navigation sector a critical potential emission source on both the local and regional scales.

2.4.4 Large rivers are subject to multiple pressures, and water quality varies on longitudinal and cross-sectional scales

Fecal pollution can change over time and along the investigated river reach because of changing river morphology, confluence with tributaries and point and nonpoint sources. Therefore, longitudinal investigations are frequently performed in river water quality analyses (Ballesté et al., 2019; Fernández et al., 2022; Kirschner et al., 2009; Kirschner et al., 2017); however, cross-sections are seldom investigated (Kirschner et al., 2017). In contrast in coastal regions, several studies have been performed to study water quality variations at high spatial resolution (along the shore and in transects (Ahn et al., 2005; Amorim et al., 2014; Manini et al., 2022)).

Our spatially highly resolved water quality investigation at the Danube River showed that there were neither significant longitudinal differences in *E. coli* concentrations along the 223 km Danube River reach nor significant cross-sectional variations at most of the transects (see **Figure 7 and 8**). The observed concentration of *E. coli*, indicative of general fecal pollution, ranged from \log_{10} 0.9–3.38 MPN/100 mL, with a median of 2.10 MPN/100 mL for the Danube River in the monitoring timeframe, consistent with former surveys of the Danube River (Demeter et al., 2021; Kirschner et al., 2009). This is a typical concentration range for a moderately polluted water body with input from state-of-the-art WWTPs. Other navigable rivers show similar *E. coli* concentration levels, for example, the Rhine River with concentrations between $< \log_{10}$ 1.18 and \log_{10} 4.10 and an average of \log_{10} 2.91 MPN/100 mL (Herrig et al., 2019), or the upper Mississippi River with mean values of \log_{10} 1.89 in 2011 and \log_{10} 1.18 CFU/100 mL in 2012 (Staley et al., 2014). However, many rivers are considerably more polluted, such as the rivers of the Bogotá basin in Columbia, with maximum concentrations up to \log 6 and \log 7 *E. coli* MPN/100 mL at many of the sites (Fernández et al., 2022). Although there are approaches towards global and freely available data concerning the water quality of surface water, such as the GEMStat Water Quality Dashboard project by the UN (<https://gemstat.org/>), profound and standardized microbial fecal pollution analysis of

large rivers on a global scale is scarce. Additionally, in the EU, there is data scarcity, as microbial fecal pollution monitoring is not included in the Water Framework Directive (European Parliament, 2000); hence, we can conclude that the herein published highly resolved multiparametric water quality dataset is one of its kind.

2.4.5 Increasing use of AIS and RIS in research

The use of AIS data as a big data source for ship-associated research purposes has been increasing in recent decades (Chen et al., 2022; Yang et al., 2019). Especially for maritime research, this data source is used for investigations, *e.g.*, ship behavior analysis for the detection of illegal fishing (Iacarella et al., 2023; Kurekin et al., 2019). AIS and inland AIS were already used for an environmental impact evaluation of exhaust gas emissions from ships in maritime waters (Goldsworthy and Goldsworthy, 2015; Toscano et al., 2021) and from inland navigation at the Yangtze River (Huang et al., 2022a; Zhang et al., 2023). Despite providing comprehensive navigational information, AIS data-based research must consider that only vessels equipped with turned-on AIS transponders are incorporated in the database and that manually edited information might be wrong or not up to date (Harati-Mokhtari et al., 2007).

Inland AIS is one essential tool of RIS, beginning in 1998 in Europe and implemented increasingly globally, such as in India (Trivedi et al., 2021) and the United States of America (Creemers, 2023). RIS is an integral part of the trend towards digitalization in the navigational and water sector, *i.e.*, Intelligent Transport Systems (ITS) and e-Navigation (e-Nav) (Creemers, 2023); hence, inland AIS/RIS data will be increasingly available for research purposes in the future.

2.5 Conclusions

- We developed and applied a novel integrated approach for evaluating the impact of inland navigation on the microbial fecal water quality of navigable rivers, based on the three pillars (1) pollution source profiling (PSP), allowing for theoretical (*in silico*) impact scenario analysis, (2) highly resolved and advanced field-analysis (*in situ*) of fecal pollution levels, chemo-physical water quality and ship traffic and (3) statistical analysis between pollution patterns and ships on regional and local scales.

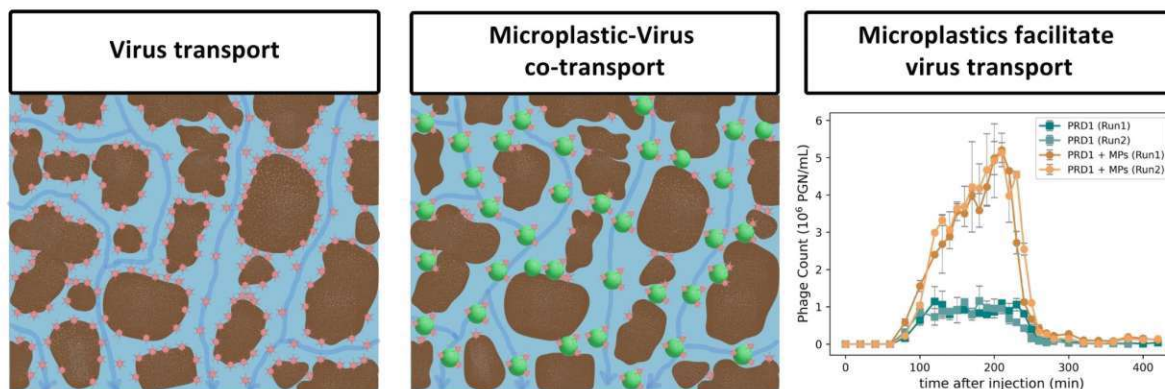
- Ship tracking data was extracted from inland AIS data by a specifically developed script, enabling retrospective back tracing of the individual ships per type (*i.e.*, cruise, passenger, freight) on regional and local scale.
- High resolution multi-parametric water quality analysis at the investigated Danube River reach revealed low longitudinal and cross-sectional pollution gradients, from dominant human origin (demonstrated by genetic fecal pollution diagnostics, GFPD), hence identifying *E. coli* as a suitable proxy for human wastewater from municipal WWTPs or ships.
- PSP highlighted a high theoretical fecal pollution potential from ships (regionally, with highest pollution capacity locally), which was not detected during the investigated period, indicating correct management of ship wastewater.
- Minor local impact was detectable and attributable to the associated docked cruise ships, highlighting the sensitivity of the approach, and showing its possible extensions towards investigation of *e.g.*, the docking times of individual ships.

The approach is transferable to any other water body with available AIS data over the world, enabling detailed understanding of local and regional navigational fecal pollution characteristics, with highest potential for research and authorities worldwide, heading towards a digitalization of the water management sector.

Chapter 3 Microplastics as vectors for virus transport in saturated porous media

Abstract

The prevalence of microplastics in skin cleaning products and clothing results in microplastics being present in sewage due to personal hygiene and laundry. During wastewater treatment, viruses can come into contact with microplastics, potentially forming aggregates. After agricultural sludge application these aggregates could infiltrate into deeper soils, threatening shallow groundwater. The mechanisms behind microplastic-virus aggregation and their effect on virus survival and co-transport in soils remain unknown. To investigate this, batch experiments were conducted by mixing PRD1 phage (a surrogate for adenovirus) with microplastics in groundwater under different temperatures. Subsequently, column experiments were performed to understand the effect of microplastics on virus transport in saturated quartz sand. Microplastic quantification was done using solid-phase cytometry, while virus enumeration was performed by qPCR and culture-based methods. The findings highlight that the surface charge of microplastics played an important role in governing virus attachment and transport. Batch experiments revealed a significant reduction in the persistence of infective viruses in the presence of microplastics. The co-transport experiments showed that microplastics act as vectors, enhancing the transport of both total and infective viruses through saturated quartz sand, posing a risk for waterborne viral transmission.



3.1 Introduction

Microplastics in the form of microbeads are widely used in personal care and consumer products due to their stability, durability, low cost, and ease of production (Fendall and Sewell, 2009; Lei et al., 2017). Approximately 6% of the liquid skin cleaning products marketed in the European Union, Norway and Switzerland contained microplastics (Gouin et al., 2015). A survey by Cosmetics Europe reported that 4360 tons of microplastics were used in 2012 (Duis and Coors, 2016). It is estimated that 4594 to 94,500 microplastics can be released into the environment in a single use of an exfoliant (Napper et al., 2015). Once used, these microplastics are washed directly into sewers and cannot be filtered or removed during wastewater treatment due to their small size (Deng et al., 2022), with over 90% accumulating in sludge (Murphy et al., 2016; Wu et al., 2022a). Unlike natural materials, the surface charge of virgin microplastics rapidly changes in the aquatic environment, allowing nutrients and contaminants to adsorb (Bowley et al., 2021). This attachment of nutrients promotes biofilm formation, enabling microplastics to host diverse microbial communities on their surfaces, known as a Plastisphere (Amaral-Zettler et al., 2020; Kesy et al., 2019; Li et al., 2019b; Oberbeckmann et al., 2018). Plastisphere formation can influence environmental behavior of microplastics, creating favorable conditions for the dispersion and prolonged survival of microplastic-associated pathogens (Tang and Li, 2024; Zhai et al., 2023; Zhong et al., 2023). Enteric viruses are the most common pathogens in wastewater and sludge (Corpuz et al., 2020) and can have very long survival times (Sidhu et al., 2010). During wastewater treatment processes, microplastics are exposed to high concentrations of enteric viruses, creating a perfect environment for the viruses to interact with microplastics (Moresco et al., 2022). Eventually, microplastic-associated pathogens in wastewater treatment will end up as treated sewage sludge (Gholipour et al., 2022). About 50% of treated sludge (biosolids) is used in agricultural applications (Huang et al., 2023; US EPA, 2016). Due to the recurring application of treated sludge to enhance soil quality for crop yield, these newly formed microplastic-associated pathogens could impact human health and the environment. These impacts include effects on soil fertility, surface and groundwater contamination, destruction of biodiversity, and the potential to affect crop yield (Eisfeld et al., 2022). Moreover, this emerging microplastic-associated pathogen risk has the potential to contaminate drinking water sources, triggering disease outbreaks.

Compared to other contaminants, less focus has been placed on the potential interaction and transport of microplastics with microbial pollutants (Lu et al., 2022). In this context, research

has demonstrated that microplastics could play a crucial role in influencing both the composition of microbial communities and the dissemination of microorganisms, including antibiotic-resistance genes (Deng et al., 2020; Karkman et al., 2019; Liu et al., 2021a; Moon et al., 2020; Slizovskiy et al., 2020; Syranidou and Kalogerakis, 2022). Several studies have focused on the interactions of microplastics and enteric viruses using batch tests (Lu et al., 2022; Moresco et al., 2022; Ochirbat et al., 2023; Pastorino et al., 2020; Zhang et al., 2022a); however, research on the co-transport of microplastic-associated pathogens in porous media has predominantly focused on bacterial pathogens (Gao et al., 2021; He et al., 2021; He et al., 2018). To the best of our knowledge, no study has explicitly investigated microplastic-virus co-transport in saturated porous media and it is still unclear whether microplastic-virus co-transport can prolong virus survival and transmission in groundwater. Therefore, given the potential risks to public health, a comprehensive study was done to unravel the mechanisms driving microplastic-virus co-transport and to evaluate the potential for groundwater contamination.

This study aims to investigate the mechanisms responsible for the persistence and mobility of a human enteric virus (using a surrogate) and microplastics in saturated porous media. PRD1 bacteriophage has been widely used as a surrogate for rotavirus and adenovirus, due to its similar properties (Bales et al., 1991; Sinton et al., 1997; Stevenson et al., 2015; Yahya et al., 1993), and long survival time in the environment (Blanc and Nasser, 1996). The research was conducted in two phases. First, batch experiments were conducted to evaluate the survival and infectivity of PRD1 phages, under different temperature conditions (both with and without MPs). Secondly, column co-transport experiments were carried out in quartz sand, mixing PRD1 phages with polystyrene (PS) microplastics, as well as injecting them separately. Experimental breakthrough data were analyzed to understand the transport and retention of total and infective PRD1 phages (with and without MPs) in quartz sand. Additionally, a two-site kinetic model accounting for attachment and detachment was used to simulate the experimental breakthrough curves (BTCs). Finally, colloid filtration theory (CFT) and Derjaguin-Landau-Verwey-Overbeek theory (DLVO) were used to examine the interactions between quartz sand and PRD1 or the MP-PRD1 aggregate, within the porous media.

3.2 Materials and methods

3.2.1 Polystyrene microplastics

A study on microplastic distribution in groundwater revealed polystyrene as the most prevalent polymer detected (Esfandiari et al., 2022). Therefore, to mimic microplastics in the environment, commercially available 1 μm plain polystyrene yellow-green fluorescent microspheres (Polysciences Inc., Warrington, PA, USA) were used in the experiments. The major benefit of using these microspheres for laboratory experiments is the ease with which they can be detected by solid-phase cytometry (Stevenson et al., 2014). For characterization of the microplastics, the zeta potential was measured with a Zetasizer Pro ZSU3200 (Malvern, Worcestershire, UK) and each measurement was repeated three times.

3.2.2 Laboratory preparation of viruses

PRD1 phage is an icosahedral phage with a diameter of 62 nm and an isoelectric point between pH 3 and 4 and negatively charged at pH values between 5 and 8 (Blanc and Nasser, 1996; Loveland et al., 1996). PRD1 was purchased from the German Collection of Microorganisms and Cell Cultures (DSMZ, Braunschweig, Germany; DSM No. 19107). For enumeration and propagation of PRD1, the related bacterial strain *Salmonella enterica* (*S. enterica*) (DSMZ, Braunschweig, Germany; DSM No. 19207) was used. Bacteria were grown overnight in tryptone soya broth (TSB) with 0.6% (w/v) yeast extract (Oxoid Ltd., Hampshire, UK) at 37 °C. Afterwards, the overnight culture was diluted ten-fold in fresh medium and incubated at 37 °C for 3-6 hours to obtain a maximum number of viable cells in the logarithmic growth phase (log phase). For propagation of virus stocks, virus solutions were used for plaque assays, according to the protocol of Kropinski et al. (2009) and plates with confluent lysates continued to be used. These plates were overlaid with 5 mL TSB or saline-magnesium (SM) buffer (5.8 g NaCl, 2.4 g Tris HCl, 1.0 g CaCl₂, 0.1 g gelatine, add 1.0 mL H₂O, pH 7.5) and shaken for about 3 hours, and then stored overnight at 4 °C. Afterwards the medium was separated and centrifuged at 8000 rpm for 2 minutes. The supernatant was filtered (0.02 μm), aliquoted, and stored at -20 °C.

3.2.3 Batch experiments

The persistence of the viruses (with and without MPs) was determined by performing two independent batch experiments. Each experiment was performed with three independent vials per condition (with and without microplastics) and stored at different temperatures i.e. 4 °C, ambient temperature ~22 °C, 30 °C and 37 °C, respectively. These temperatures were chosen

because between 4 and 22 °C (typical groundwater temperatures fall within this range), minimal differences in inactivation are expected, whereas inactivation rates should increase at 30 and 37 °C. For each condition, we investigated a total of 6 samples and 3 independent vials on two separate days. The initial phage concentration was determined, and samples were taken after 1, 3, 7, and 10 days respectively, and quantified for their presence (qPCR, phage genome number PGN/mL) and infectivity (small drop plaque assay, plaque forming unit PFU)/mL). Statistical analyses were performed in SPSS 28 (IBM, New York, USA). Differences were assessed with one-way ANOVA followed by post-hoc comparisons (Tukey HSD) and paired t-tests after confirming the normal distribution of the studied PRD1 phages (total and infective) under different temperatures and experimental conditions (with and without microplastics).

3.2.4 Column experiments

Column experiments were performed using quartz sand (grain size diameter: 0.6–1.3 mm, bulk density: 2.65 g/cm³) purchased from Carl Roth GmbH + Co. KG, Karlsruhe, Germany. The median grain diameter (d₅₀) of 0.95 mm was assumed. The details of the experimental parameters are provided in **Table 2**. Based on the standard gravimetric method, the porosity of the porous media was calculated by measuring the volume of water needed to saturate the dry soil used to pack the column (pore volume), divided by the total column volume. The zeta potential of the quartz sand was measured using a SurPASS electrokinetic analyzer (Anton Paar) based on a streaming potential and streaming current measurement (Luong and Sprik, 2013). This zeta potential indicates the surface charge at the solid-liquid interface.

Transport experiments were performed under saturated flow conditions using a Plexiglas column (70 mm inner diameter and 300 mm length). The column diameter met the minimum d_{col}/d₅₀ ratio (the ratio of the column diameter to the effective particle diameter of the porous media) and was much higher than the recommended value of 50, to ensure minimal potential wall effects in the column (Knappett et al., 2008). Stainless-steel-mesh screens (Spectrum Labs, New Brunswick, USA) were placed on both ends of the column to prevent the loss of quartz sand. The column was filled with quartz sand and saturated with Viennese tap water (chemical analysis shown in **Table B1, Appendix-B**), which is sourced from karst groundwater. To ensure homogenous packing and minimize air entrapment, the column was filled with porous media and tap water from the bottom up, in 2 cm increments while gently stirring with a small steel rod. Before the experiment, the columns were flushed with tap water for a minimum of 20 pore volumes.

A solution of sodium bromide, NaBr, (1.0 mM/L, 102.89 mg/L) prepared in tap water (1 pore-volume) served as a conservative tracer to investigate the transport properties of the packed column. The electrical conductivity (EC) of the injected tracer was measured by a hand-held portable EC meter (WTW ProfiLine Cond 3310, Xylem Analytics Weilheim, Germany) in a flow-through cell. Three different influent solution scenarios were performed in the experiments: (i) PRD1 in tap water, (ii) a mixture of PRD1 and microplastics in tap water, and (iii) microplastics in tap water. During the experiment, 2 pore-volumes (approx. 980 mL) of the influent solution was pumped in the upward direction at a constant flow rate of 6.5 mL/min (Darcy velocity = 2.45 m/day), and afterwards, the columns were flushed with 5 pore-volumes of tap water, at the same flow rate. A magnetic stirrer was used to stir the suspension constantly during the experiments to ensure that microplastics were evenly dispersed in the influent solution. A fraction collector (CF2 Fraction Collector, Spectrum Chromatography, Texas, USA) automatically collected column effluent samples in 15 mL test tubes after every 2-minute time interval. All column tests were done in duplicate (each column test contained freshly packed material).

3.2.5 Microplastic and virus enumeration

The enumeration of microplastics in the effluent solution was done with solid-phase cytometry (SPC) using a ChemScan™ RDI (bioMérieux, Marcy l'Étoile, France). The detailed procedure for the microplastic counting has been previously published (Ameen et al., 2024; Stevenson et al., 2014) and is available in the Section 4.2.6 (Chapter 4). Additionally, to enumerate the total and infective PRD1 phages in the influent and effluent samples, quantitative polymerase chain reaction (qPCR) and small-drop plaque assay (culture-based) methods were used, respectively. The details of these methods are included in Appendix **B1**.

Table 2: Overview of column experimental parameters.

Experimental Scenario	Run	Measured flow rate	Injected concentration C_0	pH
		cm/min	– PGN/mL or PFU/mL or MPs/mL –	
Total Phages^a				
PRD1	A1	0.17	1.18×10^9	7.55
	A2	0.17	1.27×10^9	7.45
PRD1 with MPs	B1	0.17	2.83×10^9	7.95
	B2	0.17	1.54×10^9	7.85
Infective Phages^b				
PRD1	A1	0.17	2.77×10^6	7.55
	A2	0.17	1.77×10^6	7.45
PRD1 with MPs	B1	0.17	1.36×10^7	7.95
	B2	0.17	7.0×10^6	7.85
Microplastics^c				
MPs	C1	0.17	4.45×10^7	7.82
	C2	0.17	4.51×10^7	7.78
MPs with PRD1	B1	0.17	4.55×10^7	7.95
	B2	0.17	4.32×10^7	7.85

^a Counted by quantitative polymerase chain reaction (qPCR) method.

^b Counted by single drop plaque assay method.

^c Counted by solid-phase cytometry.

3.2.6 Numerical analysis

3.2.6.1 Transport modeling

The breakthrough curves of the total and infective PRD1 phages (with and without microplastics) were modeled using the HYDRUS-1D software package (Simunek et al., 2013). Advection–dispersion equations for colloid transport are implemented in a numerical model using a two-site attachment-detachment model and the following equations (Schijven and Šimůnek, 2002):

$$\frac{\partial C}{\partial t} + \frac{\rho_b}{\theta} \frac{\partial S_1}{\partial t} + \frac{\rho_b}{\theta} \frac{\partial S_2}{\partial t} = D v \frac{\partial^2 C}{\partial x^2} - v \frac{\partial C}{\partial x} \quad (3.1)$$

$$\frac{\rho_b}{\theta} \frac{\partial S_1}{\partial t} = k_{a1} C - \frac{\rho_b}{\theta} k_{d1} S_1 \quad (3.2)$$

$$\frac{\rho_b}{\theta} \frac{\partial S_2}{\partial t} = k_{a2} C - \frac{\rho_b}{\theta} k_{d2} S_2 \quad (3.3)$$

where C is the concentration of PRD1 with and without microplastics (PGN/mL or PFU/mL), t is time (min), ρ_b is dry bulk density (g/cm^3), θ (dimensionless) is porosity, S_1 and S_2 are the concentrations of adsorbed PRD1 at the first and second kinetic sorption sites (PGN/mL or PFU/mL), D is dispersivity (cm), v is pore water velocity (cm/min), x is the distance along the flow path (cm), k_{a1} and k_{a2} are attachment rate coefficients (min^{-1}), while k_{d1} and k_{d2} are detachment rate coefficients (min^{-1}), at the first and second kinetic sorption sites, respectively.

3.2.6.2 Colloid filtration theory

The removal of the PRD1 phage (with and without microplastics) was quantified using colloid filtration theory, which calculates the attachment efficiency, α (dimensionless), and can be computed using the following equation (Tufenkji and Elimelech, 2004a):

$$\alpha = -\frac{2}{3} \frac{d}{(1-\theta)x\eta_0} \ln \frac{C}{C_0} \quad (3.4)$$

where d is the mean soil grain (d_{50}) size (mm), θ is the porosity (dimensionless), x is the column length (cm), C/C_0 represents the normalized concentration of colloids at the breakthrough plateau (dimensionless). The maximum value from the HYDRUS-1D modeled values was used for C/C_0 because the observed values did not produce a steady C_{max} . The predicted single collector contact efficiency, η_0 (dimensionless), was computed using the following equation (Tufenkji and Elimelech, 2004a):

$$\eta_0 = \eta_D + \eta_I + \eta_G \quad (3.5)$$

where η_0 is dependent on hydrodynamic interactions, van der Waals, and gravitational forces. η_D is the contact due to Brownian forces (diffusion), η_I is the contact due to interception, and η_G is the contact due to gravity (settling). Equation 3.5 relies on additional equations and parameters which are outlined in the **Appendix B2**. The calculations governing microplastic-associated virus filtration and their respective contributions are provided in **Table B2 (Appendix-B)**. The contact and attachment efficiencies for the co-transport scenario (i.e. PRD1-MP aggregates) were estimated considering transport dominated by microplastic colloidal properties (e.g., colloid size and density, Hamaker constant and approach velocity).

3.2.6.3 DLVO theory

The DLVO theory (Derjaguin and Landau, 1993; Verwey and Overbeek, 1955) was applied to further understand the interactions and attachment of the PRD1, microplastics, and the microplastic-associated PRD1 with the quartz sand grains. To quantify these interactions, we calculated the inter-surface potential energy as the sum of van der Waals attraction (VDW) (Gregory, 1981) and electrical double layer repulsion (EDL) (Feriancikova and Xu, 2012) energies over the separation distance between approaching surfaces. Since microplastics behave like a colloid due to their shape, size and surface charge, the classical DLVO theory is applicable (Wang et al., 2022b). All of the interaction energies were normalized by $K_B T$. Details about the DLVO can be found in the **Appendix B3**.

3.3 Results and discussion

3.3.1 Influence of microplastics on virus quantification

To determine the optimal DNA extraction protocol and to investigate a possible interference or inhibitory effect of microplastics on qPCR analysis of PRD1, both the qPCR efficacy and DNA-extraction efficacy in the presence of microplastics were tested. For this purpose, four different PRD1 concentrations ($4-8-\log_{10}$ PFU/100 μ L) were mixed with microplastics and either directly inserted into the qPCR reaction or used as input for NucleoSpin-based DNA extraction and subsequent qPCR. The results of the control samples (PRD1 without microplastics) demonstrate that both DNA extraction methods show good performance and efficiency, with R^2 values of 0.93 for direct insertion and 0.90 for the NucleoSpin when compared to the infective phage numbers (**Figure 11a**). As expected, qPCR-based quantification leads to $\sim 1-\log_{10}$ higher PGN values compared to the PFU values, as not all viral particles are infective while the genome can still be quantified. The quantitative results from

PRD1 with microplastics showed no significant difference between any of the conditions tested (**Figure 11b**), demonstrating an inhibitory effect on neither the PCR reaction nor the DNA extraction efficacy. Overall, the results demonstrate that the presence of microplastics does not interfere with qPCR-based quantification of PRD1 from aqueous samples and that both direct as well as NucleoSpin DNA extraction are suitable for the subsequent analysis of experimental samples. Following the evaluation, it was decided that the direct extraction method would be used when analyzing the effluent samples. Throughout the sample analysis, the accuracy of detecting PRD1 genomes remained consistent in tap water, whether microplastics were present or not. These findings align with previous studies that investigated the detection and stability of enteric virus genomes in surface and groundwater (Espinosa et al., 2008; Gassilloud and Gantzer, 2005; Gassilloud et al., 2003; Helmi et al., 2008). It is important to mention here that the detection of viral genome copies by the qPCR method does not necessarily imply the presence of active and infective viruses (Hamza et al., 2011), therefore, culture-based methods are used to detect infectivity. On average, the detected number of viral genome copies by qPCR was 1–3- \log_{10} units higher than the plaque assay method and is consistent with findings from other studies that compared the detection of enteric viruses to infectivity in environmental samples (Fongaro et al., 2012; Moresco et al., 2022; Moresco et al., 2015). Care must be taken and a comparison should be done because the composition and concentration of a bacterial strain (*S. enterica*) and the elution buffer composition (TSB) are known to inhibit PCR amplification (Skraber et al., 2009), suggesting that the detected genome copies may underestimate the actual number of viral genomes present, in some cases.

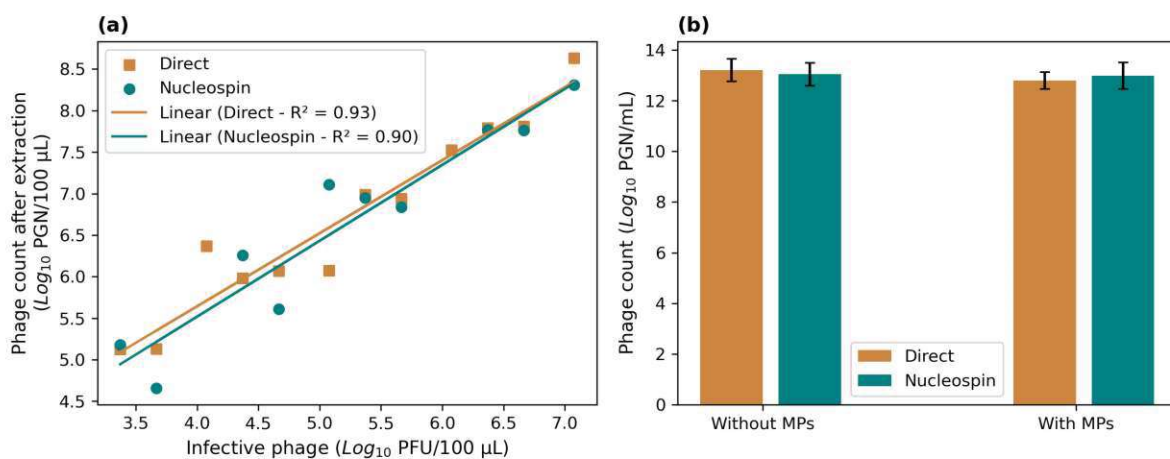


Figure 11 Comparison of DNA extraction methods

Correlation between (a) PFU and PGN numbers using either direct or NucleoSpin-based DNA extraction and (b) mean PGN/mL numbers of samples without MPs (control), and with MPs using either direct or NucleoSpin-based DNA extraction, including 95% confidence intervals.

3.3.2 Microplastics reduce virus infectivity

3.3.2.1 Total phages

To evaluate whether the attachment onto microplastics prolongs or hinders virus infectivity, PRD1 was mixed with microplastics and stored at four different temperatures for up to 10 days. As a baseline, total phages were enumerated using qPCR. During the 10 days, a minor loss of 0.51 log₁₀ was observed, as would be expected, for total phages determined via qPCR in the absence of microplastics (paired t-test, $p < 0.001$) (**Figure 12a**). In the presence of microplastics, the loss of total phages was 1.03 log₁₀ (paired t-test, $p < 0.001$) (**Figure 12b**). No significant differences were observed between the four temperatures investigated for both scenarios with and without microplastics (ANOVA, $p > 0.05$) (**Figure 12a-b**). As already after one day, a slight (0.3 log₁₀) but significant decrease in total phage particles was observed (paired t-test, $p < 0.01$), experimental error (e.g. a possible aggregation or adsorption of phages to the test tube or loss during pipetting) and DNA breakage during storage cannot be excluded. Overall, the results show high stability over 10 days.

3.3.2.2 Infective phages

In contrast to the qPCR results (total phages), a much stronger decrease in the number of infective PRD1 phages could be detected during the 10-day experiment for all scenarios tested (**Figure 12c-d**). Significant differences between the various temperature conditions occurred (ANOVA, $p < 0.001$ for both with and without microplastics present), however, without microplastics, the results obtained at 4°C and 22°C were not significantly different from each other (Tukey HSD post hoc test, $p > 0.05$). Without microplastics, the loss of infective PRD1 phages over 10 days was 0.41 and 1.15 log₁₀ at 4 °C and 22 °C (paired T-test, $p < 0.001$), respectively, while at 30 °C, 3.88 log₁₀, and 37 °C, 5.39 log₁₀ infective phages were lost after 10 days (paired T-test, $p < 0.001$). With microplastics, an even higher loss of infective phages was observed; at 4°C, 22°C and 30°C already 2.93-5.02 log₁₀ were lost after 10 days, while in the samples stored at 37 °C no infective phages could be found after 7 days (corresponding to a loss of 6.75 log₁₀, $p < 0.001$).

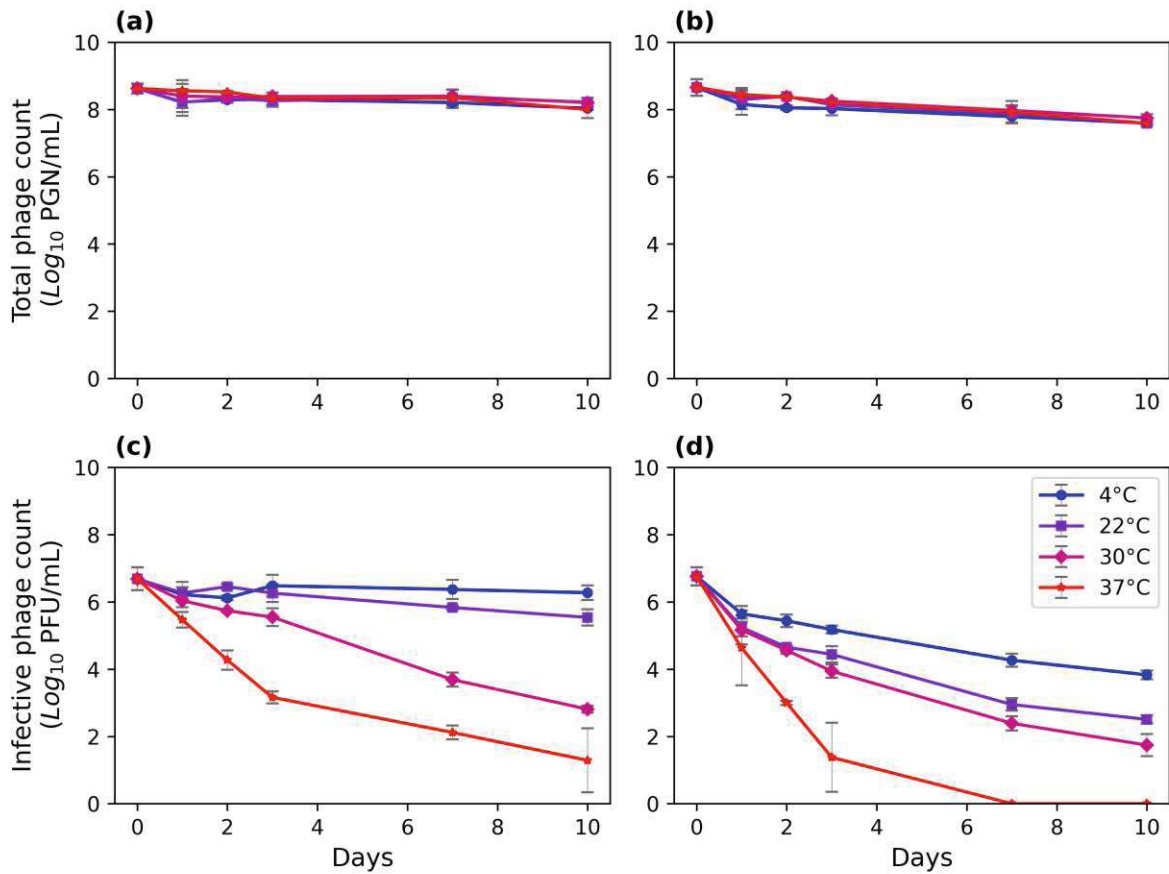


Figure 12 Virus persistence with and without microplastics

Persistence of PRD1 bacteriophages in the absence and presence of microplastics (MPs) under varying temperature conditions (4°C, ambient temperature ~ 22°C, 30°C, and 37°C) over 10 days. Panels (a) and (b) illustrate the persistence of total PRD1 phages without and with MPs, respectively. Panels (c) and (d) demonstrate the persistence of infective PRD1 phages under identical conditions (i.e. without and with MPs, respectively). Error bars represent the standard deviation from replicate experiments ($n \geq 2$).

The findings of this study suggest that temperature significantly influenced the survival of infective PRD1 phages, with their infectivity decreasing over time, especially when mixed with microplastics. The presence of microplastics accelerated the inactivation of infective viruses, even at low temperatures (4 and 22 °C), and this inactivation rate significantly increased at high temperatures. The majority of the observed loss of infectivity can be attributed to temperature and, to a lesser degree, the attachment of the phages to the microplastics, which is a potential inactivation mechanism (Schijven and Hassanizadeh, 2000), possibly due to the surface structure being disturbed upon attachment. Studies have shown that overall virus stability and infectivity decreased with time when they co-existed with microplastics (Lu et al., 2022;

Moresco et al., 2022). Lu et al. (2022) reported that over half of the infectious viruses (T4 phage) mixed with 2 μm polystyrene microplastics remained detectable after 10 days at 24 $^{\circ}\text{C}$ whereas, in the present study, no PRD1 phages were infective at 37 $^{\circ}\text{C}$ after 6 days. This may be due to the internal lipid membrane of the PRD1 phage capsid, which makes it more susceptible to inactivation, while, the T4 phage, with its tail structure, demonstrates greater infectivity and thermostability (Firquet et al., 2015; Moresco et al., 2022; Wigginton and Kohn, 2012). Our work clearly indicates, when compared to Lu et al. (2022), that the structural formation of viruses exhibits different behavior regarding their persistence in the presence of microplastics. At high temperatures (30 and 37 $^{\circ}\text{C}$), the viruses (without MPs) retained infectivity even after 10 days. Since groundwater temperatures typically range from 10 to 22 $^{\circ}\text{C}$ (Yates et al., 1985), and virus migration is relatively slow in deep groundwater but can be significantly faster in shallow groundwater, the prolonged survival of viruses in groundwater can pose substantial risks to drinking water safety (Zhang et al., 2022b).

3.3.3 Electrostatic interaction facilitating co-transport

Variations in the surface charge (measured as zeta potential) of viruses and microplastics can lead to charge-dependent repulsion or aggregation of colloids. Most viruses are negatively charged at environmentally relevant pH values, and most porous media in aquifers are negatively charged under similar conditions, indicating low potential attraction between the two surfaces (e.g. pure quartz); however, viruses can attach electrostatically where patches of positive charge are present due to impurities, for example iron or calcite. In this study, the zeta potential of quartz sand was -43 mV (pH = 8.2), while microplastics and PRD1 had zeta potential values of -42.4 ± 2.2 mV (pH = 7.82, EC = 372 $\mu\text{S}/\text{cm}$) and -8.9 ± 2.16 mV (pH = 7.5, EC = 381 $\mu\text{S}/\text{cm}$), respectively. The zeta potential values of PRD1 reported in this study align well with previously reported values, ranging from -7.8 ± 2.6 mV in 10 mM NaCl at pH 7.9 (Stevenson et al., 2015) to -9.8 mV (Mesquita et al., 2010). Upon mixing PRD1 with microplastics, the net zeta potential of the microplastic-associated PRD1 solution decreased to -17.74 ± 2.16 mV (pH = 7.9, EC = 379 $\mu\text{S}/\text{cm}$). Therefore, it is likely that the less negative PRD1 was attracted to the more negative microplastics, which may have caused attachment. Consistent with these findings, Lu et al. (2022) and Dang and Tarabara (2021) showed that polystyrene-microplastics adsorbed over 90% of a viral dose (T4 phage and adenovirus), highlighting the potential for electrostatic interactions being the predominant attachment

mechanism between the two types of colloids. Due to the large-sized microplastic being more negative than the PRD1, and the overall surface charge of the microplastic-associated PRD1 also being more negative than PRD1, it would be expected that the mobility of the PRD1 would be enhanced (more repulsion with sand grains) and the mobility of the microplastics would remain the same or would slightly decrease, due to the decreased negative charge of the microplastics in the presence of PRD1. This effect was observed by Stevenson et al. (2015) when they injected polystyrene-microplastics of the same size but different charge; the mobility of the less negative microplastics were enhanced and the mobility of the more negative microplastics decreased.

In order to evaluate to what extent surface charge facilitated attachment, the DLVO interaction energy profiles were calculated for three interaction scenarios over a range of different ionic strengths: (1) microplastics and the quartz sand; (2) PRD1 and the quartz sand; and (3) MP- PRD1 aggregates and the quartz sand (**Figure B1, Appendix B**). For microplastics and the quartz sand system, repulsion is predicted due to their similar charge. The interaction energy calculations reveal the presence of a high repulsive energy barrier ($\Phi_{DLVO}/k_B T$ maximum value being 108.53) to deposition at a low ionic strength (3 mM), and therefore, indicates less attachment of microplastics to sand grains in the Viennese tap water matrix, which has an ionic strength of approximately 3 mM. For ionic strengths ≥ 10 mM, the presence of a secondary energy minimum is observed ($\Phi_{DLVO}/k_B T = -0.05$ to -0.49) at a greater separation distance than that of the energy barrier. This is because the EDL interaction decreases exponentially with respect to separation distance, whereas the VDW attraction exhibits a power-law dependency with a slower decay (Tufenkji and Elimelech, 2004b). When repulsion dominates, a secondary minima can occur; however, the magnitude is quite small, and the separation between surfaces is significant (Gentile et al., 2021). Still, microplastics' removal is observed even at the lowest ionic strength examined, with straining being the most likely dominant removal mechanism. Similarly, repulsion is predicted between PRD1 and quartz, as both have a negative charge. The interaction energy indicates a low energy barrier to deposition at all ionic strengths ($\Phi_{DLVO}/k_B T$ maximum value for 3 mM being 4.65), which means that PRD1 shows weak repulsion but aggregation at the primary minima and at greater separation distances, thus predicting more potential for attachment of PRD1 to quartz sand. At a low ionic strength (3 mM) a primary minimum is observed ($\Phi_{DLVO}/k_B T = -11.66$), indicating high virus attachment to sand grains ($C_{max}/C_0 = 0.9 \times 10^{-3}$). For MP-PRD1 aggregates and the quartz sand system, repulsion is expected to be dominant due to negative

charge of aggregates and sand. The interaction energy calculations reveal the presence of a low repulsive energy barrier to deposition at all ionic strengths ($\Phi_{DLVO}/k_B T = 6.27$) and, therefore, aggregates are expected to attach to the quartz sand surfaces more than microplastics alone, but less than PRD1 alone. The MP-PRD1 aggregate removal is observed at the lowest ionic strength examined ($C_{max}/C_0 = 3.34 \times 10^{-3}$ at 3 mM in tap water). The values of each energy barrier, as well as the primary and secondary minima are shown in **Table B3 (Appendix B)**. DLVO calculations showed that the change in zeta potential affects the depth of the energy minima and the height of the energy barrier of interacting colloids (Bradford et al., 2017). If the energy barrier remains greater than $7 k_B T$ (e.g., microplastics and their co-transport with viruses), primary minima interactions are unlikely to occur, except at sites with surface roughness or charge heterogeneity (Bradford et al., 2017; Torkzaban et al., 2013). Additionally, if the secondary minimum is less than $1.5 k_B T$ in magnitude, it is considered insignificant (Shen et al., 2018).

3.3.4 Microplastics enhance virus transport in porous media

To understand the impact of microplastics on the transport of viruses and the reciprocal influence of viruses on microplastics within porous media, PRD1 and microplastics were enumerated in the effluent solution after column breakthrough. Total and infective PRD1 concentration curves (**Figure 13a-b**) show that the presence of microplastics influenced the transport of viruses by enhancing their transport (more viruses came through with the MPs, as opposed to without MPs). PRD1 concentration data was highly scattered, and concentrations did not reach a constant plateau, which was also observed with the conservative tracer (**Figure 14a**). The maximum concentration of infective phages passing through the column was approximately 2 orders of magnitude lower than what was injected (10^4 vs. 10^6 PFU/mL). The influent concentration of infective phages was 10^6 PFU/mL, as compared to the total number of phages injected (10^9 /mL), counted by qPCR. In the presence of microplastics, the concentration of infective viruses exhibited a more rapid increase and a fluctuating dynamic, with both increases and decreases occurring more dramatically. This interaction between the PRD1 and microplastics suggests a complex dynamic (e.g. straining, blocking and/or electrostatic interaction), where the presence of microplastics influences the movement and distribution of viruses within the porous media.

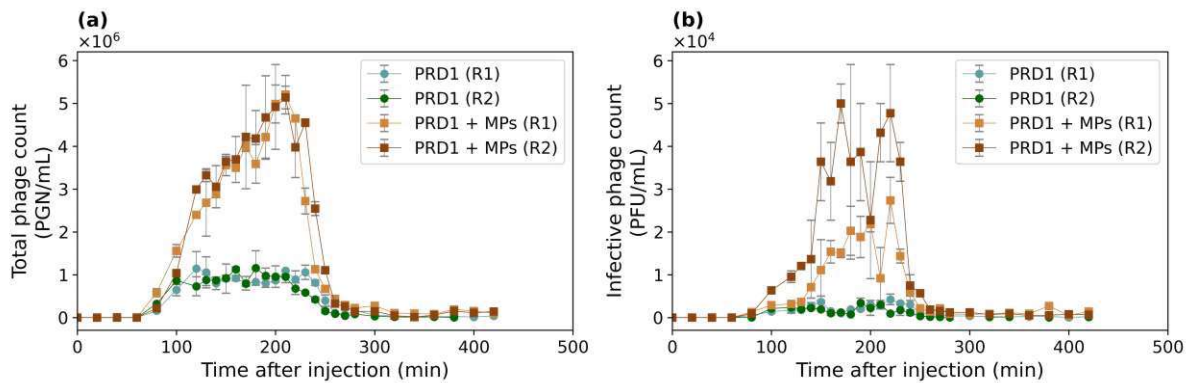


Figure 13 Virus concentration in effluent solution

Observed virus concentrations of (a) total PRD1 and (b) infective PRD1 phages plotted over time with and without MPs. Error bars represent standard deviation from replicate column experiments (≥ 2). R1 and R2 refer to experimental run 1 and 2, respectively. Experiments were conducted at ambient temperature (22 °C) and flow velocity = 2.45 m/day.

Figure 14a illustrates the breakthrough of a conservative tracer (NaBr) and the shape of the curve (two peaks) shows that the porous material is heterogeneous, with strong preferential flow paths. The early and sharp rise of NaBr (first peak) represents the extremely rapid movement of water and solute through the macropores. A second NaBr peak occurred after approximately 82 minutes due to the breakthrough of solute from the matrix material. **Figure 14b** demonstrates the reciprocal effect of PRD1 phages on the breakthrough of microplastics, showing that the presence of PRD1 slightly enhances microplastic transport. This enhancement is evident from the slightly higher breakthrough and the observed delay in the microplastic peak and is possibly due to the breakthrough of microplastics from the matrix material (slower flow region).

The experimental (observed) breakthrough curves for total PRD1 (**Figure 14c-d**), revealed that the peak C_{\max}/C_0 values of PRD1 were 0.97×10^{-3} and 0.91×10^{-3} (without MPs) and 1.84×10^{-3} and 3.34×10^{-3} (with MPs). The maximum effluent recovery of total PRD1 was remarkably enhanced in the presence of microplastics, increasing from 0.1% and 0.09% to 0.18% and 0.33%, respectively. When transported alone, PRD1 exhibited relatively constant (flat) breakthrough curves, and the maximum breakthrough of PRD1 alone was reduced, due to high attachment in the absence of the microplastics. On the other hand, the breakthrough of total PRD1 (with MPs) showed that the time to peak breakthrough was retarded (increasing breakthrough with time). This is possibly due to the heterogeneity of the quartz sand and virus transport occurring through the matrix (slower-moving water zones) which can also be

observed from the NaBr tracer breakthrough curve (**Figure 14a**). Another explanation is that the presence of microplastics can alter the available number of deposition sites in quartz sand for PRD1 phage attachment, thereby enhancing their transport as ideal attachment sites become filled (a phenomenon known as blocking) and competition for adsorption sites increases (Pelley and Tufenkji, 2008). However, it is unlikely that this observed increasing breakthrough with time is due to blocking, as the infective phages do not mimic this pattern. Whether this effect is due to blocking or not, the initial breakthrough of PRD1 with microplastics is clearly higher than PRD1 alone.

Examination of the breakthrough curves for infective PRD1 (**Figure 14e-f**) indicates that the peak C_{\max}/C_0 values for infective PRD1 phages were 1.53×10^{-3} and 1.93×10^{-3} (without MPs) and 2.01×10^{-3} and 7.14×10^{-3} (with MPs). The effluent recovery of infective PRD1 was 0.15% and 0.19% (without MPs), compared to 0.20% and 0.71% (with MPs). The relative concentration values of infective PRD1 are higher compared to the total PRD1 because the initial concentration (C_0) of infective phages is much lower. The presence of microplastics enhanced the recovery of infective PRD1 in the effluent solution, just like it facilitated the transport of total phages. No blocking or retardation was observed for infective PRD1 phages. Most likely, the dual porosity of the heterogeneous quartz sand allowed infective phages to travel through various pore systems at different velocities, resulting in two breakthrough peaks. These observations demonstrate that the coexistence of microplastics affects virus (both total and infective) transport and enhances the mobility of viruses in saturated porous media.

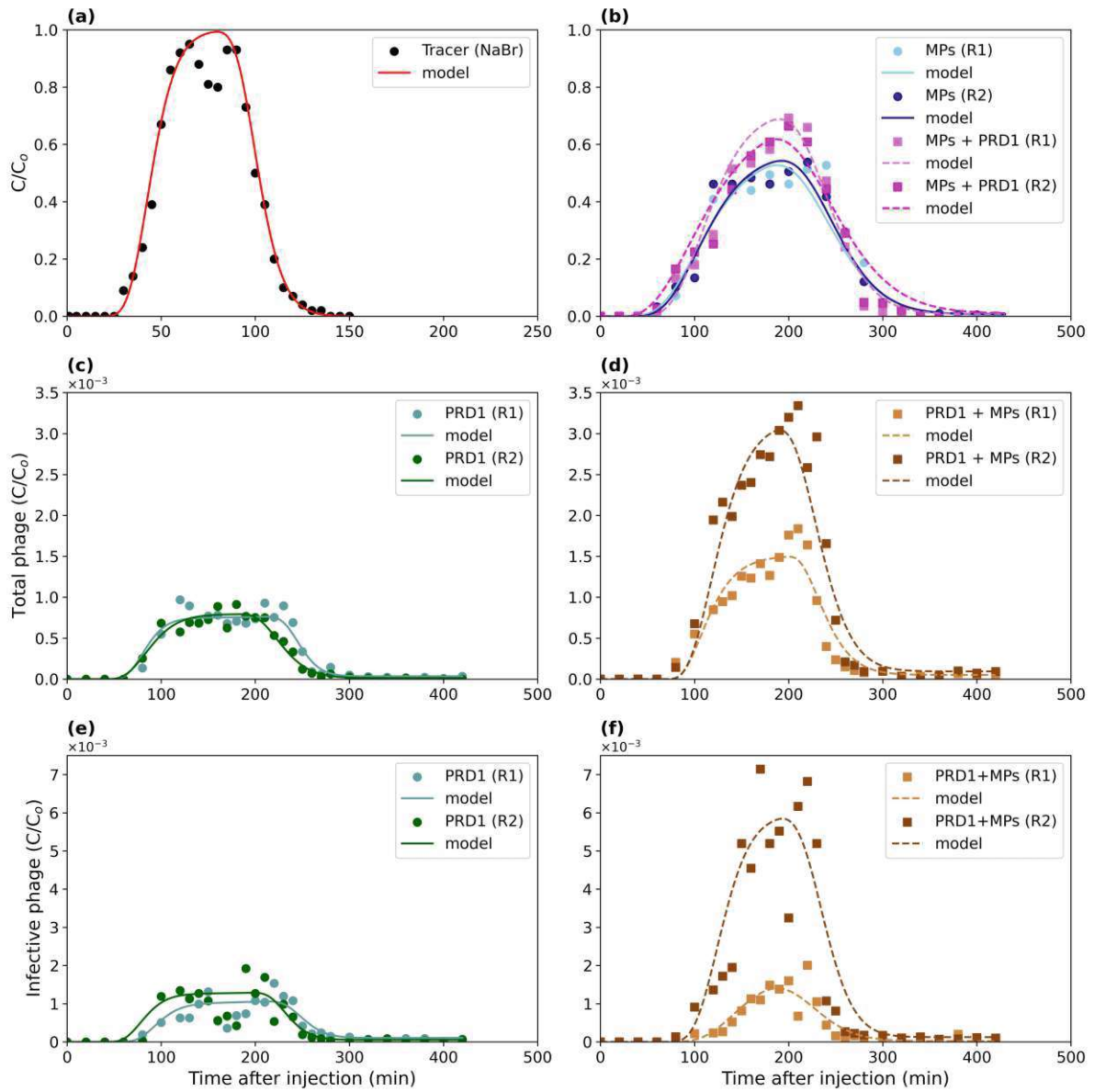


Figure 14 Observed and modeled breakthrough curves

Experimental and Hydrus 1D modeled (attachment/detachment) breakthrough curves (BTCs). (a) NaBr tracer, (b) MPs with and without virus transport scenario. Total PRD1 phage BTCs: (c) without MPs and (d) with MPs, measured via qPCR. Infective PRD1 phage BTCs: (e) without MPs and (f) with MPs, measured using plaque assay method. R1 and R2 refer to experimental runs 1 and 2, respectively. Scattered points represent observed experimental data, while solid and dashed lines indicate modeled data. C/C_0 is the effluent concentration normalized by the influent concentration.

Furthermore, to gain a deeper understanding about the attachment and detachment processes and to comprehensively characterize the transport of total and infective PRD1 in the porous media, HYDRUS-1D was used to simulate breakthrough curves (**Figure 14**). Two attachment

and detachment rate coefficients were necessary for accurately modeling the BTCs observed in the experiments (Table 3). When transported alone, both total and infective PRD1 demonstrate a higher degree of attachment, as evidenced by their elevated primary attachment rate coefficients ($k_{a1} = 0.18$ and 0.17 min^{-1}) and their smaller size resulted in higher relative dispersivity ($\lambda = 0.60 \text{ cm}$). However, when co-transported with microplastics, both total and infective PRD1 show reduced primary attachment rate coefficients ($k_{a1} = 0.12$ and 0.11 min^{-1}) and lower dispersivity ($\lambda = 0.33 \text{ cm}$), due to the larger size of the aggregates. This is to be expected as larger colloids have lower dispersivity, since smaller colloids can access smaller pore spaces. In the absence of microplastics, high attachment of PRD1 could be attributed to the smaller size of the viruses accessing the smaller dead-end pores and the less negative charge causing more attachment to the negative porous media. However, the modeled BTCs for microplastics, both with and without PRD1 phages, exhibit almost similar λ , k_{a2} , and k_{d2} values (Table 3), indicating a minimal impact of viruses on the transport of microplastics.

Generally, when two different contaminants co-exist, the one with higher mobility can act as a vehicle and facilitate the transport of the other contaminant with relatively lower mobility in the porous media (Abdel-Fattah et al., 2013; Li et al., 2019a; Peng et al., 2017), a phenomenon that can be referred to as "hitchhiking" (Kirstein et al., 2016). Consistent to the findings of this work, studies indicate that microplastics not only serve as carriers for pathogens (Gao et al., 2021; He et al., 2021; Yan et al., 2020), but also for heavy metals (Cu and Pb), enhancing their mobility in aquifers (Duan et al., 2021; Purwiyanto et al., 2020; Wang et al., 2022a). Enhanced transport could be observed due to blocking of ideal transport sites by other colloids, but the $10^7/\text{mL}$ influent concentrations of microplastics should be insignificant compared to the $10^9/\text{mL}$ influent concentrations of PRD1 (Camesano et al., 1999; Pelley and Tufenkji, 2008), although the relative size is larger. Furthermore, the size aspect must be taken into account and the co-transport of microplastics and viruses in porous media is also possibly governed by straining processes (Zhang et al., 2022b). The ratio of PRD1 phage to median grain size ($d_p/d_{50} = 0.00007$) is less than 0.0017, indicating that straining is not expected to occur (Bradford et al., 2002). Similarly, the ratio of PRD1-MP aggregate (assuming the $1 \mu\text{m}$ diameter of the MPs) to median grain size is 0.00105, which also falls below the threshold ratio. Additionally, when transported alone, PRD1 could deposit in immobile zones, like grain junctions, small pores, and/or pore constrictions causing higher removal (Bradford et al., 2002), which they would not be able to access if attached to the microplastics. For these reasons, the removal of PRD1 in this study is assumed to be governed by electrostatic interactions causing attachment, as well

as removal in small pore spaces and immobile zones, when transported alone. The transport of microplastics (with or without PRD1) is much higher than PRD1, probably due to the enhanced mobility in coarse sand ($d_{50} = 0.95$ mm) of larger colloids, as mentioned above, as well as the stronger negative charge.

Table 3: Overview of CFT and Hydrus modeled parameters

Summary and comparison of collision coefficients and the calculated and modeled parameters using HYDRUS-1D for PRD1 phage with and without microplastics: contact efficiency (η_0), attachment efficiency (α), dispersivity (D), attachment rate coefficients at primary and secondary sorption sites (k_{a1} and k_{a2}), detachment rate coefficients at secondary sorption sites (k_{d2}). C/C_0 , for CFT calculations, is maximum effluent concentration/influent concentration.

Experimental Scenario	Run	C/C_0	η_0	α	D (cm)	k_{a1} (min^{-1})	k_{a2} (min^{-1})	k_{d2} (min^{-1})	R^2
Total Phages									
PRD1	A1	7.62×10^{-4}	0.046	0.58	0.60	0.18	0.31	0.40	0.93
	A2	7.92×10^{-4}							0.20
PRD1 with MPs	B1	1.50×10^{-3}	0.006	0.23	0.33	0.12	0.07	0.13	0.92
	B2	3.04×10^{-3}							0.14
Infective Phages									
PRD1	A1	1.06×10^{-3}	0.046	0.55	0.60	0.17	0.25	0.30	0.72
	A2	1.29×10^{-3}							0.22
PRD1 with MPs	B1	1.40×10^{-3}	0.046	0.23	0.33	0.11	0.28	0.20	0.80
	B2	5.84×10^{-3}							0.26
Microplastics									
MPs	C1	5.27×10^{-1}	0.006	0.40	0.40	0.012	0.18	0.12	0.94
	C2	5.43×10^{-1}							0.38
MPs with PRD1	B1	6.88×10^{-1}	0.006	0.23	0.40	0.005	0.13	0.16	0.96
	B2	6.18×10^{-1}							0.30

3.3.5 Virus removal in porous media

Colloid filtration theory (CFT) was also applied to compare the removal of total and infective PRD1 in the porous media (**Table 3**). Calculations for the MP-PRD1 aggregate assumed that the physical characteristics of the MP size and density dominate. The single-collector contact efficiency η_0 (ratio of the rate at which colloids collide with the porous media to the rate at which colloids flow) of both total and infective PRD1 is 0.046, whereas, for the MP-PRD1 aggregate it is 0.006. High values of η_0 indicate PRD1 are expected to experience more collisions with the quartz sand surface in comparison to MP-PRD1 aggregates. The attachment efficiency α (the number of successful contacts resulting in attachment divided by the total number of collisions), is found to be high for PRD1 (total: 0.58, infective: 0.55). For MP-PRD1 co-transport, α is further reduced (0.23 and 0.30 for both total and infective phages). Theoretically, large values of α for PRD1 suggest higher removal by attachment, which is in agreement with the experimental BTCs (**Figure 14c-f**).

The calculation of single-collector contact efficiency took into account aspect ratio (N_R) and van der Waals forces (N_{vdw}). The MP-PRD1 aggregates had a high aspect ratio (**Table B2, Appendix B**) compared to PRD1 alone, but retention did not necessarily increase with increasing aspect ratio (Liu et al., 2010). Similarly, high van der Waals forces indicate a strong attraction between the MP-PRD1 aggregates and quartz sand, which would typically promote their retention (**Table B2, Appendix B**). However, experimental breakthrough data showed less removal of these aggregates suggesting that, rather than van der Waals forces alone, electrostatic interactions (Lu et al., 2022) and hydrophobic effects (Dika et al., 2015) played a dominant role in influencing the interactions between microplastics and viruses. These factors have likely reduced the overall attachment between the aggregates and quartz sand. Moreover, PRD1 exhibited greater Brownian diffusion as compared to the MP-PRD1 aggregates (**Table B2, Appendix B**), implying more removal by attachment, which is also evident by the higher attachment efficiency (**Table 3**). Several studies identified 60 nm as the critical diameter below which virus transport can occur over significantly longer distances, and removal is mainly due to electrostatic interactions (Cao et al., 2010; Chrysikopoulos et al., 2010; Dowd and Pillai, 1997; Walshe et al., 2010). At 62 nm, the size of PRD1 sits right on the cusp of this threshold, however, it seems that in the present study, electrostatic interactions were dominant.

3.3.6 Environmental implications

The potential for microplastics to serve as vectors for virus transmission in the environment remains unclear and is a matter of ongoing scientific discussion (Li et al., 2022; Lu et al., 2022; Moresco et al., 2022; Wang et al., 2024). The co-transport experiments in quartz sand clearly demonstrate that microplastics enhanced the transport of viruses in porous media and, therefore, could pose greater health risks. The long lifespan, low density, and hydrophobic nature of microplastics allow them to accumulate various organic and inorganic compounds, potentially serving as nutrient sources for diverse microbes, including plant pathogens. This raises concerns about their potential role in enhancing transmission of viruses in various environmental settings. Moreover, the widespread presence of microplastics and viruses together in wastewater and sludge (Gholipour et al., 2022), along with their current application of improving agricultural soil properties for high crop yields (Dhanker et al., 2021), raises substantial concerns about their potential to transport pathogens to shallow groundwater aquifers. More importantly, the accumulation of microplastic-virus aggregates in porous media can further be amplified due to recurrent irrigation and surface runoff. Therefore, the enhanced transport of viruses in the presence of microplastics in saturated porous media could play a significant role in waterborne viral infections and outbreaks (Gerba et al., 1996; Murphy et al., 2017), particularly in groundwater systems where microplastics and viral contamination co-exist.

3.4 Conclusions

The present work represents a pioneering effort to study the influence of microplastics on the interactions and transport dynamics of both total and infective viruses within saturated quartz sand. Research findings validate the efficacy of qPCR and plaque assay enumeration techniques for quantifying viruses in the presence of microplastics. This study provides compelling evidence that microplastics could play a critical role in facilitating virus transport through porous media. On the other hand, interactions between infective viruses and microplastics can cause virus inactivation and may reduce their persistence in the environment. The co-transport of microplastics and viruses is an emerging concern, requiring further research in natural aquifer materials, in order to assess the extent of potential groundwater contamination and subsequent health risks.

Chapter 4 Fate and transport of fragmented and spherical microplastics in saturated gravel and quartz sand

Abstract

Microplastics in urban runoff undergo rapid fragmentation and accumulate in the soil, potentially endangering shallow groundwater. To improve the understanding of microplastic transport in groundwater, column experiments were performed to compare the transport behavior of fragmented (FMPs ~1 μm diameter) and spherical (SMPs ~1, 10, and 20 μm diameter) microplastics in natural gravel (medium and fine) and quartz sand (coarse and medium). Polystyrene microspheres were physically abraded with glass beads to mimic the rapid fragmentation process. The experiments were conducted at a constant flow rate of 1.50 meter day⁻¹ by injecting two pore volumes of SMPs and FMPs. Key findings indicate that SMPs showed higher breakthrough, compared to FMPs in natural gravel, possibly due to size exclusion of the larger SMPs. Interestingly, FMPs exhibited higher breakthrough in quartz sand, likely due to tumbling and their tendency to align with flow paths, while both sizes (larger and smaller relative to FMPs) of SMPs exhibited higher removal in quartz sand. Therefore, an effect due to shape and size was observed.

4.1 Introduction

Plastics are undoubtedly a marvel of the modern era, which have benefited society across many sectors and outpaced almost any other material with a global annual production of 368 million metric tonnes (da Costa et al., 2020). Improper handling and disposal of plastics in the environment lead to various degradation processes including mechanical abrasion, in-situ weathering, ultraviolet (UV) induced degradation, photo-degradation, bio-degradation, oxidative degradation, and hydrolysis (Andrady, 2011; Cai et al., 2018; Fournier et al., 2021; Mendoza and Balcer, 2019; Ren et al., 2020; Song et al., 2017), ultimately resulting in the formation of microplastic particles smaller than 5 mm (Thompson et al., 2004). The European Commission defines microplastics as ranging in size from 0.1 μm to 5 mm and can be found in

various forms such as filaments, fragments, spheres, and foams (Mendoza and Balcer, 2019). Microplastics are also released directly into the environment due to anthropogenic activities (Rochman, 2018); the main sources being cosmetic products (Habib et al., 2020), wastewater effluent and sludge (Edo et al., 2020; Kosuth et al., 2018), apparel and home textiles (Belzagui et al., 2019; Henry et al., 2019), abrasion of vehicle tires (Knight et al., 2020; Luo et al., 2021) and paint fragments generated from boats and ships, road markings and buildings (Gaylarde et al., 2021; Turner, 2021). Over the past few years, there has been increasing concern regarding the widespread presence and distribution of microplastics (Kershaw and Rochman, 2015; Marsden et al., 2019) across various environments, including marine habitats, rivers, surface runoff, lakes, groundwater, sediments, soil, glaciers, and in such isolated places as Arctic and Antarctic regions (Aves et al., 2022; Cha et al., 2023; Chia et al., 2021; Koutnik et al., 2021; Miranda et al., 2020; Wu et al., 2019).

Microplastics, often referred to as colloidal contaminants, can quickly migrate in the environment, posing ecological and health risks (Flury and Aramrak, 2017; Liu et al., 2021b; Molnar et al., 2015; Senathirajah et al., 2021). Due to their small size and altered surface properties, they can act as carriers for contaminants (Cortés-Arriagada, 2021; Liu et al., 2019). As microplastics age, their physical and chemical properties can change, making their fate more unpredictable (Luo et al., 2020). Physical fragmentation, the breaking down of microplastics into smaller pieces, is an important aging mechanism that is often overlooked. Microplastics that accumulate in urban stormwater runoff experience physical aging due to mechanical abrasion, as stormwater runoff contains a mixture of precipitation, suspended sediment, natural and anthropogenic debris, and chemical pollutants (Gilbreath and McKee, 2015; McKee and Gilbreath, 2015; Werbowski et al., 2021).

Microplastics that accumulate from surface and urban stormwater runoff have the potential to move downwards into the subsurface through infiltration enhanced by rainfall and natural freeze-thaw cycles (Koutnik et al., 2022a; Koutnik et al., 2022b; Li et al., 2023). Although groundwater is a critical resource for many regions of the world, the presence of microplastics in groundwater has been neglected as a potential risk, due to the assumption that soil serves as an effective barrier against microplastic contamination (Alimi et al., 2018; Goepfert and Goldscheider, 2021; Panno et al., 2019; Re, 2019; Samandra et al., 2022). On the contrary, O'Connor et al. (2019) argued that soil is not only a microplastic sink but a viable route to deeper soils and groundwater. Goepfert and Goldscheider (2021) have experimentally

demonstrated the transport of microplastics up to a distance of 200 meters (in the groundwater flow direction) in an alluvial aquifer. Samandra et al. (2022) also identified the presence of eight most commonly found microplastics, ranging in size from 18 to 491 μm , within an unconfined alluvial aquifer in Australia. Mintenig et al. (2019a) analyzed groundwater and drinking water samples for the presence of microplastics (50 to 150 μm) and found polyethylene, polyamide, polyester, polyvinylchloride and epoxy resin. Susceptible to pollution from surface runoff due to fracture networks and preferential flow, karst groundwater systems are especially at risk (Panno et al., 2019).

Several factors such as microplastic shape and size, porous media properties, and groundwater chemistry influence the transport of microplastics in the subsurface environment (Hou et al., 2020). Koutnik et al. (2021) found that only 20% of global research on microplastics considers particles smaller than 20 μm , which are more likely to be transported to groundwater. Nonetheless, the potential impact of these smaller particles (diameter $< 20 \mu\text{m}$) is likely underestimated. A limited number of studies have investigated microplastics at the micron level even though most fragmented particles found in soil environments are micron-sized (Hou et al., 2020). It is generally agreed upon that larger microplastics have less mobility in saturated porous environments, as they are likely to get filtered out by the pore structure in aquifer material (Dong et al., 2018). The most recent research demonstrates that smaller microplastics have increased vertical transport in porous media, and also the morphology of microplastics can play a critical role in attachment and detachment within the subsurface environment (Dong et al., 2021; Dong et al., 2022; Hou et al., 2020; O'Connor et al., 2019; Rillig et al., 2017; Waldschläger and Schüttrumpf, 2020). The aquifer material characteristics also play a significant role in the transport of microplastics. Coarse-grained porous media promote the transport of microplastics due to their larger pores and preferential flow paths (Hou et al., 2020). Recently, the focus has been directed towards studying the transport of microplastics in groundwater, but limited to investigating uniform-shaped microspheres, while in nature, most microplastics found are fragmented and irregular in shape (He et al., 2020; He et al., 2019; Hitchcock, 2020; Piñon-Colin et al., 2020). Despite this, the impact of various parameters (e.g. fragmentation, size, shape etc.) on the transport of microplastics in different aquifer materials has not yet been extensively studied.

The present study aims to understand and investigate the transport behavior of spherical (SMPs) and fragmented (FMPs) microplastics in two different sizes of gravel and quartz sand.

Polystyrene microspheres were chosen to replicate the impact of fragmentation on microplastics within an urban environment. The reason for using polystyrene is due to its abundance in the natural environment, low weathering, and heat resistance (Alimi et al., 2018). These microspheres have a density ranging from 1.04–1.11 gram cm⁻³ and can exist as submerged or floating in the aquatic environment (Duis and Coors, 2016). The present research focused on the rapid physical breakdown of 10 and 20 µm microplastics through mechanical abrasion, resulting in a random size distribution (approx. average diameter ~1 µm). In gravel, 20 µm SMPs are compared to 1.60 and 1.80 µm FMPs, whereas in quartz sand 10 µm SMPs are compared to 1.20 and 1.40 µm FMPs. Also, 1.40 µm FMPs were compared to their corresponding similar sized SMPs (1 µm) in coarse quartz sand, for a better understanding of the role of shape and size during subsurface transport.

4.2 Materials and methods

4.2.1 Preparations of microplastics

Commercially available plain polystyrene yellow-green fluorescent microspheres were used in the column transport experiments: 1, 10, and 20 µm (Fluoresbrite® YG Microspheres, Polysciences Inc., Warrington, PA, USA). The major benefit of using these microspheres for laboratory experiments is the ease with which they are detected by solid-phase cytometry and epifluorescence applications due to their strong fluorescent intensity and emission/excitation spectra (Stevenson et al., 2014). To mimic irregular-shaped microplastics present in the terrestrial environment, 10 and 20 µm polystyrene microspheres were physically fragmented through a mechanical abrasion process, based on the method developed by Ranhand (1974). To achieve rapid and reproducible fragmentation, 1 mL of the microsphere stock solution was mixed with 1 gram of glass beads (1 mm diameter) in a FastPrep-24™ Classic homogenizer (MP Biomedicals, Eschwege, Germany). To ensure consistent fragmented particle size, a controlled constant mixing speed (impact velocity) of 20 revolutions per minute was applied to provide consistent impact force between the microspheres and the glass beads. The abrasion process was conducted for a duration of 10-15 minutes. This time duration was chosen based on trials to achieve the target FMP size range of approximately 1 µm. The abrasion time was varied depending on the microsphere size: 10 minutes for 10 µm and 15 minutes for 20 µm microspheres. The mixing time for 20 µm microspheres was extended due to the Zetasizer measurement limit of 10 µm. The fragmented particles were extracted from the solution, using

a pipette, after the heavier glass beads were allowed to settle. For the characterization of microplastics, the zeta potential and mean diameter (**Table C1, Appendix C**) were measured with a Zetasizer Pro ZSU3200 (Malvern, Worcestershire, UK). Each measurement was repeated using at least three different samples.

4.2.2 Properties of influent water

The influent water used for the column experiments was standard Viennese tap water, sourced from an Alpine karstic spring. In this study, tap water offered several advantages over local groundwater, exhibiting lower electrical conductivity, reduced levels of iron and sulfate, and being free from emerging contaminants (Oudega et al., 2021). Also, tap water is of a consistent quality (**Table B1, Appendix B**) and is readily available in large volumes, making it an ideal choice for maintaining controlled conditions during experiments. Furthermore, the use of tap water provided a more realistic simulation of microplastic fate in the natural environment, enabling accurate determination of critical transport parameters like attachment, detachment, and dispersion coefficients within different porous media.

Throughout the column experiments, from injection to effluent collection, the pH, temperature, and electrical conductivity remained stable. Zhao et al. (2024) found that many water quality parameters are poorly correlated with the microplastics in an urban drinking water source. Also, studies in freshwater ecosystems suggest total dissolved solids and electrical conductivity have a minimal influence on microplastic aggregation. While pH, temperature, total suspended solids, and dissolved oxygen have a significant impact (Buwono et al., 2021; Khoironi et al., 2023; Rakib et al., 2023; Zhao et al., 2024).

4.2.3 Tracer preparation and analysis

A solution of sodium bromide (1 mM L^{-1} , 102.89 mg L^{-1}) prepared in tap water served as a conservative tracer to investigate the transport properties of the packed columns. The bromide concentration and electrical conductivity (EC) of the injected tracer were measured by a flow-through cell (WTW TetraCon 325) and a hand-held portable EC meter (WTW ProfiLine Cond 3310, Xylem Analytics Weilheim, Germany).

4.2.4 Porous media

Four different soil materials were used as porous media to study the transport behavior of microplastics. Natural aquifer material was extracted from a borehole depth of 5 to 6 m below the ground surface, at a site southeast of Vienna, Austria, and the portions held back on the 8 and 4 mm sieves were used for the “medium gravel” and “fine gravel” columns, respectively

(both with a bulk density of $1.52 \text{ gram cm}^{-3}$). The median grain diameters (d_{50}) values of 4 and 8 mm for medium and fine gravel respectively. Similarly, two types of quartz sand (grain size: 0.6–1.3 and 0.4–0.8 mm, bulk density: 2.65 g cm^{-3}) were purchased for the “coarse quartz” and “medium quartz” sand column experiments (Carl Roth GmbH + Co. KG, Karlsruhe, Germany). The median grain diameters (d_{50}) of 0.95 and 0.60 mm for coarse and medium quartz respectively. Based on the standard gravimetric method, the porosity of the porous media was calculated by measuring the volume of water needed to saturate the dry soil used to pack the column, divided by the total column volume (**Table C1, Appendix C**).

4.2.5 Column experiments

Transport experiments were conducted under saturated flow conditions using Plexiglas columns (70 mm inner diameter and 300 mm length). For quartz sand experiments, the column diameters met the minimum d_{col}/d_{50} ratio (the ratio of the column diameter to the media effective particle diameter) that was much higher than the recommended value of 50, to ensure minimal potential wall effects in the column (Knappett et al., 2008). Although the d_{col}/d_{50} ratio in the gravel experiments was below 50, the symmetrical shapes of both the tracer and microplastic breakthrough curves resemble those observed with quartz sand, suggesting negligible wall effects (**Figure C1, Appendix C**). Stainless steel-mesh screens (Spectrum Labs, New Brunswick, USA) were placed on both ends of the column to prevent the loss of porous media and the caps were threaded to tighten against the outside of the column. A rubber O-ring was embedded in the column end to create a tight seal. All tubings were made of Teflon. To ensure homogeneous packing and minimize air entrapment, the column was filled with the porous media in 2 cm increments while gently stirring with a small steel rod. This careful filling procedure ensured uniform flow throughout the column, as evidenced by the good recovery rates of the tracer (NaBr) and the nearly identical, symmetrical breakthrough curves with minimal tailing (**Figure C1, Appendix C**), as expected for a homogeneously packed soil column (Sobotkova and Snehota, 2014). The pore volume (PV) for the influent solution was calculated by the product of porosity and the volume of the column. Before the experiment, the columns were flushed for a minimum of 20 PV with tap water. The influent microplastics concentration (**Table 4**) was prepared by mixing 1 mL of microplastics stock solution (spherical or fragmented) and two pore volumes of tap water. To preclude the possibility of ripening or blocking, relatively low microplastic concentrations (approx. $10^4 \text{ particles mL}^{-1}$) were introduced in the influent suspension solution, which was pumped in an upward direction at a constant flow rate of 4 mL min^{-1} (Darcy velocity = $1.5 \text{ meter day}^{-1}$). Afterward, the columns

were flushed with 5 PV of tap water, at the same flow rate. A magnetic stirrer was used to stir the suspension constantly during the experiments to ensure that microplastics were evenly dispersed in the influent. A fraction collector (CF2 Fraction Collector, Spectrum Chromatography, Texas, USA) automatically collected column effluent sample in a 15 mL test tube every 5 minutes. All column tests were done with at least two replicates (each column freshly packed).

4.2.6 Microplastic enumeration

The enumeration of FMPs and SMPs in the effluent solution was carried out by Solid-Phase Cytometer (SPC) using the ChemScan™ RDI (Biomérieux, Craponne, France). The SPC system has been used in the past mainly for the detection of colloids in environmental samples (Baudart et al., 2002; Mignon-Godefroy et al., 1997; Schauer et al., 2012). Stevenson et al. (2014) used this simple and efficient method for enumerating microspheres in natural water samples. Details on the SPC system and the enumeration process are described by Mignon-Godefroy et al. (1997). The following section provides a comprehensive explanation of the microplastic enumeration procedure.

- a) Filtration: 1 mL of effluent solution was filtered onto a 25 mm black polyester 0.4 μm pore size filters (AES Chemunex, bioMérieux, Marcy l'Étoile, France) using a Multifold Vacuum Filtration Device (Pall, Port Washington, NY). The black polyester filter was then carefully placed on a support pad (AES Chemunex, bioMérieux, Marcy l'Étoile, France), which was already saturated with 100 μL of phosphate-buffered saline to hold the filter in place.
- b) Automated enumeration with SPC: The filter was placed on the ChemScan™ RDI sample holder, and the scan was initiated. An argon laser (488 nm emission wavelength) scanned the entire 25 mm filter area in 3 to 5 minutes. Microplastic particles (referred to as fluorescent events) were distinguished from other background interferences based on their fluorescence intensity (500 – 530 nm wavelength with the green channel) and then counted. Following a complete scan, the system generates raw data and result maps based on discriminant settings, highlighting fluorescent events. These maps mark the exact location of each microplastic on the filter. Subsequently, these microplastics were visually examined and confirmed using a microscope equipped with a motorized stage. The most important discriminant parameters are the number of “lines” and the number of “samples” for the shape and the peak intensity of the signal. The ratio of the fluorescent light detected in the

secondary channel (fluorescence from microplastics) to the fluorescent light detected in the primary channel (fluorescence from the probe) is another important discriminant parameter and is referred to as the S/P ratio. The discriminant settings were set as follows: number of “lines,” 1 to 50; number of “samples,” 1 to 250; peak intensity, 250 to 65536; and S/P ratio, 0 to 0.898 (Table C2, Appendix C).

- c) Validation of counted microplastics: The verification of microplastics was achieved through a visual inspection by a Nikon Eclipse 80i epifluorescence microscope directly connected to the ChemScan™ RDI system. The microscope employs a 100x magnification objective, resulting in a final magnification of 1000x for detailed analysis of each fluorescent particle identified by the laser scan. The microscope is equipped with an automatic stage that can be driven by the user such that the whole filtration area can be scanned. Up to 250 events were validated per filter, with a ratio being used if above, and all events were validated when enumeration results were less than 250. For each effluent sample, a minimum of three replicates was analyzed.

4.3 Theoretical considerations

4.3.1 Filtration efficiency

The transport and deposition behavior of the microplastics (SMPs and FMPs) in the saturated porous media was quantified using colloid filtration theory (CFT), which calculates the attachment (collision) efficiency (α). The attachment efficiency represents the fraction of collisions (contacts) between suspended microplastic particles and collector sand grains that result in successful attachment (Elimelech and O'Melia, 1990). It is common to use column experiments to determine the attachment efficiency for given physicochemical conditions. The collision efficiency was computed using the following equation by Tufenkji and Elimelech (2004a):

$$\alpha = -\frac{2}{3} \frac{d}{(1-\theta)x\eta_0} \ln \frac{C}{C_0} \quad (4.1)$$

where d is the mean soil grain size (mm), θ is the porosity, x is the column length (cm), C/C_0 is the normalized steady-state breakthrough microplastic concentration (particles mL⁻¹), and η_0 is the predicted single-collector contact efficiency and can be computed using the following equation (Tufenkji and Elimelech, 2004a):

$$\eta_0 = \eta_D + \eta_I + \eta_G \quad (4.2)$$

where η_0 is the overall contact efficiency between microplastics and soil grain and is dependent on hydrodynamic interactions, van der Waals, and gravitational forces. η_D is the contact due to Brownian force (diffusion), η_I is the contact due to interception, and η_G is the contact due to gravity (settling). Equation 4.2 relies on additional equations and parameters outlined in **Table C3 (Appendix C)**. The respective contribution of different filtration mechanisms was computed by dividing the individual contact efficiency by the total contact efficiency (i.e. diffusion: η_D/η_0 , interception: η_I/η_0 , gravitation: η_G/η_0). The calculations governing microplastic filtration and their respective contributions in different soils are provided in **Table C4 (Appendix C)**. The removal efficiency (η) is computed using the following equation (Tufenkji and Elimelech, 2004a):

$$\eta = \eta_0 \times \alpha \quad (4.3)$$

4.3.2 Transport modeling

The breakthrough curves (BTCs) of the microplastics (SMPs and FMPs) were modeled using the HYDRUS-1D computer software package (Simunek et al., 2013). HYDRUS-1D is a widely used finite-element model that can simulate the movement of water and particle-like solutes in both saturated and unsaturated porous media (Simunek et al., 2016). Several studies have already simulated the transport of microplastics in saturated gravel and quartz sand using HYDRUS-1D (Gui et al., 2022; Li et al., 2024b; Ren et al., 2021). In this study, the advection-dispersion equations were implemented in a numerical model using an attachment-detachment model comprised of the following equations:

$$\frac{\partial C}{\partial t} + \frac{\rho_b}{\theta} \frac{\partial S}{\partial t} = \lambda v \frac{\partial^2 C}{\partial x^2} - v \frac{\partial C}{\partial x} \quad (4.4)$$

$$\frac{\rho_b}{\theta} \frac{\partial S}{\partial t} = k_{att} C - \frac{\rho_b}{\theta} k_{det} S \quad (4.5)$$

where C is microplastics concentration (particles mL^{-1}), t is time (min), ρ_b is dry bulk density (gram cm^{-3}), S is microplastic concentration (particles mL^{-1}), D is dispersivity (cm), x is the distance along the flow path (cm), v is pore water velocity (cm min^{-1}), k_{att} is an attachment rate coefficient (min^{-1}), and k_{det} is a detachment rate coefficient (min^{-1}).

4.4 Results

4.4.1 Microplastic fragmentation

The fragmentation rate of a material is influenced by the number, mass, and impact velocity of colliding particles (Arnold and Hutchings, 1989). During the abrasion process, the impact velocity remained constant, but the abrasion time was varied (high for 20 μm SMPs), which increased the number of particle strikes and reduced the SMP diameter. The hardness of the particles also impacts the fragmentation rate. The glass beads used in this study were harder (>5000 HV) than the sand (1200 HV) and polystyrene (20 HV) (Barlet et al., 2015), resulting in high abrasion and significant particle size reduction (**Figure 15**).

Another key factor regarding the effectiveness of the fragmentation process is the microplastic shape. Visual observation showed the plowing impact of the glass beads on the smooth and regular surface of the microspheres, by displacing them to the side and causing a frontal impact. Perfect spherical particles (SMPs) now become rough and irregular in shape, after abrasion, and are broken down into smaller particles and debris (FMPs). Walley et al. (1987) found that at equal impact velocities, angular particles like sand caused more damage to polyethylene surfaces due to increased contact points. Although spherical glass beads were used in this study to simulate abrasion of microplastics, particles in the environment are often angular, which can significantly increase fragmentation and wear rates, potentially by a factor of 10 or more (Hutchings, 1992).

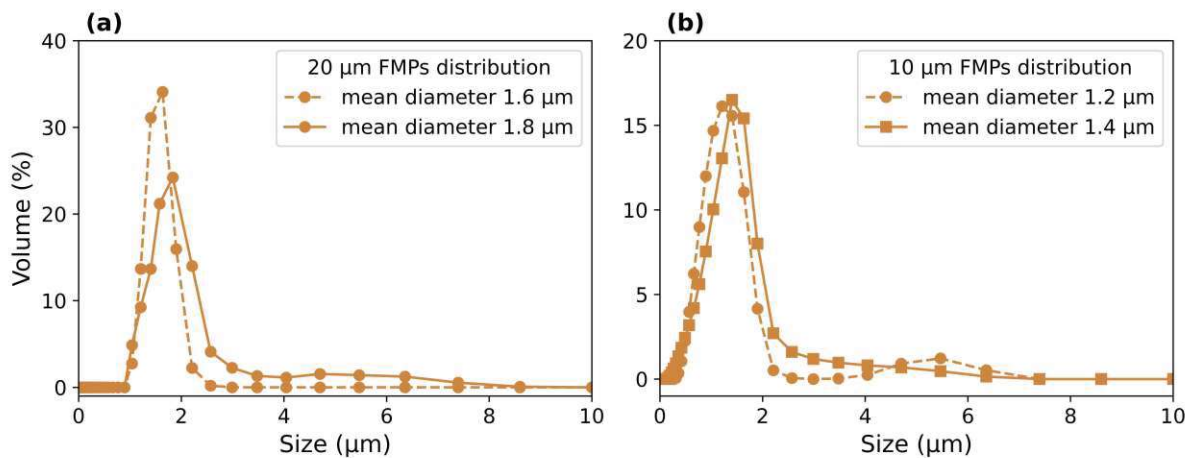


Figure 15 Particle size distribution of MPs after fragmentation

Particle size distribution of microplastics after going through an abrasion process. FMPs generated from 20 μm (a) and 10 μm (b). The mean diameter values are the volume-based distribution median.

4.4.2 Microplastic transport in natural gravel and quartz sand

The transport behavior of SMPs and FMPs was analyzed by comparing BTCs in two different grain size ranges and two textural classes each (natural gravel and quartz sand). In gravel, a higher removal of FMPs was observed, whereas in quartz sand, there was more removal of SMPs (**Figure 16**). In coarse gravel (8 mm), the percent mass recovery was 88–90% for SMPs and 74–76% for FMPs (**Figure 16a**). In fine gravel (4 mm), there was a decrease in mass recovery ranging from 72–74% for SMPs and 59–62% for FMPs (**Figure 16b**), indicating more FMP retention in gravel than for SMPs. The percent mass recovery of microplastics was further reduced in both quartz sands but, in contrast to the findings in the gravel experiment, more retention of SMPs compared to FMPs was observed (**Figure 16c-d**). In coarse quartz sand (0.6–1.3 mm), the mass recovery ranged from 12–14% for SMPs, whereas it was 30–31% for FMPs. A similar trend was observed in the medium quartz sand (0.4–0.8 mm), where the percent mass recovery was 5 to 6% for SMPs and 19 to 23% for FMPs.

Irrespective of the porous media, larger-sized SMPs (10 and 20 μm diameter) experienced straining (**Table C1, Appendix C**), defined by $d_p/d_{50} > 0.0017$ (Bradford et al., 2002). To characterize the SMPs and FMPs behavior in the porous media, BTCs were modeled using HYDRUS-1D (**Figure 16**). For gravel media, high values of dispersivity (D) and the detachment rate (k_{det}) highlight the importance of grain size and type of porous media (**Table 4**). The attachment rates (k_{att}) in medium and fine gravel were 0.0028 and 0.0060 cm^{-1} for FMPs, and 0.0012 and 0.0032 cm^{-1} , for SMPs respectively, indicating higher attachment of FMPs compared to SMPs, in gravel, which was also evident from the percent recovery results (mentioned above). In contrast, in coarse and medium quartz sand, the attachment rates were 0.0090 and 0.0136 cm^{-1} for FMPs, and 0.0182 and 0.0245 cm^{-1} for SMPs, respectively, indicating higher attachment of SMPs compared to FMPs, which is also in accordance with the percent recovery results.

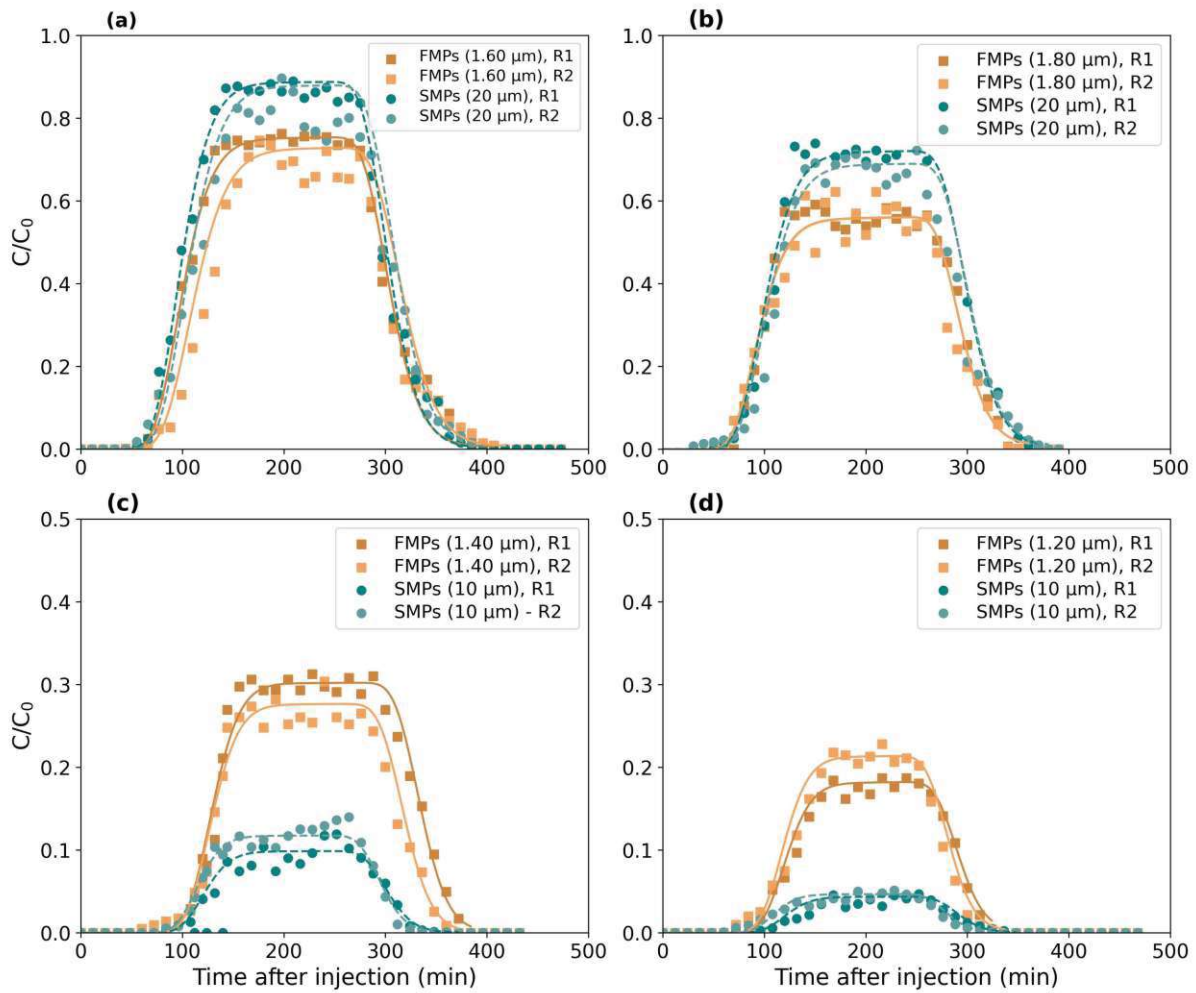


Figure 16 Breakthrough of SMPs and FMPs in different soils

Observed and simulated BTCs for SMPs and FMPs in four different materials (a: medium gravel 8 mm; b: fine gravel 4 mm; c: coarse quartz sand 0.6–1.3 mm; d: medium quartz sand 0.4–0.8 mm). Symbols represent experimental data, and the lines are the fitted breakthrough curves using HYDRUS-1D. SMPs = spherical microplastics (10 and 20 μm only), FMPs = fragmented microplastics. R1 and R2 are experimental runs 1 and 2 respectively. The column was packed with fresh material for each run. BTCs were plotted in the form of the normalized effluent concentration (C/C_0). Particle size distribution of microplastics after going through an abrasion process. FMPs generated from 20 μm (a) and 10 μm (b). The mean diameter values are the volume-based distribution median.

4.4.3 Effect of particle shape on microplastic transport

To investigate the role of particle shape during microplastic transport in the porous medium, column experiments were conducted using FMPs and SMPs with a similar average diameter of approximately 1 μm in saturated coarse quartz sand (experiments E1, E2, G1, and G2, **Table 4**). The FMPs were visually classified as asymmetrical with uneven and fractured surfaces. The average diameter of injected FMPs was 1.40 μm . The FMPs showed higher values of C_{max}/C_0 (**Table 4**), and higher values of percent mass recovery (31%), compared to SMPs (24.5%), indicating higher mobility (**Figure 17**).

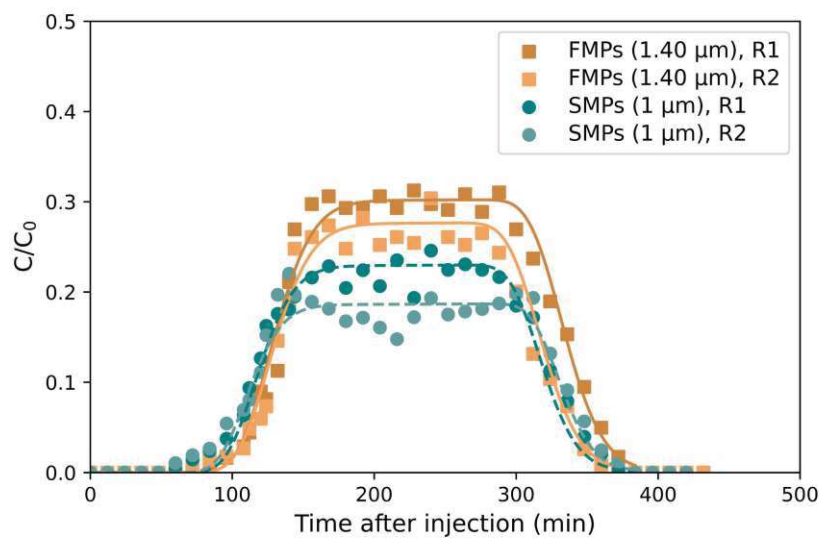


Figure 17 Comparison of 1 μm SMPs and FMPs in coarse quartz sand

Average values of observed breakthrough curves (BTCs) of FMPs and SMPs (both $\sim 1 \mu\text{m}$) in coarse quartz sand (0.6–1.3 mm). Symbols represent experimental data, and the lines are the fitted breakthrough curves using HYDRUS-1D. R1 and R2 are experimental runs 1 and 2, respectively. The column was packed with fresh material for each run. BTCs were plotted in the form of the normalized effluent concentration (C/C_0).

4.4.4 Filtration efficiency of microplastics

CFT was applied to better understand the filtration, retention, and transport of microplastics in different saturated aquifer materials. **Figure 18** shows the values based on averages of column test runs 1 and 2, each run being done in a freshly packed column. As shown in **Figure 18a**, the single-collector contact efficiency “ η_0 ” of SMPs ranged from 0.58 (medium gravel) to 0.49 (fine gravel), while FMPs exhibited lower values of 0.0051 to 0.0063, respectively. Whereas, in the case of coarse and medium quartz sand, η_0 ranged from 0.092 to 0.087 for SMPs and

0.0078 to 0.0096 for FMPs, respectively. High values of η_0 indicate that SMPs are expected to experience more collisions with the collector surface (**Figure 18a**).

As illustrated in **Figure 18b**, the attachment efficiency “ α ” of FMPs ranged from 1.62 (medium gravel) to 1.11 (fine gravel), whereas SMPs exhibited lower values of 0.006 and 0.009, respectively. This indicates a high removal rate of FMPs compared to SMPs through attachment in gravel (**Figure 18d**). However, the computed α values for FMPs are reduced to 0.54 (coarse quartz sand) and 0.38 (medium quartz sand), whereas SMPs exhibited increased values of 0.079 and 0.084, respectively (**Figure 18b**). Compared to gravel, the significantly higher α values of SMPs in both quartz sands result in a higher removal rate of SMPs by attachment (**Figure 18d**). Moreover, SMPs also experience straining phenomena in quartz sand (**Table C1, Appendix C**), leading to high removal rates despite having lower α values compared to FMPs. Since the colloid filtration theory does not apply to gravel porous media ($\alpha > 1$) and irregular colloids, a comparison of attachment rate coefficient k_{att} (min^{-1}) clearly showed high attachment of FMPs in gravel and high attachment of SMPs in quartz sand (**Figure 18c**). Furthermore, a comparison was made between the attachment efficiency of 1 μm -sized SMPs ($\alpha=0.60$) to similar-sized FMPs ($\alpha=0.54$) in coarse quartz sand (experiments E and G), which clearly showed high attachment of 1 μm -sized SMPs, which is consistent with the experimental data (**Figure 17**).

Figures 18e-f present a summary of the contribution of different filtration mechanisms (gravity settling, interception, and Brownian diffusion) to microplastic retention and transport in porous media. In medium and fine gravel, the retention of FMPs (1.60 and 1.80 μm diameter) was mostly influenced by settling (0.71 and 0.65 respectively) and, to a lesser degree, diffusion (0.29 and 0.34), while the behavior of the SMPs (20 μm diameter) is entirely controlled by settling. On the contrary, in coarse and medium sand, respectively, the filtration of FMPs (1.40 and 1.20 μm diameter) is influenced mostly by diffusion (0.73 and 0.85) and, to a lesser degree, settling (0.24 and 0.12), while the behavior of the SMPs (10 μm diameter) is almost entirely controlled by settling (0.95 and 0.90) and interception (0.04 and 0.08).

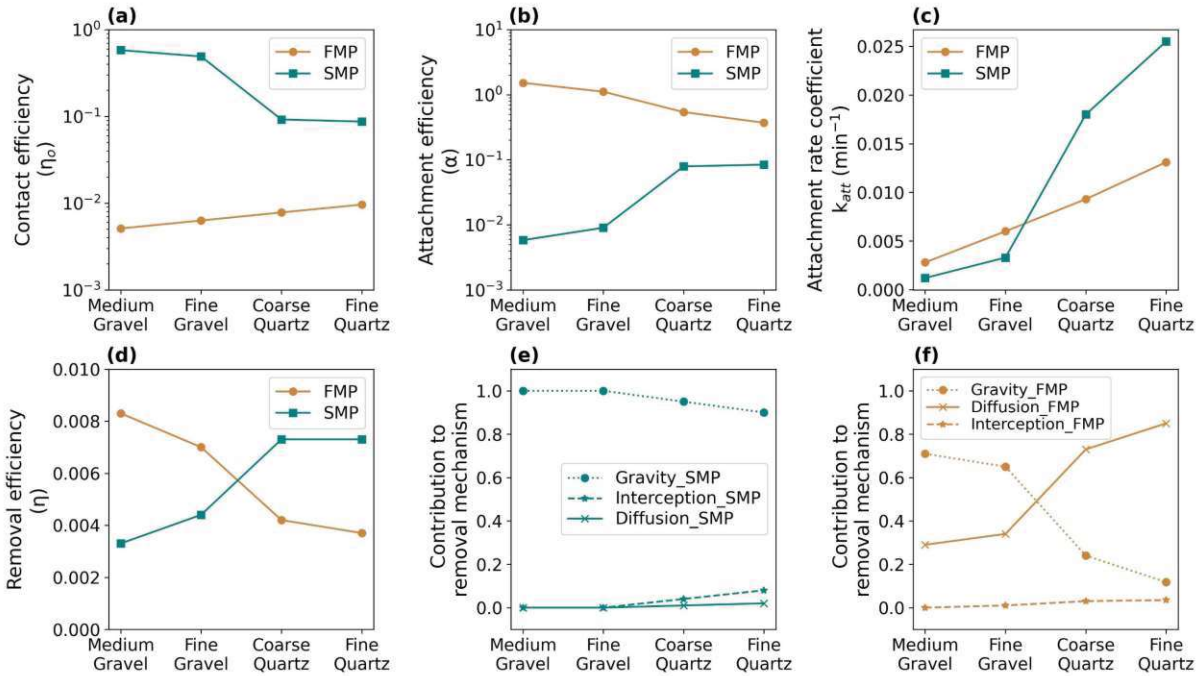


Figure 18 Filtration efficiencies of FMPs and SMPs in various soils

Filtration efficiencies of fragmented (FMPs) and spherical (SMPs) microplastics in various porous media. Panels (a-d) show single-collector contact efficiency, attachment efficiency, attachment rate coefficient (k_{att}), and removal efficiency, respectively. Panels (e-f) depict the contribution of SMPs and FMPs to different transport mechanisms. Data represents the average of the column test runs 1 and 2 with fresh soil material.

4.5 Discussion

4.5.1 Role of different aquifer materials in microplastic transport

Both gravel types (medium and fine) had a similar impact on the transport of FMPs under saturated conditions, resulting in a high retention of FMPs ($\sim 1 \mu\text{m}$) when compared to the larger-sized SMPs ($20 \mu\text{m}$). In such coarse material, it is surprising that the smaller particles were retained more. One potential reason for this phenomenon is that in natural gravel, the presence of clay particles may fill up the concave locations within the pore spaces and decrease the availability of these locations to retain larger SMPs (Liang et al., 2022). Another important explanation involves the size exclusion of the SMPs from small pore spaces. In comparison to the conservative tracer BTCs, earlier peak times of SMPs BTCs were observed in gravel (Figure C1, Appendix C). This suggests that SMPs can only be transported through the larger pores of gravel, resulting in an earlier detection peak. Similar observations have been reported regarding MPs and colloidal particles, which are compelled to navigate through the broader preferential flow paths to facilitate their transport (Bradford et al., 2003; Li et al., 2024b). In

this context, Sirivithayapakorn and Keller (2003) experimentally demonstrated that the observed preferential flow paths are less evident in the case of smaller colloids (0.05 μm), compared to the larger colloids (1–3 μm). On the contrary, size exclusion phenomena were not observed in the BTCs for either type of quartz sand.

In the coarse and medium sands, FMPs showed higher mobility, compared to the 10 μm SMPs, due to the effect of straining of the SMPs (**Table C1, Appendix C**), which is the removal of colloids due to small pore spaces acting as a sieve and is dependent on median grain size. Minimum values of d_p/d_{50} (d_p is colloid diameter and d_{50} is median grain size), where straining has been observed in angular silica sand, range from 0.0017 (Bradford et al., 2002) to 0.02 (Tufenkji et al., 2004). Since some straining values in the experiments are in the above-mentioned range (**Table C1, Appendix C**), straining could provide a possible explanation for the increased retention of SMPs in both quartz sands; however, none are above the 0.02 threshold from Tufenkji et al. (2004).

The zeta potential represents surface charge and serves as a key factor for microplastic stability in solutions (Dong et al., 2018). Variations in the zeta potential reflect size-dependent dispersion and aggregation of microplastics. The zeta-potential of FMPs ranged from -21.75 ± 3.79 to -22.17 ± 2.05 mV, while the zeta potential of the SMPs ranged from -18.22 ± 1.51 to -19.55 ± 3.61 mV (**Table C1, Appendix C**). These values indicate strong repulsive forces between the microplastics, causing them to disperse more easily from each other. The zeta potential influences the electrostatic interactions (Mei and Lu, 2014), which are crucial for microplastic attachment to porous media. A more negative zeta potential is more conducive to adsorb to less negatively charged particles (Shen et al., 2020).

Since no tailing was observed in any of the experiments (**Figure 16**), both FMPs and SMPs were likely deposited in the primary minimum, with no energy barrier hindering their interaction with the porous media (Knappett et al., 2008). Moreover, the calculation of single-collector contact efficiency took into account hydrodynamic interactions and van der Waals forces (**Table C4, Appendix C**). The primary interaction mechanism between SMPs and porous media across all soils was gravitational force (**Figure 18e**), whereas, for FMPs, Brownian diffusion was the key mechanism in quartz sand (**Figure 18f**), as reflected by aspect ratio and van der Waals number (**Table C4, Appendix C**). Consistent with previous experimental observations (Elimelech, 1994; Knappett et al., 2008; Zhuang et al., 2005) and theoretical computation (Huber et al., 2000), microplastics-collector interaction changes nonlinearly with microplastic size. Retention and transport of smaller colloids are more

subjected to the influence of diffusion, while behaviors of larger colloids are mainly controlled by interception and sedimentation (Close et al., 2006; Knappett et al., 2008).

4.5.2 Microplastic shape affects its environmental fate and transport

The experiments (tests E1, E2, G1, and G2) examining the influence of microplastic shape on transport were performed with a similar size of microplastic in coarse quartz sand, for which straining due to large particle sizes is not a removal mechanism ($d_p/d_{50} < 0.0017$), and zeta potential is similar for both particle types (**Table C1, Appendix C**). It was found that the FMPs ($\sim 1.40 \mu\text{m}$) exhibit a higher degree of mobility compared to SMPs ($\sim 1 \mu\text{m}$). This may be due to the unique ability of FMPs to align themselves with the direction of flow, thereby significantly enhancing their overall transport efficiency. Previous studies have found that microplastics with a smaller diameter had higher mobility in the quartz sand (O'Connor et al., 2019; Pradel et al., 2020), which contradicts the findings of tests E and G where the $1 \mu\text{m}$ SMPs are transported less than the slightly larger FMPs (**Figure 17**). Therefore, the observed enhanced mobility of FMPs may be due to shape instead of size; an explanation for this could be that the higher aspect ratio of FMPs (**Table C4, Appendix C**) exposes them to larger surface tension forces, causing them to re-orient or re-align with the flow direction to counteract the dynamic fluid forces (Liu et al., 2010; Xu et al., 2008). This could also be described as a tumbling (rotational) movement leading to greater mobility within saturated quartz sand (Aramrak et al., 2013). Comparable to this study, Tumwet et al. (2022) also reported high mobility of FMPs in quartz sand, due to velocity fluctuations because of the asymmetrical shapes, and experimentally demonstrated that the shape of microplastics is one of the critical factors during transport. The current study found that even though FMPs had a larger average particle diameter and would be anticipated to have higher removal, the irregular shape of the particles emerged as the primary factor influencing mobility within saturated coarse quartz sand.

4.5.3 Microplastic response to filtration mechanisms

Considering the transport of FMPs in natural gravel, high values of attachment efficiencies predicted that more removal of FMPs would occur (**Figure 18b**), which was in agreement with the experimental breakthrough data (**Figure 16a-b**). However, there were inconsistencies in the case of quartz sand. Despite higher values of the attachment efficiency for FMPs, compared to the larger $10 \mu\text{m}$ SMPs (which would imply more removal), experimental breakthrough data showed less removal of FMPs (**Figure 16c-d**). Several factors can potentially contribute to these inconsistencies, including the size, shape, and roughness of the FMPs. One explanation

is that since the majority of the FMPs used in the current study were approximately 1.20 to 1.80 μm in diameter (**Table 4**), this diameter range falls in the transition zone where all three filtration mechanisms can act simultaneously (i.e. Brownian diffusion, interception, and gravity settling). Moreover, straining is also likely playing a role, as Bradford et al. (2002) advised using caution when applying CFT when the d_p/d_{50} ratio is above the 0.0017 threshold, which is the case for the 10 and 20 μm SMPs, but especially (high d_p/d_{50}) in the coarse and medium quartz sand. Additionally, the particle shape and surface roughness of FMPs may influence the kinetic interactions with collector surfaces during the filtration process leading to more breakthrough. Several researchers suggest that grain surface area, angularity, and roughness can all play a role in physicochemical filtration (Bhattacharjee et al., 1998; Saiers and Ryan, 2005; Shellenberger and Logan, 2002). These inconsistencies indicate that additional factors beyond those accounted for by CFT should be taken into account, such as the shape of microplastics.

4.5.4 Implications for groundwater management

Understanding microplastic retention and transport behavior in saturated porous media is imperative to be able to evaluate the potential risks of microplastics in groundwater. The results of this study suggest that the size and shape of microplastics were important factors influencing groundwater transport in various aquifer materials, and fragmented particles showed greater mobility in quartz sand (**Figure 16c-d**). Concerning microplastic shape and size, Pivokonsky et al. (2018) reported fragments as the most abundant morphotype (size range: 1–10 μm), whereas spherical particles were the least prevalent in raw drinking water. Despite this fact, there is a lack of comprehensive data concerning the size, shape, and rates at which microplastics undergo fragmentation and how they are transported in various aquifer materials. The findings of the current study showed that these fragmented particles could pose a more significant threat to sandy aquifers, as they can potentially be transported further than spherical particles of the same size and could act as vectors for long-distance transport due to their co-existence with pathogens in wastewater effluents and sludge (Edo et al., 2020; Pham et al., 2021).

The experiments in the current study are focused on saturated conditions, whereas in the terrestrial environment, microplastic transport to groundwater via infiltrating water primarily occurs through the unsaturated (vadose) zone. The transport processes in the vadose zone are highly complex, characterized by intricate air-water interfaces within pore spaces (Bradford and Torkzaban, 2008). This complexity results in the formation of liquid film entrainment,

which contributes to the fate of microplastics influenced by flow velocity, volume fraction, and pore sizes (He et al., 2023; Wu et al., 2021). In natural environments, soil saturation conditions fluctuate, underscoring the importance of studying both conditions together to improve predictions of microplastic mobility and potential contamination risks.

4.6 Conclusions

This study aimed to understand the transport of microplastics in saturated porous media based on their size and shape. The transport behavior of FMPs and SMPs was compared in different aquifer materials, such as natural gravel and quartz sand. The experiments showed that the soil type and the size and shape of microplastics influence the transport of microplastics. In gravel, the larger SMPs experienced higher breakthrough than FMPs, possibly due to size exclusion. The irregular shape and rough surface of FMPs may increase their attachment to impurities (e.g., clay particles) present on the natural gravel surface. Due to straining, the larger SMPs showed higher retention in quartz sand. It was found that FMPs were more mobile than similar-sized SMPs in the coarse quartz sand, possibly due to the high aspect ratio forcing them to re-align with the flow direction. The results indicate that settling was the primary retention mechanism for SMPs in gravel, while diffusion was dominant for FMPs in quartz sand. The outcome of this study suggests that future research should use irregularly shaped plastic materials to closely replicate microplastics in the natural environment and to better assess the risks of microplastic transport in soil and groundwater.

5.1 Conclusions

This dissertation addressed the pressing environmental issue of microplastic pollution and its potential risks to groundwater systems, employing a multi-faceted research approach. First, it focuses on the development and monitoring of microplastic-rich fecal pollution originating from commercial ships and vessels. Second, it investigates the complex interactions and co-transport mechanisms between pathogens and microplastic particles. Lastly, it examines how the shape and size of spherical and fragmented microplastics influence their transport dynamics within diverse riverbank sediments.

To tackle these emerging problems, the first study (Chapter 2) developed and implemented an innovative integrated framework to evaluate the impact of commercial and recreational ships on (microplastic-rich) fecal water quality of the River Danube. Built on three pillars, pollution source profiling (PSP), high-resolution field analysis, and statistical analysis between pollution patterns and ships, this approach offers a comprehensive method for understanding the interplay between ship traffic and water quality dynamics. By extracting and analyzing Danube River Information Services (DoRIS) data with a python-language-based script, we enabled precise tracking and retrospective analysis of individual ships by type, laying the foundation for detailed pollution assessments on both regional and local scales. Our high-resolution analysis of the River Danube demonstrated minimal longitudinal and cross-sectional pollution gradients, with human wastewater identified as the dominant pollution source, confirmed by genetic fecal pollution diagnostics (GFPD). While PSP suggested a high theoretical pollution potential from ships, effective wastewater management prevented significant pollution during the study period. Nonetheless, localized impacts linked to docked cruise ships were detected, underscoring the sensitivity and applicability of this methodology for identifying fine-scale pollution sources. This novel methodology is not only adaptable to other rivers worldwide with available AIS data but also holds immense potential for advancing digitalization in water sector. By providing actionable insights into the interactions between inland navigation and water quality, this research supports the global pursuit of improved environmental protection

and public health, offering an innovative tool for researchers and authorities aiming to safeguard aquatic ecosystems and human well-being.

Secondly, building upon the exploration of microbial pollution in aquatic environments, Chapter 3 extends the investigation to understand the role of microplastics in facilitating pathogen transport and survival in groundwater. Using qPCR and plaque assay (culture-based) techniques for virus quantification in the presence of microplastics, this study establishes a robust methodological foundation for studying these complex microplastic-virus interactions and processes. Through this dissertation, we established that microplastics can facilitate virus transport, enhancing mobility and potential contamination pathways. However, their interactions with viruses can lead to virus inactivation, potentially reducing environmental persistence. Our work provides a baseline that emphasizes the co-transport of microplastics, and different viruses emerge as a critical concern, underscoring the need for further research in natural aquifer materials to further understand the mechanisms governing these interactions. Such studies are essential to accurately evaluate the risks of groundwater contamination and the associated public health implications. By advancing our knowledge of microplastic-virus dynamics, this work lays the groundwork for developing strategies to mitigate emerging environmental and health challenges posed by these pollutants.

Expanding upon the investigation of microplastic-virus interactions and the role of microplastics in enhancing virus transport in saturated quartz sand, Chapter 4 investigated the transport of microplastics in various saturated porous media, focusing on the influence of size and shape. Comparative experiments with fragmented microplastics (FMPs) and spherical microplastics (SMPs) in natural gravel and quartz sand revealed significant effects of soil grain particle size and microplastic characteristics (shape and size) on transport behavior. In gravel, SMPs exhibited higher breakthrough rates than FMPs, likely due to size exclusion, while the irregular shape and rough surface of FMPs increased their attachment to surface impurities. In quartz sand, SMPs showed higher retention due to straining, whereas FMPs were more mobile in coarse sand, potentially because their high aspect ratio facilitated alignment with flow paths. The study identified settling as the primary retention mechanism for SMPs in gravel, while diffusion dominated for FMPs in quartz sand. This study emphasizes the critical role of microplastic shape and size in groundwater transport dynamics and suggests that future research should prioritize using irregularly shaped plastics (size less than 20 μm) to better mimic natural environmental conditions.

5.2 Challenges

Although there is growing interest in studying the presence of microplastics in natural environments, only a limited number of studies provide data on the properties of different porous media and their relationship to groundwater. The absence of standardized analytical detection methods and a lack of hydrogeological information relevant to groundwater transport of microplastics, make it challenging to compare results, significantly influencing the understanding of the transport dynamics in groundwater. This dissertation aims to address this gap by investigating microplastic transport through various soil types, emphasizing the importance of soil characterization for a thorough evaluation of microplastic occurrence in groundwater.

Fourier Transform Infrared Spectroscopy (FTIR) is widely recognized as one of the most effective methods for identifying plastic fragments with sub-micrometer dimensions. However, these microplastics are often similar in size to the pore throats of various soil types, but the size of many microplastics fall below FTIR's detection threshold when present in saturated porous media. This limitation has contributed to the global underestimation of microplastic contamination in groundwater. This dissertation overcomes the challenge of detecting sub-micron microplastics by introducing the solid-phase cytometry technique, providing a more accurate approach for identifying these particles in environmental samples.

The complex and poorly understood dynamics of microplastic transport in groundwater, combined with the limitations of existing modeling and detection methods, call for a proactive approach. To protect vital drinking water resources, it is imperative to implement strict regulations on industrial and agricultural activities that could contribute to microplastic contamination in vulnerable aquifers.

The recent increase in plastic production, along with continuous degradation and fragmentation of existing plastic waste, is set to intensify microplastic pollution on a global scale. This growing threat not only jeopardizes the environment but also extends its reach into previously untouched and pristine ecosystems, creating long-term, far-reaching consequences.

5.3 Recommendations

In recent years, biodegradable plastics (BPs) have gained attention as a promising alternative to conventional petroleum-based plastics. However, although it was not the topic of this

dissertation, it is important to recognize that not all BPs fully degrade in natural conditions, and it is recommended that future research should investigate the unique properties of BPs. Some may fragment into microplastics more quickly than traditional plastics, creating new environmental challenges. Additionally, the impact of BPs on microbial contaminants in water and soil is not well understood, particularly in relation to their ability to interact with pathogens and promote their transport. Given the increasing use of biodegradable plastics, it is crucial to prioritize the ecological safety of these materials before their widespread commercialization. Future research should focus on understanding how BPs degrade, their interactions with pathogens, and the potential for increased microbial contamination in water and agricultural soils. This knowledge will be vital for assessing the environmental risks of BPs, ensuring that their use does not inadvertently exacerbate existing pollution problems. Therefore, it is essential to develop and implement comprehensive safety standards for biodegradable plastics to mitigate potential environmental and health impacts.

Furthermore, to address the growing environmental concerns of the plastisphere (fate of biofilms on plastics), future research should focus on the overland transport of microplastic-pathogen aggregates in agricultural soils. Specifically, future research should explore how biosolids application (to enhance soil quality for agricultural yield), irrigation, and rainfall influence the vertical infiltration of these aggregates into deeper soils and their runoff into freshwater systems. Investigating the factors such as soil type, rainfall intensity, and catchment topography that govern this transport is critical. This knowledge would help develop effective management strategies to reduce microplastic contamination and protect freshwater resources.

References

- Abdel-Fattah, A. I., Zhou, D., Boukhalfa, H., Tarimala, S., Ware, S. D., & Keller, A. A. (2013). Dispersion Stability and Electrokinetic Properties of Intrinsic Plutonium Colloids: Implications for Subsurface Transport. *Environmental Science & Technology*, 47(11), 5626-5634. <https://doi.org/10.1021/es304729d>
- Ahn, J. H., Grant, S. B., Surbeck, C. Q., DiGiacomo, P. M., Nezhin, N. P., & Jiang, S. (2005). Coastal Water Quality Impact of Stormwater Runoff from an Urban Watershed in Southern California. *Environmental Science & Technology*, 39(16), 5940-5953. <https://doi.org/10.1021/es0501464>
- Alimi, O. S., Farner Budarz, J., Hernandez, L. M., & Tufenkji, N. (2018). Microplastics and Nanoplastics in Aquatic Environments: Aggregation, Deposition, and Enhanced Contaminant Transport. *Environmental Science & Technology*, 52(4), 1704-1724. <https://doi.org/10.1021/acs.est.7b05559>
- Amaral-Zettler, L. A., Zettler, E. R., & Mincer, T. J. (2020). Ecology of the plastisphere. *Nature Reviews Microbiology*, 18(3), 139-151. <https://doi.org/10.1038/s41579-019-0308-0>
- Amato-Lourenço, L. F., Carvalho-Oliveira, R., Júnior, G. R., dos Santos Galvão, L., Ando, R. A., & Mauad, T. (2021). Presence of airborne microplastics in human lung tissue. *Journal of Hazardous Materials*, 416, 126124. <https://doi.org/https://doi.org/10.1016/j.jhazmat.2021.126124>
- Ameen, A., Stevenson, M. E., Kirschner, A. K. T., Jakwerth, S., Derx, J., & Blaschke, A. P. (2024). Fate and transport of fragmented and spherical microplastics in saturated gravel and quartz sand. *Journal of Environmental Quality*, 53(5), 727-742. <https://doi.org/https://doi.org/10.1002/jeq2.20618>
- Amorim, E., Ramos, S., & Bordalo, A. A. (2014). Relevance of temporal and spatial variability for monitoring the microbiological water quality in an urban bathing area. *Ocean and Coastal Management*, 91, 41-49. <https://doi.org/10.1016/j.ocecoaman.2014.02.001>
- Andrady, A. L. (2011). Microplastics in the marine environment. *Marine Pollution Bulletin*, 62(8), 1596-1605. <https://doi.org/https://doi.org/10.1016/j.marpolbul.2011.05.030>
- Aramrak, S., Flury, M., Harsh, J. B., Zollars, R. L., & Davis, H. P. (2013). Does Colloid Shape Affect Detachment of Colloids by a Moving Air-Water Interface? *Langmuir*, 29(19), 5770-5780. <https://doi.org/10.1021/la400252q>
- Arnold, J. C., & Hutchings, I. M. (1989). Flux rate effects in the erosive wear of elastomers. *Journal of Materials Science*, 24(3), 833-839. <https://doi.org/10.1007/BF01148765>
- Aves, A. R., Revell, L. E., Gaw, S., Ruffell, H., Schuddeboom, A., Wotherspoon, N. E., LaRue, M., & McDonald, A. J. (2022). First evidence of microplastics in Antarctic snow. *The Cryosphere*, 16(6), 2127-2145. <https://doi.org/10.5194/tc-16-2127-2022>
- Bales, R. C., Hinkle, S. R., Kroeger, T. W., Stocking, K., & Gerba, C. P. (1991). Bacteriophage Adsorption during Transport through Porous Media: Chemical Perturbations and Reversibility [Article]. *Environmental Science and Technology*, 25(12), 2088-2095. <https://doi.org/10.1021/es00024a016>
- Ballesté, E., Pascual-Benito, M., Martín-Díaz, J., Blanch, A. R., Lucena, F., Muniesa, M., Jofre, J., & García-Aljaro, C. (2019). Dynamics of crAssphage as a human source tracking marker in potentially faecally polluted environments. *Water Research*, 155, 233-244. <https://doi.org/10.1016/j.watres.2019.02.042>
- Barlet, M., Delaye, J.-M., Charpentier, T., Gennisson, M., Bonamy, D., Rouxel, T., & Rountree, C. L. (2015). Hardness and toughness of sodium borosilicate glasses via Vickers's indentations. *Journal of Non-Crystalline Solids*, 417-418, 66-79. <https://doi.org/https://doi.org/10.1016/j.jnoncrysol.2015.02.005>
- Baudart, J., Coallier, J., Laurent, P., & Prévost, M. (2002). Rapid and Sensitive Enumeration of Viable Diluted Cells of Members of the Family Enterobacteriaceae in Freshwater and Drinking Water. *Applied and Environmental Microbiology*, 68(10), 5057-5063. <https://doi.org/10.1128/AEM.68.10.5057-5063.2002>
- Belzagui, F., Crespi, M., Álvarez, A., Gutiérrez-Bouzán, C., & Vilaseca, M. (2019). Microplastics' emissions: Microfibers' detachment from textile garments. *Environmental Pollution*, 248, 1028-1035.
- Bhattacharjee, S., Ko, C.-H., & Elimelech, M. (1998). DLVO Interaction between Rough Surfaces. *Langmuir*, 14(12), 3365-3375. <https://doi.org/10.1021/la971360b>
- Blanc, R., & Nasser, A. (1996). Effect of effluent quality and temperature on the persistence of virus in soil. *Water Science and Technology*, 33(10), 237-242. [https://doi.org/https://doi.org/10.1016/0273-1223\(96\)00425-8](https://doi.org/https://doi.org/10.1016/0273-1223(96)00425-8)
- Boos, J.-P., Gilfedder, B. S., & Frei, S. (2021). Tracking Microplastics Across the Streambed Interface: Using Laser-Induced-Fluorescence to Quantitatively Analyze Microplastic Transport in an Experimental

Flume. *Water Resources Research*, 57(12), e2021WR031064.
<https://doi.org/https://doi.org/10.1029/2021WR031064>

- Bowley, J., Baker-Austin, C., Porter, A., Hartnell, R., & Lewis, C. (2021). Oceanic Hitchhikers – Assessing Pathogen Risks from Marine Microplastic. *Trends in Microbiology*, 29(2), 107-116.
<https://doi.org/https://doi.org/10.1016/j.tim.2020.06.011>
- Bradford, S. A., Kim, H., Shen, C., Sasidharan, S., & Shang, J. (2017). Contributions of Nanoscale Roughness to Anomalous Colloid Retention and Stability Behavior. *Langmuir*, 33(38), 10094-10105.
<https://doi.org/10.1021/acs.langmuir.7b02445>
- Bradford, S. A., Simunek, J., Bettahar, M., van Genuchten, M. T., & Yates, S. R. (2003). Modeling Colloid Attachment, Straining, and Exclusion in Saturated Porous Media. *Environmental Science & Technology*, 37(10), 2242-2250. <https://doi.org/10.1021/es025899u>
- Bradford, S. A., & Torkzaban, S. (2008). Colloid Transport and Retention in Unsaturated Porous Media: A Review of Interface-, Collector-, and Pore-Scale Processes and Models. *Vadose Zone Journal*, 7(2), 667-681. <https://doi.org/https://doi.org/10.2136/vzj2007.0092>
- Bradford, S. A., Yates, S. R., Bettahar, M., & Simunek, J. (2002). Physical factors affecting the transport and fate of colloids in saturated porous media. *Water Resources Research*, 38(12), 63-61-63-12.
<https://doi.org/https://doi.org/10.1029/2002WR001340>
- Buwono, N. R., Risjani, Y., & Soegianto, A. (2021). Distribution of microplastic in relation to water quality parameters in the Brantas River, East Java, Indonesia. *Environmental Technology & Innovation*, 24, 101915. <https://doi.org/https://doi.org/10.1016/j.eti.2021.101915>
- Cai, L., Wang, J., Peng, J., Wu, Z., & Tan, X. (2018). Observation of the degradation of three types of plastic pellets exposed to UV irradiation in three different environments. *Science of The Total Environment*, 628, 740-747.
- Camesano, T. A., Unice, K. M., & Logan, B. E. (1999). Blocking and ripening of colloids in porous media and their implications for bacterial transport. *Colloids and Surfaces A: Physicochemical and Engineering Aspects*, 160(3), 291-307. [https://doi.org/https://doi.org/10.1016/S0927-7757\(99\)00156-9](https://doi.org/https://doi.org/10.1016/S0927-7757(99)00156-9)
- Cao, H., Tsai, F. T.-C., & Rusch, K. A. (2010). Salinity and Soluble Organic Matter on Virus Sorption in Sand and Soil Columns. *Groundwater*, 48(1), 42-52. <https://doi.org/https://doi.org/10.1111/j.1745-6584.2009.00645.x>
- Cao, Y. l., Wang, X., Yin, C. q., Xu, W. w., Shi, W., Qian, G. r., & Xun, Z. m. (2018). Inland Vessels Emission Inventory and the emission characteristics of the Beijing-Hangzhou Grand Canal in Jiangsu province. *Process Safety and Environmental Protection*, 113, 498-506. <https://doi.org/10.1016/j.psep.2017.10.020>
- Carić, H., & Mackelworth, P. (2014). Cruise tourism environmental impacts – The perspective from the Adriatic Sea. *Ocean & Coastal Management*, 102, 350-363.
<https://doi.org/https://doi.org/10.1016/j.ocecoaman.2014.09.008>
- CCNR. (2022). Roadmap for reducing inland navigation emissions.
- Cha, J., Lee, J.-Y., & Chia, R. W. (2023). Microplastics contamination and characteristics of agricultural groundwater in Haeon Basin of Korea. *Science of The Total Environment*, 864, 161027.
<https://doi.org/https://doi.org/10.1016/j.scitotenv.2022.161027>
- Chen, R., Liu, C., Xue, Q., & Rui, R. (2022). Research on Fine Ship Sewage Generation Inventory Based on AIS Data and Its Application in the Yangtze River. *Water (Switzerland)*, 14(19).
<https://doi.org/10.3390/w14193109>
- Chia, R. W., Lee, J.-Y., Kim, H., & Jang, J. (2021). Microplastic pollution in soil and groundwater: a review. *Environmental Chemistry Letters*, 19(6), 4211-4224. <https://doi.org/10.1007/s10311-021-01297-6>
- Chrysikopoulos, C. V., Masciopinto, C., La Mantia, R., & Manariotis, I. D. (2010). Removal of biocolloids suspended in reclaimed wastewater by injection into a fractured aquifer model [Article]. *Environmental Science and Technology*, 44(3), 971-977. <https://doi.org/10.1021/es902754n>
- Close, M. E., Pang, L., Flintoft, M. J., & Sinton, L. W. (2006). Distance and Flow Effects on Microsphere Transport in a Large Gravel Column. *Journal of Environmental Quality*, 35(4), 1204-1212.
<https://doi.org/https://doi.org/10.2134/jeq2005.0286>
- Cole, M., Lindeque, P., Halsband, C., & Galloway, T. S. (2011). Microplastics as contaminants in the marine environment: A review. *Marine Pollution Bulletin*, 62(12), 2588-2597.
<https://doi.org/https://doi.org/10.1016/j.marpolbul.2011.09.025>

- Corpuz, M. V. A., Buonerba, A., Vigliotta, G., Zarra, T., Ballesteros, F., Campiglia, P., Belgiorno, V., Korshin, G., & Naddeo, V. (2020). Viruses in wastewater: occurrence, abundance and detection methods. *Science of The Total Environment*, 745, 140910. <https://doi.org/https://doi.org/10.1016/j.scitotenv.2020.140910>
- Cortés-Arriagada, D. (2021). Elucidating the co-transport of bisphenol A with polyethylene terephthalate (PET) nanoplastics: A theoretical study of the adsorption mechanism. *Environmental Pollution*, 270, 116192. <https://doi.org/https://doi.org/10.1016/j.envpol.2020.116192>
- Creemers, P. (2023). A New Era for River Information Services (Wg125). *Proceedings of PIANC Smart Rivers 2022, Singapore*. https://doi.org/https://doi.org/10.1007/978-981-19-6138-0_66
- da Costa, J. P., Mouneyrac, C., Costa, M., Duarte, A. C., & Rocha-Santos, T. (2020). The role of legislation, regulatory initiatives and guidelines on the control of plastic pollution. *Frontiers in Environmental Science*.
- Dang, H. T. T., & Tarabara, V. V. (2021). Attachment of human adenovirus onto household paints. *Colloids and Surfaces B: Biointerfaces*, 204, 111812. <https://doi.org/https://doi.org/10.1016/j.colsurfb.2021.111812>
- Danube Commission. (2021). *MARKET OBSERVATION FOR DANUBE NAVIGATION RESULTS IN 2020*. https://www.danubecommission.org/uploads/doc/2021/Market_observation_2020/en_market_observation_2020.pdf
- David, A., Mako, P., Galieriková, A., & Stupalo, V. (2021). Transshipment Activities in the Rhine Ports. *Transportation Research Procedia*, 53, 188-195. <https://doi.org/https://doi.org/10.1016/j.trpro.2021.02.025>
- Demeter, K., Derx, J., Komma, J., Parajka, J., Schijven, J., Sommer, R., Cervero-Aragó, S., Lindner, G., Zoufal-Hruza, C. M., Linke, R., Savio, D., Ixenmaier, S. K., Kirschner, A. K. T., Kromp, H., Blaschke, A. P., & Farnleitner, A. H. (2021). Modelling the interplay of future changes and wastewater management measures on the microbiological river water quality considering safe drinking water production. *Science of The Total Environment*, 768, Fsurface-Fsurface. <https://doi.org/10.1016/j.scitotenv.2020.144278>
- Demeter, K., Linke, R., Ballesté, E., Reischer, G., Mayer, R. E., Vierheilig, J., Kolm, C., Stevenson, M. E., Derx, J., Kirschner, A. K. T., Sommer, R., Shanks, O. C., Blanch, A. R., Rose, J., Ahmed, W., & Farnleitner, A. H. (2023). Have genetic targets for faecal pollution diagnostics and source tracking revolutionised water quality analysis yet? *FEMS Microbiology Reviews*(June), 1-36. <https://doi.org/10.1093/femsre/fuad028>
- Deng, C., Liu, X., Li, L., Shi, J., Guo, W., & Xue, J. (2020). Temporal dynamics of antibiotic resistant genes and their association with the bacterial community in a water-sediment mesocosm under selection by 14 antibiotics. *Environment International*, 137, 105554. <https://doi.org/https://doi.org/10.1016/j.envint.2020.105554>
- Deng, L., Li, G., Peng, S., Wu, J., & Che, Y. (2022). Microplastics in personal care products: Exploring public intention of usage by extending the theory of planned behaviour. *Science of The Total Environment*, 848, 157782. <https://doi.org/https://doi.org/10.1016/j.scitotenv.2022.157782>
- Derjaguin, B., & Landau, L. (1993). Theory of the stability of strongly charged lyophobic sols and of the adhesion of strongly charged particles in solutions of electrolytes. *Progress in Surface Science*, 43(1), 30-59. [https://doi.org/https://doi.org/10.1016/0079-6816\(93\)90013-L](https://doi.org/https://doi.org/10.1016/0079-6816(93)90013-L)
- Derx, J., Blaschke, A. P., & Blöschl, G. (2010). Three-dimensional flow patterns at the river-aquifer interface — a case study at the Danube. *Advances in Water Resources*, 33(11), 1375-1387. <https://doi.org/https://doi.org/10.1016/j.advwatres.2010.04.013>
- Derx, J., Kılıç, H. S., Linke, R., Cervero-Aragó, S., Frick, C., Schijven, J., Kirschner, A. K. T., Lindner, G., Walochnik, J., Stalder, G., Sommer, R., Saracevic, E., Zessner, M., Blaschke, A. P., & Farnleitner, A. H. (2023). Probabilistic fecal pollution source profiling and microbial source tracking for an urban river catchment. *Science of The Total Environment*, 857(October 2022). <https://doi.org/10.1016/j.scitotenv.2022.159533>
- Dhanker, R., Chaudhary, S., Goyal, S., & Garg, V. K. (2021). Influence of urban sewage sludge amendment on agricultural soil parameters. *Environmental Technology & Innovation*, 23, 101642. <https://doi.org/https://doi.org/10.1016/j.eti.2021.101642>
- Dheenani, P. S., Jha, D. K., Das, A. K., Vinithkumar, N. V., Devi, M. P., & Kirubakaran, R. (2016). Geographic information systems and multivariate analysis to evaluate fecal bacterial pollution in coastal waters of Andaman, India. *Environmental Pollution*, 214, 45-53. <https://doi.org/10.1016/j.envpol.2016.03.065>
- Dika, C., Duval, J. F. L., Francius, G., Perrin, A., & Gantzer, C. (2015). Isoelectric point is an inadequate descriptor of MS2, Phi X 174 and PRD1 phages adhesion on abiotic surfaces. *Journal of Colloid and Interface Science*, 446, 327-334. <https://doi.org/https://doi.org/10.1016/j.jcis.2014.08.055>

- Dong, S., Xia, J., Sheng, L., Wang, W., Liu, H., & Gao, B. (2021). Transport characteristics of fragmental polyethylene glycol terephthalate (PET) microplastics in porous media under various chemical conditions. *Chemosphere*, 276, 130214. <https://doi.org/https://doi.org/10.1016/j.chemosphere.2021.130214>
- Dong, S., Zhou, M., Su, X., Xia, J., Wang, L., Wu, H., Suakollie, E. B., & Wang, D. (2022). Transport and retention patterns of fragmental microplastics in saturated and unsaturated porous media: A real-time pore-scale visualization. *Water Research*, 214, 118195. <https://doi.org/https://doi.org/10.1016/j.watres.2022.118195>
- Dong, Z., Qiu, Y., Zhang, W., Yang, Z., & Wei, L. (2018). Size-dependent transport and retention of micron-sized plastic spheres in natural sand saturated with seawater. *Water Research*, 143, 518-526. <https://doi.org/https://doi.org/10.1016/j.watres.2018.07.007>
- Dowd, S. E., & Pillai, S. D. (1997). Survival and transport of selected bacterial pathogens and indicator viruses under sandy aquifer conditions. *Journal of Environmental Science and Health . Part A: Environmental Science and Engineering and Toxicology*, 32(8), 2245-2258. <https://doi.org/10.1080/10934529709376680>
- Drummond, J. D., Schneidewind, U., Li, A., Hoellein, T. J., Krause, S., & Packman, A. I. (2022). Microplastic accumulation in riverbed sediment via hyporheic exchange from headwaters to mainstems. *Science Advances*, 8(2), eabi9305. <https://doi.org/doi:10.1126/sciadv.abi9305>
- Duan, J., Bolan, N., Li, Y., Ding, S., Atugoda, T., Vithanage, M., Sarkar, B., Tsang, D. C. W., & Kirkham, M. B. (2021). Weathering of microplastics and interaction with other coexisting constituents in terrestrial and aquatic environments. *Water Research*, 196, 117011. <https://doi.org/https://doi.org/10.1016/j.watres.2021.117011>
- Duis, K., & Coors, A. (2016). Microplastics in the aquatic and terrestrial environment: sources (with a specific focus on personal care products), fate and effects. *Environmental Sciences Europe*, 28(1), 2. <https://doi.org/10.1186/s12302-015-0069-y>
- Eder, A., Sotier, B., Klebinder, K., Sturmlechner, R., Dorner, J., Markart, G., Schmid, G., & Strauss, P. (2011). *Hydrologische Bodenkenndaten der Böden Niederösterreichs (HydroBodNÖ) 1 Endbericht (Data on hydrological soil characteristics of soils in Lower Austria)*. <https://data.europa.eu/data/datasets/203fbf07-9da2-40d2-bc7f-328dae43dafc/embed?locale=en>
- Edo, C., González-Pleiter, M., Leganés, F., Fernández-Piñas, F., & Rosal, R. (2020). Fate of microplastics in wastewater treatment plants and their environmental dispersion with effluent and sludge. *Environmental Pollution*, 259, 113837.
- Eisfeld, C., Schijven, J. F., van der Wolf, J. M., Medema, G., Kruisdijk, E., & van Breukelen, B. M. (2022). Removal of bacterial plant pathogens in columns filled with quartz and natural sediments under anoxic and oxygenated conditions. *Water Research*, 220, 118724. <https://doi.org/https://doi.org/10.1016/j.watres.2022.118724>
- Elimelech, M. (1994). Effect of particle size on the kinetics of particle deposition under attractive double layer interactions [Article]. *Journal of Colloid and Interface Science*, 164(1), 190-199. <https://doi.org/10.1006/jcis.1994.1157>
- Elimelech, M., Gregory, J., Jia, X., Williams, R., Gregory, J., Jia, X., & Williams, R. (1995). Chapter 2-Electrical properties of interfaces. Particle Deposition & Aggregation. In: Woburn: Butterworth-Heinemann.
- Elimelech, M., & O'Melia, C. R. (1990). Kinetics of deposition of colloidal particles in porous media. *Environmental Science & Technology*, 24(10), 1528-1536. <https://doi.org/10.1021/es00080a012>
- Eriksen, M., Cowger, W., Erdle, L. M., Coffin, S., Villarrubia-Gómez, P., Moore, C. J., Carpenter, E. J., Day, R. H., Thiel, M., & Wilcox, C. (2023). A growing plastic smog, now estimated to be over 170 trillion plastic particles afloat in the world's oceans—Urgent solutions required. *PLOS ONE*, 18(3), e0281596. <https://doi.org/10.1371/journal.pone.0281596>
- Esfandiari, A., Abbasi, S., Peely, A. B., Mowla, D., Ghanbarian, M. A., Oleszczuk, P., & Turner, A. (2022). Distribution and transport of microplastics in groundwater (Shiraz aquifer, southwest Iran). *Water Research*, 220, 118622. <https://doi.org/https://doi.org/10.1016/j.watres.2022.118622>
- Espinosa, A. C., Mazari-Hiriart, M., Espinosa, R., Maruri-Avidal, L., Méndez, E., & Arias, C. F. (2008). Infectivity and genome persistence of rotavirus and astrovirus in groundwater and surface water. *Water Research*, 42(10), 2618-2628. <https://doi.org/https://doi.org/10.1016/j.watres.2008.01.018>
- EU Regulation 2020/741. (2022). Proposal for a DIRECTIVE OF THE EUROPEAN PARLIAMENT AND OF THE COUNCIL concerning urban wastewater treatment (recast). *Off. J. Eur. Union*, 0345(October), 1-68.

- European Commission. (2024). Supplementing Directive (EU) 2020/2184 of the European Parliament and of the Council by laying down a methodology to measure microplastics in water intended for human consumption. *Official Journal of the European Union*. http://data.europa.eu/eli/dec_del/2024/1441/oj
- European Parliament. (2000). EU DIRECTIVE 2000/60/EC establishing a framework for Community action in the field of water policy. *Official Journal of the European Communities*.
- European Parliament. (2005). DIRECTIVE 2005/44/EC on harmonised river information services (RIS) on inland waterways in the Community. *Official Journal of the European Union*, L255/159. <https://eur-lex.europa.eu/legal-content/en/ALL/?uri=CELEX:32005L0044>
- Falk, M. (2014). Impact of weather conditions on tourism demand in the peak summer season over the last 50 years. *Tourism Management Perspectives*, 9, 24-35. <https://doi.org/10.1016/j.tmp.2013.11.001>
- Farazi, N. P., Zou, B., Sriraj, P. S., Dirks, L., Lewis, E., & Manzanarez, J. P. (2022). State-level performance measures and database development for inland waterway freight transportation: A US context and a case study. *Research in Transportation Business & Management*, 45, 100866-100866. <https://doi.org/https://doi.org/10.1016/j.rtbm.2022.100866>
- Faust, M. A. (1982). Contribution of pleasure boats to fecal bacteria concentrations in the Rhode River estuary, Maryland, U.S.A. *Science of The Total Environment*, 25(3), 255-262. [https://doi.org/https://doi.org/10.1016/0048-9697\(82\)90018-3](https://doi.org/https://doi.org/10.1016/0048-9697(82)90018-3)
- Fendall, L. S., & Sewell, M. A. (2009). Contributing to marine pollution by washing your face: Microplastics in facial cleansers. *Marine Pollution Bulletin*, 58(8), 1225-1228. <https://doi.org/https://doi.org/10.1016/j.marpolbul.2009.04.025>
- Feriancikova, L., & Xu, S. (2012). Deposition and remobilization of graphene oxide within saturated sand packs [Article]. *Journal of Hazardous Materials*, 235-236, 194-200. <https://doi.org/10.1016/j.jhazmat.2012.07.041>
- Fernández, M. F. C., Manosalva, I. R. C., Quintero, R. F. C., Marín, C. E. M., Cuesta, Y. E. D., Mahecha, D. E., & Vásquez, P. A. P. (2022). Multitemporal Total Coliforms and Escherichia coli Analysis in the Middle Bogotá River Basin, 2007–2019. *Sustainability (Switzerland)*, 14(3), 2007-2019. <https://doi.org/10.3390/su14031769>
- Firquet, S., Beaujard, S., Lobert, P.-E., Sané, F., Caloone, D., Izard, D., & Hober, D. (2015). Survival of Enveloped and Non-Enveloped Viruses on Inanimate Surfaces. *Microbes and Environments*, 30(2), 140-144. <https://doi.org/10.1264/jsme2.ME14145>
- Fister, S., Fuchs, S., Mester, P., Kilpeläinen, I., Wagner, M., & Rossmannith, P. (2015). The use of ionic liquids for cracking viruses for isolation of nucleic acids. *Separation and Purification Technology*, 155, 38-44. <https://doi.org/https://doi.org/10.1016/j.seppur.2015.03.035>
- Flury, M., & Aramrak, S. (2017). Role of air-water interfaces in colloid transport in porous media: A review. *Water Resources Research*, 53(7), 5247-5275. <https://doi.org/https://doi.org/10.1002/2017WR020597>
- Folbert, M. E. F., Corbin, C., & Löhr, A. J. (2022). Sources and Leakages of Microplastics in Cruise Ship Wastewater [Original Research]. *Frontiers in Marine Science*, 9. <https://doi.org/10.3389/fmars.2022.900047>
- Fongaro, G., Nascimento, M. A., Viancelli, A., Tonetta, D., Petrucio, M. M., & Barardi, C. R. M. (2012). Surveillance of human viral contamination and physicochemical profiles in a surface water lagoon. *Water Science and Technology*, 66(12), 2682-2687. <https://doi.org/10.2166/wst.2012.504>
- Fournier, E., Etienne-Mesmin, L., Grootaert, C., Jelsbak, L., Syberg, K., Blanquet-Diot, S., & Mercier-Bonin, M. (2021). Microplastics in the human digestive environment: A focus on the potential and challenges facing in vitro gut model development. *Journal of Hazardous Materials*, 415, 125632. <https://doi.org/https://doi.org/10.1016/j.jhazmat.2021.125632>
- Frei, S., Piehl, S., Gilfedder, B. S., Löder, M. G. J., Krutzke, J., Wilhelm, L., & Laforsch, C. (2019). Occurrence of microplastics in the hyporheic zone of rivers. *Scientific Reports*, 9(1), 15256. <https://doi.org/10.1038/s41598-019-51741-5>
- Frick, C., Vierheilg, J., Nadiotis-Tsaka, T., Ixenmaier, S., Linke, R., Reischer, G. H., Komma, J., Kirschner, A. K. T., Mach, R. L., Savio, D., Seidl, D., Blaschke, A. P., Sommer, R., Derox, J., & Farnleitner, A. H. (2020). Elucidating fecal pollution patterns in alluvial water resources by linking standard fecal indicator bacteria to river connectivity and genetic microbial source tracking. *Water Research*, 184, 116132-116132. <https://doi.org/10.1016/j.watres.2020.116132>
- Fu, Z., & Wang, J. (2019). Current practices and future perspectives of microplastic pollution in freshwater ecosystems in China. *Science of The Total Environment*, 691, 697-712. <https://doi.org/https://doi.org/10.1016/j.scitotenv.2019.07.167>

- Galafassi, S., Nizzetto, L., & Volta, P. (2019). Plastic sources: A survey across scientific and grey literature for their inventory and relative contribution to microplastics pollution in natural environments, with an emphasis on surface water. *Science of The Total Environment*, 693, 133499. <https://doi.org/https://doi.org/10.1016/j.scitotenv.2019.07.305>
- Gao, M., Peng, H., & Xiao, L. (2021). The influence of microplastics for the transportation of E. coli using column model. *Science of The Total Environment*, 786, 147487. <https://doi.org/https://doi.org/10.1016/j.scitotenv.2021.147487>
- Gassilloud, B., & Gantzer, C. (2005). Adhesion-Aggregation and Inactivation of Poliovirus 1 in Groundwater Stored in a Hydrophobic Container. *Applied and Environmental Microbiology*, 71(2), 912-920. <https://doi.org/10.1128/AEM.71.2.912-920.2005>
- Gassilloud, B., Schwartzbrod, L., & Gantzer, C. (2003). Presence of Viral Genomes in Mineral Water: a Sufficient Condition To Assume Infectious Risk? *Applied and Environmental Microbiology*, 69(7), 3965-3969. <https://doi.org/doi:10.1128/AEM.69.7.3965-3969.2003>
- Gaylarde, C. C., Neto, J. A. B., & da Fonseca, E. M. (2021). Paint fragments as polluting microplastics: A brief review. *Marine Pollution Bulletin*, 162, 111847. <https://doi.org/https://doi.org/10.1016/j.marpolbul.2020.111847>
- Gentile, G. J., Blanco Fernández, M. D., & Fidalgo de Cortalezzi, M. M. (2021). Interparticle effects in the cotransport of viruses and engineered nanoparticles in saturated porous media. *Journal of Environmental Chemical Engineering*, 9(5), 106058. <https://doi.org/https://doi.org/10.1016/j.jece.2021.106058>
- Gerba, C. P., Rose, J. B., Haas, C. N., & Crabtree, K. D. (1996). Waterborne rotavirus: A risk assessment. *Water Research*, 30(12), 2929-2940. [https://doi.org/https://doi.org/10.1016/S0043-1354\(96\)00187-X](https://doi.org/https://doi.org/10.1016/S0043-1354(96)00187-X)
- Gholipour, S., Ghalhari, M. R., Nikaeen, M., Rabbani, D., Pakzad, P., & Miranzadeh, M. B. (2022). Occurrence of viruses in sewage sludge: A systematic review. *Science of The Total Environment*, 824, 153886. <https://doi.org/https://doi.org/10.1016/j.scitotenv.2022.153886>
- Gilbreath, A. N., & McKee, L. J. (2015). Concentrations and loads of PCBs, dioxins, PAHs, PBDEs, OC pesticides and pyrethroids during storm and low flow conditions in a small urban semi-arid watershed. *Science of The Total Environment*, 526, 251-261. <https://doi.org/https://doi.org/10.1016/j.scitotenv.2015.04.052>
- Goeppert, N., & Goldscheider, N. (2021). Experimental field evidence for transport of microplastic tracers over large distances in an alluvial aquifer. *Journal of Hazardous Materials*, 408, 124844. <https://doi.org/https://doi.org/10.1016/j.jhazmat.2020.124844>
- Goldsworthy, L., & Goldsworthy, B. (2015). Modelling of ship engine exhaust emissions in ports and extensive coastal waters based on terrestrial AIS data - An Australian case study. *Environmental Modelling and Software*, 63, 45-60. <https://doi.org/10.1016/j.envsoft.2014.09.009>
- Gouin, T., Avalos, J., Brunning, I., Brzuska, K., De Graaf, J., Kaumanns, J., Koning, T., Meyberg, M., Rettinger, K., & Schlatter, H. (2015). Use of micro-plastic beads in cosmetic products in Europe and their estimated emissions to the North Sea environment. *SOFW J*, 141(4), 40-46.
- Gregory, J. (1981). Approximate expressions for retarded van der waals interaction [Article]. *Journal of Colloid and Interface Science*, 83(1), 138-145. [https://doi.org/10.1016/0021-9797\(81\)90018-7](https://doi.org/10.1016/0021-9797(81)90018-7)
- Gui, X., Ren, Z., Xu, X., Chen, X., Chen, M., Wei, Y., Zhao, L., Qiu, H., Gao, B., & Cao, X. (2022). Dispersion and transport of microplastics in three water-saturated coastal soils. *Journal of Hazardous Materials*, 424, 127614. <https://doi.org/https://doi.org/10.1016/j.jhazmat.2021.127614>
- Guo, X., Wang, L., Wang, X., Li, D., Wang, H., Xu, H., Liu, Y., Kang, R., Chen, Q., Zheng, L., Wu, S., Guo, Z., & Zhang, S. (2024). Discovery and analysis of microplastics in human bone marrow. *Journal of Hazardous Materials*, 477, 135266. <https://doi.org/https://doi.org/10.1016/j.jhazmat.2024.135266>
- Habib, R. Z., Abdoon, M. M. S., Al Meqbaali, R. M., Ghebremedhin, F., Elkashlan, M., Kittaneh, W. F., Cherupurakal, N., Mourad, A.-H. I., Thiemann, T., & Al Kindi, R. (2020). Analysis of microbeads in cosmetic products in the United Arab Emirates. *Environmental Pollution*, 258, 113831.
- Hamza, I. A., Jurzik, L., Überla, K., & Wilhelm, M. (2011). Methods to detect infectious human enteric viruses in environmental water samples. *International Journal of Hygiene and Environmental Health*, 214(6), 424-436. <https://doi.org/https://doi.org/10.1016/j.ijheh.2011.07.014>
- Harati-Mokhtari, A., Wall, A., Brooks, P., & Wang, J. (2007). Automatic identification system (AIS): Data reliability and human error implications. *Journal of Navigation*, 60(3), 373-389. <https://doi.org/10.1017/S0373463307004298>
- Harwood, V., Shanks, O., Korajkic, A., Verbyla, M., Ahmed, W., & Iriarte, M. (2019). General and host-associated bacterial indicators of faecal pollution. In A. Farnleitner & A. Blanch (Eds.), *Water and*

Sanitation for the 21st Century: Health and Microbiological Aspects of Excreta and Wastewater Management (Global Water Pathogen Project). Michigan State University. <https://doi.org/10.14321/waterpathogens.6>

- He, B., Wijesiri, B., Ayoko, G. A., Egodawatta, P., Rintoul, L., & Goonetilleke, A. (2020). Influential factors on microplastics occurrence in river sediments. *Science of The Total Environment*, 738, 139901. <https://doi.org/https://doi.org/10.1016/j.scitotenv.2020.139901>
- He, H., Wu, T., Chen, Y.-F., & Yang, Z. (2023). A pore-scale investigation of microplastics migration and deposition during unsaturated flow in porous media. *Science of The Total Environment*, 858, 159934. <https://doi.org/https://doi.org/10.1016/j.scitotenv.2022.159934>
- He, L., Rong, H., Li, M., Zhang, M., Liu, S., Yang, M., & Tong, M. (2021). Bacteria have different effects on the transport behaviors of positively and negatively charged microplastics in porous media. *Journal of Hazardous Materials*, 415, 125550. <https://doi.org/https://doi.org/10.1016/j.jhazmat.2021.125550>
- He, L., Wu, D., Rong, H., Li, M., Tong, M., & Kim, H. (2018). Influence of Nano- and Microplastic Particles on the Transport and Deposition Behaviors of Bacteria in Quartz Sand. *Environmental Science & Technology*, 52(20), 11555-11563. <https://doi.org/10.1021/acs.est.8b01673>
- He, P., Chen, L., Shao, L., Zhang, H., & Lü, F. (2019). Municipal solid waste (MSW) landfill: A source of microplastics? -Evidence of microplastics in landfill leachate. *Water Research*, 159, 38-45. <https://doi.org/https://doi.org/10.1016/j.watres.2019.04.060>
- Helmi, K., Skraber, S., Gantzer, C., Willame, R., Hoffmann, L., & Cauchie, H.-M. (2008). Interactions of *Cryptosporidium parvum*, *Giardia lamblia*, Vaccinal Poliovirus Type 1, and Bacteriophages ϕ X174 and MS2 with a Drinking Water Biofilm and a Wastewater Biofilm. *Applied and Environmental Microbiology*, 74(7), 2079-2088. <https://doi.org/10.1128/AEM.02495-07>
- Henry, B., Laitala, K., & Klepp, I. G. (2019). Microfibres from apparel and home textiles: prospects for including microplastics in environmental sustainability assessment. *Science of The Total Environment*, 652, 483-494.
- Herrig, I., Seis, W., Fischer, H., Regnery, J., Manz, W., Reifferscheid, G., & Böer, S. (2019). Prediction of fecal indicator organism concentrations in rivers: the shifting role of environmental factors under varying flow conditions. *Environmental Sciences Europe*, 31(1). <https://doi.org/10.1186/s12302-019-0250-9>
- Hitchcock, J. N. (2020). Storm events as key moments of microplastic contamination in aquatic ecosystems. *Science of The Total Environment*, 734, 139436. <https://doi.org/https://doi.org/10.1016/j.scitotenv.2020.139436>
- Hou, J., Xu, X., Lan, L., Miao, L., Xu, Y., You, G., & Liu, Z. (2020). Transport behavior of micro polyethylene particles in saturated quartz sand: Impacts of input concentration and physicochemical factors. *Environmental Pollution*, 263, 114499. <https://doi.org/https://doi.org/10.1016/j.envpol.2020.114499>
- Huang, H., Mohamed, B. A., & Li, L. Y. (2023). Accumulation and fate of microplastics in soils after application of biosolids on land: A review. *Environmental Chemistry Letters*, 21(3), 1745-1759. <https://doi.org/10.1007/s10311-023-01577-3>
- Huang, H., Zhou, C., Huang, L., Xiao, C., Wen, Y., Li, J., & Lu, Z. (2022a). Inland ship emission inventory and its impact on air quality over the middle Yangtze River, China. *Science of The Total Environment*, 843(April), 156770-156770. <https://doi.org/10.1016/j.scitotenv.2022.156770>
- Huang, S., Huang, X., Bi, R., Guo, Q., Yu, X., Zeng, Q., Huang, Z., Liu, T., Wu, H., Chen, Y., Xu, J., Wu, Y., & Guo, P. (2022b). Detection and Analysis of Microplastics in Human Sputum. *Environmental Science & Technology*, 56(4), 2476-2486. <https://doi.org/10.1021/acs.est.1c03859>
- Huber, N., Baumann, T., & Niessner, R. (2000). Assessment of colloid filtration in natural porous media by filtration theory [Article]. *Environmental Science and Technology*, 34(17), 3774-3779. <https://doi.org/10.1021/es9903429>
- Huhta, H.-k., Rytönen, J., & Sassi, J. (2007). *Estimated nutrient load from waste waters originating from ships in the Baltic Sea area* (9789513868987). (Espoo, Issue. <https://publications.vtt.fi/pdf/tiedotteet/2007/T2370.pdf>
- Hutchings, I. M. (1992). *Tribology : friction and wear of engineering materials*. Edward Arnold.
- Iacarella, J. C., Burke, L., Clyde, G., Wicks, A., Clavelle, T., Dunham, A., Rubidge, E., & Woods, P. (2023). Application of AIS- and flyover-based methods to monitor illegal and legal fishing in Canada 's Pacific marine conservation areas. (April 2022), 1-14. <https://doi.org/10.1111/csp2.12926>
- ICPDR. (2021). Danube River Basin Management Plan - Update 2021.
- Interreg - Danube Transnational, P. (2019). *Study of the development of the cruise tourism in the Danube Region*.

- ISO. (2012). ISO 9308-2:2012 (2012) Water quality -- Enumeration of *Escherichia coli* and coliform bacteria -- Part 2: Most probable number method. In Geneva, Switzerland.: International Organization for Standardization.
- Jägerbrand, A. K., Brutemark, A., Barthel, J., & Gren, I.-m. (2019). A review on the environmental impacts of shipping on aquatic and nearshore ecosystems. *Science of The Total Environment*, 695, 133637-133637. <https://doi.org/10.1016/j.scitotenv.2019.133637>
- Jászberényi, M., & Miskolczi, M. (2020). Danube Cruise Tourism as a Niche Product—An Overview of the Current Supply and Potential. In *Sustainability* (Vol. 12).
- Karkman, A., Pärnänen, K., & Larsson, D. G. J. (2019). Fecal pollution can explain antibiotic resistance gene abundances in anthropogenically impacted environments. *Nature Communications*, 10(1), 80. <https://doi.org/10.1038/s41467-018-07992-3>
- Kavka, G. G., Kasimir, G. D., & Farnleitner, A. H. (2006). Microbiological water quality of the River Danube (km 2581 - km 15): Longitudinal variation of pollution as determined by standard parameters. *Proceedings 36th International Conference of IAD. Austrian Committee Danube Research/IAD, Vienna, ISBN: 13.*, pp. 415–421. pp. 415–421.
- Kershaw, P., & Rochman, C. (2015). Sources, fate and effects of microplastics in the marine environment: part 2 of a global assessment. *Reports and Studies-IMO/FAO/Unesco-IOC/WMO/IAEA/UN/UNEP Joint Group of Experts on the Scientific Aspects of Marine Environmental Protection (GESAMP) Eng No. 93*.
- Kesy, K., Oberbeckmann, S., Kreikemeyer, B., & Labrenz, M. (2019). Spatial Environmental Heterogeneity Determines Young Biofilm Assemblages on Microplastics in Baltic Sea Mesocosms [Original Research]. *Frontiers in Microbiology*, 10. <https://doi.org/10.3389/fmicb.2019.01665>
- Khan, M. T., Rashid, S., Yaman, U., Khalid, S. A., Kamal, A., Ahmad, M., Akther, N., Kashem, M. A., Hossain, M. F., & Rashid, W. (2024). Microplastic pollution in aquatic ecosystem: A review of existing policies and regulations. *Chemosphere*, 364, 143221. <https://doi.org/https://doi.org/10.1016/j.chemosphere.2024.143221>
- Khoironi, A., Hadiyanto, H., Hartini, E., Dianratri, I., Joelyna, F. A., & Pratiwi, W. Z. (2023). Impact of disposable mask microplastics pollution on the aquatic environment and microalgae growth. *Environmental Science and Pollution Research*, 30(31), 77453-77468. <https://doi.org/10.1007/s11356-023-27651-5>
- Kildare, B. J., Leutenegger, C. M., McSwain, B. S., Bambic, D. G., Rajal, V. B., & Wuertz, S. (2007). 16S rRNA-based assays for quantitative detection of universal, human-, cow-, and dog-specific fecal Bacteroidales: A Bayesian approach. *Water Research*, 41(16), 3701-3715. <https://doi.org/10.1016/j.watres.2007.06.037>
- Kirschner, A. K. T., Kavka, G. G., Velimirov, B., Mach, R. L., Sommer, R., & Farnleitner, A. H. (2009). Microbiological water quality along the Danube River: Integrating data from two whole-river surveys and a transnational monitoring network. *Water Research*, 43(15), 3673-3684. <https://doi.org/10.1016/j.watres.2009.05.034>
- Kirschner, A. K. T., Reischer, G. H., Jakwerth, S., Savio, D., Ixenmaier, S., Toth, E., Sommer, R., Mach, R. L., Linke, R., Eiler, A., Kolarevic, S., & Farnleitner, A. H. (2017). Multiparametric monitoring of microbial faecal pollution reveals the dominance of human contamination along the whole Danube River. *Water Research*, 124, 543-555. <https://doi.org/10.1016/j.watres.2017.07.052>
- Kirstein, I. V., Kirmizi, S., Wichels, A., Garin-Fernandez, A., Erler, R., Löder, M., & Gerds, G. (2016). Dangerous hitchhikers? Evidence for potentially pathogenic *Vibrio* spp. on microplastic particles. *Marine Environmental Research*, 120, 1-8. <https://doi.org/https://doi.org/10.1016/j.marenvres.2016.07.004>
- Kittner, M., Kerndorff, A., Ricking, M., Bednarz, M., Obermaier, N., Lukas, M., Asenova, M., Bordós, G., Eisentraut, P., Hohenblum, P., Hudcova, H., Humer, F., István, T. G., Kirchner, M., Marushevska, O., Nemejcová, D., Oswald, P., Paunovic, M., Sengl, M., . . . Bannick, C. G. (2022). Microplastics in the Danube River Basin: A First Comprehensive Screening with a Harmonized Analytical Approach. *ACS ES&T Water*, 2(7), 1174-1181. <https://doi.org/10.1021/acsestwater.1c00439>
- Knappett, P. S. K., Emelko, M. B., Zhuang, J., & McKay, L. D. (2008). Transport and retention of a bacteriophage and microspheres in saturated, angular porous media: Effects of ionic strength and grain size. *Water Research*, 42(16), 4368-4378. <https://doi.org/https://doi.org/10.1016/j.watres.2008.07.041>
- Knight, L. J., Parker-Jurd, F. N. F., Al-Sid-Cheikh, M., & Thompson, R. C. (2020). Tyre wear particles: an abundant yet widely unreported microplastic? *Environmental Science and Pollution Research*, 27(15), 18345-18354. <https://doi.org/10.1007/s11356-020-08187-4>
- Koboevi, Ž. (2022). Analysis of Sea Pollution by Sewage from Vessels.

- Koboević, Ž., Mišković, D., Capor Hrošik, R., & Koboević, N. (2022). Analysis of sea pollution by sewage from vessels. *Sustainability (Switzerland)*, 14(1). <https://doi.org/10.3390/su14010263>
- Kosuth, M., Mason, S. A., & Wattenberg, E. V. (2018). Anthropogenic contamination of tap water, beer, and sea salt. *PLOS ONE*, 13(4), e0194970.
- Koutnik, V. S., Borthakur, A., Leonard, J., Alkidim, S., Koydemir, H. C., Tseng, D., Ozcan, A., Ravi, S., & Mohanty, S. K. (2022a). Mobility of polypropylene microplastics in stormwater biofilters under freeze-thaw cycles. *Journal of Hazardous Materials Letters*, 3, 100048. <https://doi.org/https://doi.org/10.1016/j.hazl.2022.100048>
- Koutnik, V. S., Leonard, J., Alkidim, S., DePrima, F., Ravi, S., Hoek, E., & Mohanty, S. K. (2021). Distribution of microplastics in soil and freshwater environments: Global analysis and framework for transport modeling. *Environmental Pollution*, 116552.
- Koutnik, V. S., Leonard, J., Brar, J., Cao, S., Glasman, J. B., Cowger, W., Ravi, S., & Mohanty, S. K. (2022b). Transport of microplastics in stormwater treatment systems under freeze-thaw cycles: Critical role of plastic density. *Water Research*, 222, 118950. <https://doi.org/https://doi.org/10.1016/j.watres.2022.118950>
- Kropinski, A. M., Mazzocco, A., Waddell, T. E., Lingohr, E., & Johnson, R. P. (2009). Enumeration of bacteriophages by double agar overlay plaque assay. *Methods Mol Biol*, 501, 69-76. https://doi.org/10.1007/978-1-60327-164-6_7
- Kuehn, W., & Mueller, U. (2000). Riverbank Filtration: An Overview. *Journal AWWA*, 92(12), 60-69. <https://doi.org/https://doi.org/10.1002/j.1551-8833.2000.tb09071.x>
- Kurekin, A. A., Loveday, B. R., Clements, O., Quartly, G. D., Miller, P. I., Wiafe, G., & Agyekum, K. A. (2019). Operational monitoring of illegal fishing in Ghana through exploitation of satellite earth observation and AIS data. *Remote Sensing*, 11(3). <https://doi.org/10.3390/rs11030293>
- Law, K. L. (2017). Plastics in the Marine Environment. *Annual Review of Marine Science*, 9(Volume 9, 2017), 205-229. <https://doi.org/https://doi.org/10.1146/annurev-marine-010816-060409>
- Lebreton, L. C. M., van der Zwet, J., Damsteeg, J.-W., Slat, B., Andrady, A., & Reisser, J. (2017). River plastic emissions to the world's oceans. *Nature Communications*, 8(1), 15611. <https://doi.org/10.1038/ncomms15611>
- Lee, J., Disney, J. E., & Farrell, A. (2018). Exploring The Unseen: From Microplastic Pollution To The Microbial World Of Cruise Ships [Technical Report]. <https://repository.library.noaa.gov/view/noaa/38021>
- Lei, K., Qiao, F., Liu, Q., Wei, Z., Qi, H., Cui, S., Yue, X., Deng, Y., & An, L. (2017). Microplastics releasing from personal care and cosmetic products in China. *Marine Pollution Bulletin*, 123(1), 122-126. <https://doi.org/https://doi.org/10.1016/j.marpolbul.2017.09.016>
- Leslie, H. A., van Velzen, M. J. M., Brandsma, S. H., Vethaak, A. D., Garcia-Vallejo, J. J., & Lamoree, M. H. (2022). Discovery and quantification of plastic particle pollution in human blood. *Environment International*, 163, 107199. <https://doi.org/https://doi.org/10.1016/j.envint.2022.107199>
- Li, M., He, L., Hsieh, L., Rong, H., & Tong, M. (2023). Transport of plastic particles in natural porous media under freeze-thaw treatment: Effects of porous media property. *Journal of Hazardous Materials*, 442, 130084. <https://doi.org/https://doi.org/10.1016/j.jhazmat.2022.130084>
- Li, M., He, L., Zhang, M., Liu, X., Tong, M., & Kim, H. (2019a). Cotransport and Deposition of Iron Oxides with Different-Sized Plastic Particles in Saturated Quartz Sand. *Environmental Science & Technology*, 53(7), 3547-3557. <https://doi.org/10.1021/acs.est.8b06904>
- Li, R., An, X.-L., Wang, Y., Yang, Z., Su, J.-Q., Cooper, J., & Zhu, Y.-G. (2024a). Viral metagenome reveals microbial hosts and the associated antibiotic resistome on microplastics. *Nature Water*, 2(6), 553-565. <https://doi.org/10.1038/s44221-024-00249-y>
- Li, R., Zhu, L., Cui, L., & Zhu, Y.-G. (2022). Viral diversity and potential environmental risk in microplastic at watershed scale: Evidence from metagenomic analysis of plastisphere. *Environment International*, 161, 107146. <https://doi.org/https://doi.org/10.1016/j.envint.2022.107146>
- Li, W., Brunetti, G., Zafiu, C., Kunaschk, M., Debreczeby, M., & Stumpp, C. (2024b). Experimental and simulated microplastics transport in saturated natural sediments: Impact of grain size and particle size. *Journal of Hazardous Materials*, 468, 133772. <https://doi.org/https://doi.org/10.1016/j.jhazmat.2024.133772>
- Li, W., Zhang, Y., Wu, N., Zhao, Z., Xu, W. a., Ma, Y., & Niu, Z. (2019b). Colonization Characteristics of Bacterial Communities on Plastic Debris Influenced by Environmental Factors and Polymer Types in the

Haihe Estuary of Bohai Bay, China. *Environmental Science & Technology*, 53(18), 10763-10773. <https://doi.org/10.1021/acs.est.9b03659>

- Li, Z., Zheng, Y., Maimaiti, Z., Fu, J., Yang, F., Li, Z.-Y., Shi, Y., Hao, L.-B., Chen, J.-Y., & Xu, C. (2024c). Identification and analysis of microplastics in human lower limb joints. *Journal of Hazardous Materials*, 461, 132640. <https://doi.org/10.1016/j.jhazmat.2023.132640>
- Liang, Y., Luo, Y., Shen, C., & Bradford, S. A. (2022). Micro- and nanoplastics retention in porous media exhibits different dependence on grain surface roughness and clay coating with particle size. *Water Research*, 221, 118717. <https://doi.org/10.1016/j.watres.2022.118717>
- Linke, R. B., Zeki, S., Mayer, R. E., Keibliner, K., Savio, D., Kirschner, A. K. T., Reischer, G. H., Mach, R. L., Sommer, R., & Farnleitner, A. H. (2021). Identifying Inorganic Turbidity in Water Samples as Potential Loss Factor During Nucleic Acid Extraction : Implications for Molecular Fecal Pollution Diagnostics and Source Tracking. *12*(October), 1-14. <https://doi.org/10.3389/fmicb.2021.660566>
- Liro, M., Zielonka, A., & Mikuś, P. (2024). First attempt to measure macroplastic fragmentation in rivers. *Environment International*, 191, 108935. <https://doi.org/10.1016/j.envint.2024.108935>
- Liro, M., Zielonka, A., & van Emmerik, T. H. M. (2023). Macroplastic fragmentation in rivers. *Environment International*, 180, 108186. <https://doi.org/10.1016/j.envint.2023.108186>
- Liu, J., Zhang, T., Tian, L., Liu, X., Qi, Z., Ma, Y., Ji, R., & Chen, W. (2019). Aging Significantly Affects Mobility and Contaminant-Mobilizing Ability of Nanoplastics in Saturated Loamy Sand. *Environmental Science & Technology*, 53(10), 5805-5815. <https://doi.org/10.1021/acs.est.9b00787>
- Liu, Q., Lazouskaya, V., He, Q., & Jin, Y. (2010). Effect of Particle Shape on Colloid Retention and Release in Saturated Porous Media. *J Environ Qual*, 39(2), 500-508. <https://doi.org/10.2134/jeq2009.0100>
- Liu, Y., Liu, W., Yang, X., Wang, J., Lin, H., & Yang, Y. (2021a). Microplastics are a hotspot for antibiotic resistance genes: Progress and perspective. *Science of The Total Environment*, 773, 145643. <https://doi.org/10.1016/j.scitotenv.2021.145643>
- Liu, Y., Shao, H., Liu, J., Cao, R., Shang, E., Liu, S., & Li, Y. (2021b). Transport and transformation of microplastics and nanoplastics in the soil environment: A critical review. *Soil Use and Management*, 37(2), 224-242. <https://doi.org/10.1111/sum.12709>
- Liu, Z., & You, X.-y. (2023). Recent progress of microplastic toxicity on human exposure base on in vitro and in vivo studies. *Science of The Total Environment*, 903, 166766. <https://doi.org/10.1016/j.scitotenv.2023.166766>
- Loehr, L. C., Beegle-Krause, C. J., George, K., McGee, C. D., Mearns, A. J., & Atkinson, M. J. (2006). The significance of dilution in evaluating possible impacts of wastewater discharges from large cruise ships. *Marine Pollution Bulletin*, 52(6), 681-688. <https://doi.org/10.1016/j.marpolbul.2005.10.021>
- Loveland, J. P., Ryan, J. N., Amy, G. L., & Harvey, R. W. (1996). The reversibility of virus attachment to mineral surfaces. *Colloids and Surfaces A: Physicochemical and Engineering Aspects*, 107, 205-221. [https://doi.org/10.1016/0927-7757\(95\)03373-4](https://doi.org/10.1016/0927-7757(95)03373-4)
- Lu, J., Yu, Z., Ngiam, L., & Guo, J. (2022). Microplastics as potential carriers of viruses could prolong virus survival and infectivity. *Water Research*, 225, 119115. <https://doi.org/10.1016/j.watres.2022.119115>
- Luna, G. M., Manini, E., Turk, V., Tinta, T., D'Errico, G., Baldrighi, E., Baljak, V., Buda, D., Cabrini, M., Campanelli, A., Cenov, A., Del Negro, P., Drakulović, D., Fabbro, C., Glad, M., Grilec, D., Grilli, F., Jokanović, S., Jozić, S., . . . Zoffoli, S. (2019). Status of faecal pollution in ports: A basin-wide investigation in the Adriatic Sea. *Marine Pollution Bulletin*, 147(March 2018), 219-228. <https://doi.org/10.1016/j.marpolbul.2018.03.050>
- Luo, H., Zhao, Y., Li, Y., Xiang, Y., He, D., & Pan, X. (2020). Aging of microplastics affects their surface properties, thermal decomposition, additives leaching and interactions in simulated fluids. *Science of The Total Environment*, 714, 136862. <https://doi.org/10.1016/j.scitotenv.2020.136862>
- Luo, Z., Zhou, X., Su, Y., Wang, H., Yu, R., Zhou, S., Xu, E. G., & Xing, B. (2021). Environmental occurrence, fate, impact, and potential solution of tire microplastics: Similarities and differences with tire wear particles. *Science of The Total Environment*, 795, 148902. <https://doi.org/10.1016/j.scitotenv.2021.148902>
- Luong, D. T., & Sprik, R. (2013). Streaming Potential and Electroosmosis Measurements to Characterize Porous Materials. *International Scholarly Research Notices*, 2013(1), 496352. <https://doi.org/10.1155/2013/496352>

- Mammo, F. K., Amoah, I. D., Gani, K. M., Pillay, L., Ratha, S. K., Bux, F., & Kumari, S. (2020). Microplastics in the environment: Interactions with microbes and chemical contaminants. *Science of The Total Environment*, 743, 140518. <https://doi.org/https://doi.org/10.1016/j.scitotenv.2020.140518>
- Mancini, M., Francalanci, S., Innocenti, L., & Solari, L. (2023). Investigations on microplastic infiltration within natural riverbed sediments. *Science of The Total Environment*, 904, 167256. <https://doi.org/https://doi.org/10.1016/j.scitotenv.2023.167256>
- Manini, E., Baldrighi, E., Ricci, F., Grilli, F., Giovannelli, D., Intoccia, M., Casabianca, S., Capellacci, S., Marinchel, N., Penna, P., Moro, F., Campanelli, A., Cordone, A., Correggia, M., Bastoni, D., Bolognini, L., Marini, M., & Penna, A. (2022). Assessment of Spatio-Temporal Variability of Faecal Pollution along Coastal Waters during and after Rainfall Events. *Water (Switzerland)*, 14(3). <https://doi.org/10.3390/w14030502>
- Marfella, R., Prattichizzo, F., Sardu, C., Fulgenzi, G., Graciotti, L., Spadoni, T., D'Onofrio, N., Scisciola, L., Grotta, R. L., Frigé, C., Pellegrini, V., Municinò, M., Siniscalchi, M., Spinetti, F., Vigliotti, G., Vecchione, C., Carrizzo, A., Accarino, G., Squillante, A., . . . Paolisso, G. (2024). Microplastics and Nanoplastics in Atheromas and Cardiovascular Events. *New England Journal of Medicine*, 390(10), 900-910. <https://doi.org/doi:10.1056/NEJMoa2309822>
- MARPOL. (1997). Annex IV of MARPOL 73 / 78 Regulations for the Prevention of Pollution by Sewage from Ships. *Marpol*, 78(December 1979).
- Marsden, P., Koelmans, A. A., Bourdon-Lacombe, J., Gouin, T., Anglada, L. D., Cunliffe, D., Jarvis, P., Fawell, J., & France, J. D. (2019). *Microplastics in drinking water* (9789241516198). <https://edepot.wur.nl/498693>
- Mayer, R. E., Bofill-Mas, S., Egle, L., Reischer, G. H., Schade, M., Fernandez-Cassi, X., Fuchs, W., Mach, R. L., Lindner, G., Kirschner, A., Gaisbauer, M., Piringner, H., Blaschke, A. P., Girones, R., Zessner, M., Sommer, R., & Farnleitner, A. H. (2016). Occurrence of human-associated Bacteroidetes genetic source tracking markers in raw and treated wastewater of municipal and domestic origin and comparison to standard and alternative indicators of faecal pollution. *Water Research*, 90, 265-276. <https://doi.org/10.1016/j.watres.2015.12.031>
- Mayer, R. E., Reischer, G. H., Ixenmaier, S. K., Derx, J., Blaschke, A. P., Ebdon, J. E., Linke, R., Egle, L., Ahmed, W., Blanch, A. R., Byamukama, D., Savill, M., Mushi, D., Cristóbal, H. A., Edge, T. A., Schade, M. A., Aslan, A., Brooks, Y. M., Sommer, R., . . . Farnleitner, A. H. (2018). Global Distribution of Human-Associated Fecal Genetic Markers in Reference Samples from Six Continents. *Environmental Science and Technology*, 52(9), 5076-5084. <https://doi.org/10.1021/acs.est.7b04438>
- Mazzocco, A., Waddell, T. E., Lingohr, E., & Johnson, R. P. (2009). Enumeration of bacteriophages using the small drop plaque assay system. *Methods Mol Biol*, 501, 81-85. https://doi.org/10.1007/978-1-60327-164-6_9
- McKee, L. J., & Gilbreath, A. N. (2015). Concentrations and loads of suspended sediment and trace element pollutants in a small semi-arid urban tributary, San Francisco Bay, California. *Environmental Monitoring and Assessment*, 187(8), 499. <https://doi.org/10.1007/s10661-015-4710-4>
- Mei, H., & Lu, X. (2014). The quantitative description between zeta potential and fluorescent particle adsorption on Cu surface [Article]. *Surface and Interface Analysis*, 46(1), 56-60. <https://doi.org/10.1002/sia.5348>
- Mendoza, L. M. R., & Balcer, M. (2019). Microplastics in freshwater environments: A review of quantification assessment. *TrAC Trends in Analytical Chemistry*, 113, 402-408.
- Mesquita, M. M. F., Stimson, J., Chae, G. T., Tufenkji, N., Ptacek, C. J., Blowes, D. W., & Emelko, M. B. (2010). Optimal preparation and purification of PRD1-like bacteriophages for use in environmental fate and transport studies. *Water Research*, 44(4), 1114-1125. <https://doi.org/https://doi.org/10.1016/j.watres.2009.11.017>
- Microsoft Corporation. (2019). Microsoft Excel. In.
- Mieszkin, S., Furet, J. P., Corthier, G., & Gourmelon, M. (2009). Estimation of pig fecal contamination in a river catchment by real-time PCR using two Pig-Specific Bacteroidales 16S rRNA genetic markers. *Applied and Environmental Microbiology*, 75(10), 3045-3054. <https://doi.org/10.1128/AEM.02343-08>
- Mignon-Godefroy, K., Guillet, J.-G., & Butor, C. (1997). Solid phase cytometry for detection of rare events. *Cytometry*, 27(4), 336-344. [https://doi.org/https://doi.org/10.1002/\(SICI\)1097-0320\(19970401\)27:4<336::AID-CYTO4>3.0.CO;2-A](https://doi.org/https://doi.org/10.1002/(SICI)1097-0320(19970401)27:4<336::AID-CYTO4>3.0.CO;2-A)
- Mikkola, O. (2020). Estimating microplastic concentrations and loads in cruise ship grey waters.
- Mintenig, S., Löder, M., Primpke, S., & Gerdt, G. (2019a). Low numbers of microplastics detected in drinking water from ground water sources. *Science of The Total Environment*, 648, 631-635.

- Mintenig, S. M., Löder, M. G. J., Primpke, S., & Gerdts, G. (2019b). Low numbers of microplastics detected in drinking water from ground water sources. *Science of The Total Environment*, 648, 631-635. <https://doi.org/https://doi.org/10.1016/j.scitotenv.2018.08.178>
- Miranda, M. N., Silva, A. M. T., & Pereira, M. F. R. (2020). Microplastics in the environment: A DPSIR analysis with focus on the responses. *Science of The Total Environment*, 718, 134968. <https://doi.org/https://doi.org/10.1016/j.scitotenv.2019.134968>
- Molnar, I. L., Johnson, W. P., Gerhard, J. I., Willson, C. S., & O'Carroll, D. M. (2015). Predicting colloid transport through saturated porous media: A critical review. *Water Resources Research*, 51(9), 6804-6845. <https://doi.org/https://doi.org/10.1002/2015WR017318>
- Moon, K., Jeon, J. H., Kang, I., Park, K. S., Lee, K., Cha, C.-J., Lee, S. H., & Cho, J.-C. (2020). Freshwater viral metagenome reveals novel and functional phage-borne antibiotic resistance genes. *Microbiome*, 8(1), 75. <https://doi.org/10.1186/s40168-020-00863-4>
- Moresco, V., Charatzidou, A., Oliver, D. M., Weidmann, M., Matallana-Surget, S., & Quilliam, R. S. (2022). Binding, recovery, and infectiousness of enveloped and non-enveloped viruses associated with plastic pollution in surface water. *Environmental Pollution*, 308, 119594. <https://doi.org/https://doi.org/10.1016/j.envpol.2022.119594>
- Moresco, V., Damazo, N. A., & Barardi, C. R. M. (2015). Thermal and temporal stability on the enteric viruses infectivity in surface freshwater. *Water Supply*, 16(3), 620-627. <https://doi.org/10.2166/ws.2015.171>
- Murphy, F., Ewins, C., Carbonnier, F., & Quinn, B. (2016). Wastewater Treatment Works (WwTW) as a Source of Microplastics in the Aquatic Environment. *Environmental Science & Technology*, 50(11), 5800-5808. <https://doi.org/10.1021/acs.est.5b05416>
- Murphy, H. M., Prioleau, M. D., Borchardt, M. A., & Hynds, P. D. (2017). Review: Epidemiological evidence of groundwater contribution to global enteric disease, 1948–2015. *Hydrogeology Journal*, 25(4), 981-1001. <https://doi.org/10.1007/s10040-017-1543-y>
- Napper, I. E., Bakir, A., Rowland, S. J., & Thompson, R. C. (2015). Characterisation, quantity and sorptive properties of microplastics extracted from cosmetics. *Marine Pollution Bulletin*, 99(1), 178-185. <https://doi.org/https://doi.org/10.1016/j.marpolbul.2015.07.029>
- O'Connor, D., Pan, S., Shen, Z., Song, Y., Jin, Y., Wu, W.-M., & Hou, D. (2019). Microplastics undergo accelerated vertical migration in sand soil due to small size and wet-dry cycles. *Environmental Pollution*, 249, 527-534. <https://doi.org/https://doi.org/10.1016/j.envpol.2019.03.092>
- Oberbeckmann, S., Kreikemeyer, B., & Labrenz, M. (2018). Environmental Factors Support the Formation of Specific Bacterial Assemblages on Microplastics [Original Research]. *Frontiers in Microbiology*, 8. <https://doi.org/10.3389/fmicb.2017.02709>
- Ochirbat, E., Zbonikowski, R., Sulicka, A., Bończak, B., Bonarowska, M., Łoś, M., Malinowska, E., Hołyst, R., & Paczesny, J. (2023). Heteroaggregation of virions and microplastics reduces the number of active bacteriophages in aqueous environments. *J Environ Qual*, 52(3), 665-677. <https://doi.org/https://doi.org/10.1002/jeq2.20459>
- Oudega, T. J., Lindner, G., Derx, J., Farnleitner, A. H., Sommer, R., Blaschke, A. P., & Stevenson, M. E. (2021). Upscaling Transport of *Bacillus subtilis* Endospores and Coliphage phiX174 in Heterogeneous Porous Media from the Column to the Field Scale. *Environmental Science & Technology*, 55(16), 11060-11069. <https://doi.org/10.1021/acs.est.1c01892>
- Panno, S. V., Kelly, W. R., Scott, J., Zheng, W., McNeish, R. E., Holm, N., Hoellein, T. J., & Baranski, E. L. (2019). Microplastic Contamination in Karst Groundwater Systems. *Groundwater*, 57(2), 189-196. <https://doi.org/https://doi.org/10.1111/gwat.12862>
- Parks, M., Ahmasuk, A., Compagnoni, B., Norris, A., & Rufe, R. (2019). Quantifying and mitigating three major vessel waste streams in the northern Bering Sea. *Marine Policy*, 106, 103530. <https://doi.org/https://doi.org/10.1016/j.marpol.2019.103530>
- Pastorino, B., Touret, F., Gilles, M., de Lamballerie, X., & Charrel, R. N. (2020). Prolonged Infectivity of SARS-CoV-2 in Fomites. *Emerg Infect Dis*, 26(9), 2256-2257. <https://doi.org/10.3201/eid2609.201788>
- Pelley, A. J., & Tufenkji, N. (2008). Effect of particle size and natural organic matter on the migration of nano- and microscale latex particles in saturated porous media. *Journal of Colloid and Interface Science*, 321(1), 74-83. <https://doi.org/https://doi.org/10.1016/j.jcis.2008.01.046>
- Peng, G., Xu, B., & Li, D. (2022). Gray Water from Ships: A Significant Sea-Based Source of Microplastics? *Environmental Science & Technology*, 56(1), 4-7. <https://doi.org/10.1021/acs.est.1c05446>

- Peng, S., Wu, D., Ge, Z., Tong, M., & Kim, H. (2017). Influence of graphene oxide on the transport and deposition behaviors of colloids in saturated porous media. *Environmental Pollution*, 225, 141-149. <https://doi.org/https://doi.org/10.1016/j.envpol.2017.03.064>
- Perić, T., Komadina, P., & Račić, N. (2016). Wastewater pollution from cruise ships in the Adriatic Sea. *Promet-Traffic&Transportation*, 28(4), 425-433.
- Petschko, H., Brenning, A., Bell, R., Goetz, J., & Glade, T. (2014). Assessing the quality of landslide susceptibility maps - Case study Lower Austria. *Natural Hazards and Earth System Sciences*, 14(1), 95-118. <https://doi.org/10.5194/nhess-14-95-2014>
- Pham, D. N., Clark, L., & Li, M. (2021). Microplastics as hubs enriching antibiotic-resistant bacteria and pathogens in municipal activated sludge. *Journal of Hazardous Materials Letters*, 2, 100014. <https://doi.org/https://doi.org/10.1016/j.hazl.2021.100014>
- Piñon-Colin, T. d. J., Rodriguez-Jimenez, R., Rogel-Hernandez, E., Alvarez-Andrade, A., & Wakida, F. T. (2020). Microplastics in stormwater runoff in a semiarid region, Tijuana, Mexico. *Science of The Total Environment*, 704, 135411. <https://doi.org/https://doi.org/10.1016/j.scitotenv.2019.135411>
- Pivokonsky, M., Cermakova, L., Novotna, K., Peer, P., Cajthaml, T., & Janda, V. (2018). Occurrence of microplastics in raw and treated drinking water. *Science of The Total Environment*, 643, 1644-1651. <https://doi.org/https://doi.org/10.1016/j.scitotenv.2018.08.102>
- Pradel, A., Hadri, H. e., Desmet, C., Ponti, J., Reynaud, S., Grassl, B., & Gigault, J. (2020). Deposition of environmentally relevant nanoplastic models in sand during transport experiments. *Chemosphere*, 255, 126912. <https://doi.org/https://doi.org/10.1016/j.chemosphere.2020.126912>
- Presburger Ulnikovic, V., Vukic, M., & Nikolic, R. (2012). Assessment of vessel-generated waste quantities on the inland waterways of the Republic of Serbia. *Journal of Environmental Management*, 97, 97-101. <https://doi.org/https://doi.org/10.1016/j.jenvman.2011.11.003>
- Pröbstl-Haider, U., Hödl, C., Ginner, K., & Borgwardt, F. (2021). Climate change: Impacts on outdoor activities in the summer and shoulder seasons. *Journal of Outdoor Recreation and Tourism*, 34(October 2020). <https://doi.org/10.1016/j.jort.2020.100344>
- Purwiyanto, A. I. S., Suteja, Y., Trisno, Ningrum, P. S., Putri, W. A. E., Rozirwan, Agustriani, F., Fauziyah, Cordova, M. R., & Koropitan, A. F. (2020). Concentration and adsorption of Pb and Cu in microplastics: Case study in aquatic environment. *Marine Pollution Bulletin*, 158, 111380. <https://doi.org/https://doi.org/10.1016/j.marpolbul.2020.111380>
- Qiu, L., Lu, W., Tu, C., Li, X., Zhang, H., Wang, S., Chen, M., Zheng, X., Wang, Z., Lin, M., Zhang, Y., Zhong, C., Li, S., Liu, Y., Liu, J., & Zhou, Y. (2023). Evidence of Microplastics in Bronchoalveolar Lavage Fluid among Never-Smokers: A Prospective Case Series. *Environmental Science & Technology*, 57(6), 2435-2444. <https://doi.org/10.1021/acs.est.2c06880>
- R Core Team. (2022). R: A Language and Environment for Statistical Computing. In. Vienna, Austria.
- Rakib, M. R. J., Al Nahian, S., Madadi, R., Haider, S. M. B., De-la-Torre, G. E., Walker, T. R., Jonathan, M. P., Cowger, W., Khandaker, M. U., & Idris, A. M. (2023). Spatiotemporal trends and characteristics of microplastic contamination in a large river-dominated estuary [10.1039/D3EM00014A]. *Environmental Science: Processes & Impacts*, 25(5), 929-940. <https://doi.org/10.1039/D3EM00014A>
- Ranhand, J. M. (1974). Simple, Inexpensive Procedure for the Disruption of Bacteria. *Applied Microbiology*, 28(1), 66-69. <https://doi.org/doi:10.1128/am.28.1.66-69.1974>
- Re, V. (2019). Shedding light on the invisible: addressing the potential for groundwater contamination by plastic microfibers. *Hydrogeology Journal*, 27(7), 2719-2727. <https://doi.org/10.1007/s10040-019-01998-x>
- Reischer, G. H., Ebdon, J. E., Bauer, J. M., Schuster, N., Ahmed, W., Åström, J., Blanch, A. R., Blöschl, G., Byamukama, D., Coakley, T., Ferguson, C., Goshu, G., Ko, G., De Roda Husman, A. M., Mushi, D., Poma, R., Pradhan, B., Rajal, V., Schade, M. A., . . . Farnleitner, A. H. (2013). Performance characteristics of qPCR assays targeting human- and ruminant-associated bacteroidetes for microbial source tracking across sixteen countries on six continents. *Environmental Science and Technology*, 47(15), 8548-8556. <https://doi.org/10.1021/es304367t>
- Reischer, G. H., Kasper, D. C., Steinborn, R., Farnleitner, A. H., & Mach, R. L. (2007). A quantitative real-time PCR assay for the highly sensitive and specific detection of human faecal influence in spring water from a large alpine catchment area. *Letters in Applied Microbiology*, 44(4), 351-356. <https://doi.org/10.1111/j.1472-765X.2006.02094.x>
- Reischer, G. H., Kasper, D. C., Steinborn, R., Mach, R. L., & Farnleitner, A. H. (2006). Quantitative PCR method for sensitive detection of ruminant fecal pollution in freshwater and evaluation of this method in alpine

karstic regions. *Applied and Environmental Microbiology*, 72(8), 5610-5614. <https://doi.org/10.1128/AEM.00364-06>

- Reischer, G. H., Kollanur, D., Vierheilig, J., Wehrspau, C., MacH, R. L., Sommer, R., Stadler, H., & Farnleitner, A. H. (2011). Hypothesis-driven approach for the identification of fecal pollution sources in water resources. *Environmental Science and Technology*, 45(9), 4038-4045. <https://doi.org/10.1021/es103659s>
- Ren, S.-Y., Sun, Q., Ni, H.-G., & Wang, J. (2020). A minimalist approach to quantify emission factor of microplastic by mechanical abrasion. *Chemosphere*, 245, 125630.
- Ren, Z., Gui, X., Wei, Y., Chen, X., Xu, X., Zhao, L., Qiu, H., & Cao, X. (2021). Chemical and photo-initiated aging enhances transport risk of microplastics in saturated soils: Key factors, mechanisms, and modeling. *Water Research*, 202, 117407. <https://doi.org/https://doi.org/10.1016/j.watres.2021.117407>
- Rillig, M. C., Ingraffia, R., & de Souza Machado, A. A. (2017). Microplastic Incorporation into Soil in Agroecosystems [Opinion]. *Frontiers in Plant Science*, 8. <https://doi.org/10.3389/fpls.2017.01805>
- Rochman, C. M. (2018). Microplastics research—from sink to source. *Science*, 360(6384), 28-29.
- RStudio Team. (2021). RStudio: Integrated Development Environment for R. In Boston, MA.
- Saiers, J. E., & Ryan, J. N. (2005). Colloid deposition on non-ideal porous media: The influences of collector shape and roughness on the single-collector efficiency. *Geophysical Research Letters*, 32(21). <https://doi.org/https://doi.org/10.1029/2005GL024343>
- Samandra, S., Johnston, J. M., Jaeger, J. E., Symons, B., Xie, S., Currell, M., Ellis, A. V., & Clarke, B. O. (2022). Microplastic contamination of an unconfined groundwater aquifer in Victoria, Australia. *Science of The Total Environment*, 802, 149727. <https://doi.org/https://doi.org/10.1016/j.scitotenv.2021.149727>
- Sanches, V. L., Aguiar, M. R. d. C. M., de Freitas, M. A. V., & Pacheco, E. B. A. V. (2020). Management of cruise ship-generated solid waste: A review. *Marine Pollution Bulletin*, 151, 110785-110785. <https://doi.org/https://doi.org/10.1016/j.marpolbul.2019.110785>
- SAPEA. (2019). *A scientific perspective on microplastics in nature and society: Evidence review report (1.1)*. Publications Office of the European Union. <https://doi.org/10.26356/microplastics>
- Schauer, S., Sommer, R., Farnleitner Andreas, H., & Kirschner Alexander, K. T. (2012). Rapid and Sensitive Quantification of *Vibrio cholerae* and *Vibrio mimicus* Cells in Water Samples by Use of Catalyzed Reporter Deposition Fluorescence In Situ Hybridization Combined with Solid-Phase Cytometry. *Applied and Environmental Microbiology*, 78(20), 7369-7375. <https://doi.org/10.1128/AEM.02190-12>
- Schiemer, F., Baumgartner, C., & Tockner, K. (1999). Restoration of floodplain rivers: The 'Danube Restoration Project'. *Regulated Rivers: Research and Management*, 15(1-3), 231-244. [https://doi.org/10.1002/\(SICI\)1099-1646\(199901/06\)15:1/3<231::AID-RRR548>3.0.CO;2-5](https://doi.org/10.1002/(SICI)1099-1646(199901/06)15:1/3<231::AID-RRR548>3.0.CO;2-5)
- Schijven, J. F., & Hassanizadeh, S. M. (2000). Removal of Viruses by Soil Passage: Overview of Modeling, Processes, and Parameters. *Critical Reviews in Environmental Science and Technology*, 30(1), 49-127. <https://doi.org/10.1080/10643380091184174>
- Schijven, J. F., & Šimůnek, J. (2002). Kinetic modeling of virus transport at the field scale. *Journal of Contaminant Hydrology*, 55(1), 113-135. [https://doi.org/https://doi.org/10.1016/S0169-7722\(01\)00188-7](https://doi.org/https://doi.org/10.1016/S0169-7722(01)00188-7)
- Schnurr, R. E. J., & Walker, T. R. (2019). Marine Transportation and Energy Use☆. In *Reference Module in Earth Systems and Environmental Sciences*. Elsevier. <https://doi.org/https://doi.org/10.1016/B978-0-12-409548-9.09270-8>
- Senathirajah, K., Attwood, S., Bhagwat, G., Carbery, M., Wilson, S., & Palanisami, T. (2021). Estimation of the mass of microplastics ingested – A pivotal first step towards human health risk assessment. *Journal of Hazardous Materials*, 404, 124004. <https://doi.org/https://doi.org/10.1016/j.jhazmat.2020.124004>
- Shellenberger, K., & Logan, B. E. (2002). Effect of Molecular Scale Roughness of Glass Beads on Colloidal and Bacterial Deposition. *Environmental Science & Technology*, 36(2), 184-189. <https://doi.org/10.1021/es015515k>
- Shen, C., Bradford, S. A., Li, T., Li, B., & Huang, Y. (2018). Can nanoscale surface charge heterogeneity really explain colloid detachment from primary minima upon reduction of solution ionic strength? *Journal of Nanoparticle Research*, 20(6), 165. <https://doi.org/10.1007/s11051-018-4265-8>
- Shen, M., Zhu, Y., Zhang, Y., Zeng, G., Wen, X., Yi, H., Ye, S., Ren, X., & Song, B. (2019). Micro(nano)plastics: Unignorable vectors for organisms. *Marine Pollution Bulletin*, 139, 328-331. <https://doi.org/https://doi.org/10.1016/j.marpolbul.2019.01.004>
- Shen, S., Yang, S., Jiang, Q., Luo, M., Li, Y., Yang, C., & Zhang, D. (2020). Effect of dissolved organic matter on adsorption of sediments to Oxytetracycline: An insight from zeta potential and DLVO theory

[Article]. *Environmental Science and Pollution Research*, 27(2), 1697-1709. <https://doi.org/10.1007/s11356-019-06787-3>

- Shim, W. J., & Thomposon, R. C. (2015). Microplastics in the Ocean. *Archives of Environmental Contamination and Toxicology*, 69(3), 265-268. <https://doi.org/10.1007/s00244-015-0216-x>
- Sidhu, J. P. S., Toze, S., Hodgers, L., Shackelton, M., Barry, K., Page, D., & Dillon, P. (2010). Pathogen inactivation during passage of stormwater through a constructed reedbed and aquifer transfer, storage and recovery. *Water Science and Technology*, 62(5), 1190-1197. <https://doi.org/10.2166/wst.2010.398>
- Simunek, J., Jacques, D., Langergraber, G., Bradford, S. A., Šejna, M., & van Genuchten, M. T. (2013). Numerical modeling of contaminant transport using HYDRUS and its specialized modules. *Journal of the Indian institute of science*, 93(2), 265-284.
- Simunek, J., van Genuchten, M. T., & Sejna, M. (2016). Recent Developments and Applications of the HYDRUS Computer Software Packages. *Vadose Zone Journal*, 15(7). <https://doi.org/10.2136/vzj2016.04.0033>
- Sinton, L. W., Finlay, R. K., Pang, L., & Scott, D. M. (1997). Transport of bacteria and bacteriophages in irrigated effluent into and through an alluvial gravel aquifer. *Water, Air, and Soil Pollution*, 98(1), 17-42. <https://doi.org/10.1007/BF02128648>
- Sirivithayapakorn, S., & Keller, A. (2003). Transport of colloids in saturated porous media: A pore-scale observation of the size exclusion effect and colloid acceleration. *Water Resources Research*, 39(4). <https://doi.org/https://doi.org/10.1029/2002WR001583>
- Skraber, S., Ogorzaly, L., Helmi, K., Maul, A., Hoffmann, L., Cauchie, H.-M., & Gantzer, C. (2009). Occurrence and persistence of enteroviruses, noroviruses and F-specific RNA phages in natural wastewater biofilms. *Water Research*, 43(19), 4780-4789. <https://doi.org/https://doi.org/10.1016/j.watres.2009.05.020>
- Slizovskiy, I. B., Mukherjee, K., Dean, C. J., Boucher, C., & Noyes, N. R. (2020). Mobilization of Antibiotic Resistance: Are Current Approaches for Colocalizing Resistomes and Mobilomes Useful? [Original Research]. *Frontiers in Microbiology*, 11. <https://doi.org/10.3389/fmicb.2020.01376>
- Sobotkova, M., & Snehota, M. (2014). Method of In-Line Bromide Breakthrough Curve Measurements for Column Leaching Experiments. *Vadose Zone Journal*, 13(8), vzj2013.2011.0192. <https://doi.org/https://doi.org/10.2136/vzj2013.11.0192>
- Sobsey, M. D., Perdue, R., Overton, M., & Fisher, J. (2003). Factors influencing faecal contamination in coastal marinas. *Water Science and Technology*, 47(3), 199-204. <https://doi.org/10.2166/wst.2003.0195>
- Sommer, J., Bromberger, B., Robben, C., Kalb, R., Rossmannith, P., & Mester, P.-J. (2021). Liquid-liquid extraction of viral particles with ionic liquids. *Separation and Purification Technology*, 254, 117591. <https://doi.org/https://doi.org/10.1016/j.seppur.2020.117591>
- Song, Y. K., Hong, S. H., Jang, M., Han, G. M., Jung, S. W., & Shim, W. J. (2017). Combined effects of UV exposure duration and mechanical abrasion on microplastic fragmentation by polymer type. *Environmental Science & Technology*, 51(8), 4368-4376.
- Sotirelis, N. P., & Chrysikopoulos, C. V. (2015). Interaction Between Graphene Oxide Nanoparticles and Quartz Sand. *Environmental Science & Technology*, 49(22), 13413-13421. <https://doi.org/10.1021/acs.est.5b03496>
- Stadler, H., Skritek, P., Sommer, R., Mach, R. L., Zerobin, W., & Farnleitner, A. H. (2008). Microbiological monitoring and automated event sampling at karst springs using LEO-satellites. *Water Science and Technology*, 58(4), 899-909. <https://doi.org/10.2166/wst.2008.442>
- Staley, C., Gould, T. J., Wang, P., Phillips, J., Cotner, J. B., Sadowsky, M. J., & Gibbons, S. M. (2014). Bacterial community structure is indicative of chemical inputs in the Upper Mississippi River. 5(October), 1-13. <https://doi.org/10.3389/fmicb.2014.00524>
- Steiger, R., & Scott, D. (2020). Ski tourism in a warmer world: Increased adaptation and regional economic impacts in Austria. *Tourism Management*, 77(November 2019), 104032-104032. <https://doi.org/10.1016/j.tourman.2019.104032>
- Steinbacher, S. D., Savio, D., Demeter, K., Karl, M., Kandler, W., Kirschner, A. K. T., Reischer, G. H., Ixenmaier, S. K., Mayer, R. E., Mach, R. L., Derx, J., Sommer, R., Linke, R., & Farnleitner, A. H. (2021). Genetic microbial faecal source tracking: rising technology to support future water quality testing and safety management. *Österreichische Wasser- und Abfallwirtschaft*. <https://doi.org/10.1007/s00506-021-00811-1>
- Stevenson, M. E., Blaschke, A. P., Schauer, S., Zessner, M., Sommer, R., Farnleitner, A. H., & Kirschner, A. K. T. (2014). Enumerating Microorganism Surrogates for Groundwater Transport Studies Using Solid-

Phase Cytometry. *Water, Air, & Soil Pollution*, 225(2), 1827. <https://doi.org/10.1007/s11270-013-1827-3>

- Stevenson, M. E., Sommer, R., Lindner, G., Farnleitner, A. H., Toze, S., Kirschner, A. K., Blaschke, A. P., & Sidhu, J. P. (2015). Attachment and Detachment Behavior of Human Adenovirus and Surrogates in Fine Granular Limestone Aquifer Material. *J Environ Qual*, 44(5), 1392-1401. <https://doi.org/10.2134/jeq2015.01.0052>
- Syranidou, E., & Kalogerakis, N. (2022). Interactions of microplastics, antibiotics and antibiotic resistant genes within WWTPs. *Science of The Total Environment*, 804, 150141. <https://doi.org/https://doi.org/10.1016/j.scitotenv.2021.150141>
- Tamburri, M. N., Soon, Z. Y., Scianni, C., Øpstad, C. L., Oxtoby, N. S., Doran, S., & Drake, L. A. (2022). Understanding the potential release of microplastics from coatings used on commercial ships [Policy Brief]. *Frontiers in Marine Science*, 9. <https://doi.org/10.3389/fmars.2022.1074654>
- Tang, K. H. D., & Li, R. (2024). The effects of plastisphere on the physicochemical properties of microplastics. *Bioprocess and Biosystems Engineering*. <https://doi.org/10.1007/s00449-024-03059-4>
- Thompson, R. C., Olsen, Y., Mitchell, R. P., Davis, A., Rowland, S. J., John, A. W. G., McGonigle, D., & Russell, A. E. (2004). Lost at Sea: Where Is All the Plastic? *Science*, 304(5672), 838-838. <https://doi.org/doi:10.1126/science.1094559>
- Thompson, R. C., Swan, S. H., Moore, C. J., & vom Saal, F. S. (2009). Our plastic age. *Philosophical Transactions of the Royal Society B: Biological Sciences*, 364(1526), 1973-1976. <https://doi.org/doi:10.1098/rstb.2009.0054>
- Torkzaban, S., Bradford, S. A., Wan, J., Tokunaga, T., & Masoudih, A. (2013). Release of Quantum Dot Nanoparticles in Porous Media: Role of Cation Exchange and Aging Time. *Environmental Science & Technology*, 47(20), 11528-11536. <https://doi.org/10.1021/es402075f>
- Toscano, D., Murena, F., Quaranta, F., & Mocerino, L. (2021). Assessment of the impact of ship emissions on air quality based on a complete annual emission inventory using AIS data for the port of Naples. *Ocean Engineering*, 232(May), 109166-109166. <https://doi.org/10.1016/j.oceaneng.2021.109166>
- Trivedi, A., Jakhar, S. K., & Sinha, D. (2021). Analyzing barriers to inland waterways as a sustainable transportation mode in India: A dematel-ISM based approach. *Journal of Cleaner Production*, 295, 126301-126301. <https://doi.org/10.1016/j.jclepro.2021.126301>
- Tufenkji, N., & Elimelech, M. (2004a). Correlation Equation for Predicting Single-Collector Efficiency in Physicochemical Filtration in Saturated Porous Media. *Environmental Science & Technology*, 38(2), 529-536. <https://doi.org/10.1021/es034049r>
- Tufenkji, N., & Elimelech, M. (2004b). Deviation from the Classical Colloid Filtration Theory in the Presence of Repulsive DLVO Interactions. *Langmuir*, 20(25), 10818-10828. <https://doi.org/10.1021/la0486638>
- Tufenkji, N., Miller, G. F., Ryan, J. N., Harvey, R. W., & Elimelech, M. (2004). Transport of Cryptosporidium Oocysts in Porous Media: Role of Straining and Physicochemical Filtration. *Environmental Science & Technology*, 38(22), 5932-5938. <https://doi.org/10.1021/es049789u>
- Tufenkji, N., Ryan, J. N., & Elimelech, M. (2002). The Promise of Bank Filtration. *Environmental Science & Technology*, 36(21), 422A-428A. <https://doi.org/10.1021/es022441j>
- Tumwet, F. C., Serbe, R., Kleint, T., & Scheytt, T. (2022). Effect of fragmentation on the transport of polyvinyl chloride and low-density polyethylene in saturated quartz sand. *Science of The Total Environment*, 836, 155657. <https://doi.org/https://doi.org/10.1016/j.scitotenv.2022.155657>
- Turner, A. (2021). Paint particles in the marine environment: An overlooked component of microplastics. *Water Research X*, 12, 100110. <https://doi.org/https://doi.org/10.1016/j.wroa.2021.100110>
- US EPA. (2016). Basic information about biosolids [other policies and guidance]. <https://www.epa.gov/biosolids/basic-information-about-biosolids>
- van Driezum, I. H., Chik, A. H. S., Jakwerth, S., Lindner, G., Farnleitner, A. H., Sommer, R., Blaschke, A. P., & Kirschner, A. K. T. (2018). Spatiotemporal analysis of bacterial biomass and activity to understand surface and groundwater interactions in a highly dynamic riverbank filtration system. *Science of The Total Environment*, 627, 450-461. <https://doi.org/https://doi.org/10.1016/j.scitotenv.2018.01.226>
- Vaneckhaute, C., & Fazli, A. (2020). Management of ship-generated food waste and sewage on the Baltic Sea: A review. *Waste Management*, 102, 12-20. <https://doi.org/10.1016/j.wasman.2019.10.030>
- Verwey, E. J. W., & Overbeek, J. T. G. (1955). Theory of the stability of lyophobic colloids [Letter]. *Journal of Colloid Science*, 10(2), 224-225. [https://doi.org/10.1016/0095-8522\(55\)90030-1](https://doi.org/10.1016/0095-8522(55)90030-1)

- Viadonau. (2019a). Annual Report on Danube Navigation in Austria 2019. 46-46. https://www.viadonau.org/fileadmin/user_upload/Annual_Report_on_Danube_Navigation_2019.pdf
- Viadonau. (2019b). Manual on Danube Navigation. In.
- Viadonau. (2021). *Annual Report on Danube Navigation*. https://www.viadonau.org/fileadmin/user_upload/viadonau_Annual_Report_on_Danube_Navigation_2021.pdf
- Viadonau. (2022). Annual Report on Danube Navigation in Austria. https://www.viadonau.org/fileadmin/user_upload/viadonau_Annual_Report_on_Danube_Navigation_2022.pdf
- Waldschläger, K., & Schüttrumpf, H. (2020). Infiltration Behavior of Microplastic Particles with Different Densities, Sizes, and Shapes—From Glass Spheres to Natural Sediments. *Environmental Science & Technology*, 54(15), 9366-9373. <https://doi.org/10.1021/acs.est.0c01722>
- Walker, T. R. (2021). (Micro)plastics and the UN Sustainable Development Goals. *Current Opinion in Green and Sustainable Chemistry*, 30, 100497. <https://doi.org/https://doi.org/10.1016/j.cogsc.2021.100497>
- Walley, S. M., Field, J. E., & Tabor, D. (1987). The erosion and deformation of polyethylene by solid-particle impact. *Philosophical Transactions of the Royal Society of London. Series A, Mathematical and Physical Sciences*, 321(1558), 277-303. <https://doi.org/doi:10.1098/rsta.1987.0016>
- Walshe, G. E., Pang, L., Flury, M., Close, M. E., & Flintoft, M. (2010). Effects of pH, ionic strength, dissolved organic matter, and flow rate on the co-transport of MS2 bacteriophages with kaolinite in gravel aquifer media. *Water Research*, 44(4), 1255-1269. <https://doi.org/https://doi.org/10.1016/j.watres.2009.11.034>
- Wang, X., Zhang, R., Li, Z., & Yan, B. (2022a). Adsorption properties and influencing factors of Cu(II) on polystyrene and polyethylene terephthalate microplastics in seawater. *Science of The Total Environment*, 812, 152573. <https://doi.org/https://doi.org/10.1016/j.scitotenv.2021.152573>
- Wang, X., Zheng, K., Wang, Y., Hou, X., He, Y., Wang, Z., Zhang, J., Chen, X., & Liu, X. (2024). Microplastics and viruses in the aquatic environment: a mini review [Mini Review]. *Frontiers in Microbiology*, 15. <https://doi.org/10.3389/fmicb.2024.1433724>
- Wang, Y., Wang, F., Xiang, L., Bian, Y., Wang, Z., Srivastava, P., Jiang, X., & Xing, B. (2022b). Attachment of positively and negatively charged submicron polystyrene plastics on nine typical soils. *Journal of Hazardous Materials*, 431, 128566. <https://doi.org/https://doi.org/10.1016/j.jhazmat.2022.128566>
- Weingrill, R. B., Lee, M.-J., Benny, P., Riel, J., Saiki, K., Garcia, J., Oliveira, L. F. A. d. M., Fonseca, E. J. d. S., Souza, S. T. d., D'Amato, F. d. O. S., Silva, U. R., Dutra, M. L., Marques, A. L. X., Borbely, A. U., & Urschitz, J. (2023). Temporal trends in microplastic accumulation in placentas from pregnancies in Hawai'i. *Environment International*, 180, 108220. <https://doi.org/https://doi.org/10.1016/j.envint.2023.108220>
- Werbowski, L. M., Gilbreath, A. N., Munno, K., Zhu, X., Grbic, J., Wu, T., Sutton, R., Sedlak, M. D., Deshpande, A. D., & Rochman, C. M. (2021). Urban Stormwater Runoff: A Major Pathway for Anthropogenic Particles, Black Rubbery Fragments, and Other Types of Microplastics to Urban Receiving Waters. *ACS ES&T Water*, 1(6), 1420-1428. <https://doi.org/10.1021/acsestwater.1c00017>
- WHO. (2019). Microplastics in drinking-water. World Health Organization, Geneva. Licence: CC BY-NC-SA 3.0 IGO. <https://www.who.int/publications/i/item/9789241516198>
- Wigginton, K. R., & Kohn, T. (2012). Virus disinfection mechanisms: the role of virus composition, structure, and function. *Current Opinion in Virology*, 2(1), 84-89. <https://doi.org/https://doi.org/10.1016/j.coviro.2011.11.003>
- Windsor, F. M., Durance, I., Horton, A. A., Thompson, R. C., Tyler, C. R., & Ormerod, S. J. (2019). A catchment-scale perspective of plastic pollution. *Global Change Biology*, 25(4), 1207-1221. <https://doi.org/https://doi.org/10.1111/gcb.14572>
- Wondirad, A. (2019). Retracing the past , comprehending the present and contemplating the future of cruise tourism through a meta-analysis of journal publications. *Marine Policy*, 108(May), 103618-103618. <https://doi.org/10.1016/j.marpol.2019.103618>
- World Health Organization. (2017). *Guidelines for drinking-water quality: fourth edition incorporating the first addendum* (978-92-4-154995-0). (Proceedings of the Royal Society of Medicine, Issue.
- World Health Organization. (2021). *Guidelines on Recreational Water Quality* (Vol. 1).
- Wu, P., Huang, J., Zheng, Y., Yang, Y., Zhang, Y., He, F., Chen, H., Quan, G., Yan, J., Li, T., & Gao, B. (2019). Environmental occurrences, fate, and impacts of microplastics. *Ecotoxicology and Environmental Safety*, 184, 109612. <https://doi.org/https://doi.org/10.1016/j.ecoenv.2019.109612>

- Wu, T., Yang, Z., Hu, R., Chen, Y.-F., Zhong, H., Yang, L., & Jin, W. (2021). Film entrainment and microplastic particles retention during gas invasion in suspension-filled microchannels. *Water Research*, 194, 116919. <https://doi.org/https://doi.org/10.1016/j.watres.2021.116919>
- Wu, X., Lyu, X., Li, Z., Gao, B., Zeng, X., Wu, J., & Sun, Y. (2020). Transport of polystyrene nanoplastics in natural soils: Effect of soil properties, ionic strength and cation type. *Science of The Total Environment*, 707, 136065. <https://doi.org/https://doi.org/10.1016/j.scitotenv.2019.136065>
- Wu, X., Zhao, X., Chen, R., Liu, P., Liang, W., Wang, J., Teng, M., Wang, X., & Gao, S. (2022a). Wastewater treatment plants act as essential sources of microplastic formation in aquatic environments: A critical review. *Water Research*, 221, 118825. <https://doi.org/https://doi.org/10.1016/j.watres.2022.118825>
- Wu, Z., Woo, S.-H., Lai, P.-L., & Chen, X. (2022b). The economic impact of inland ports on regional development: Evidence from the Yangtze River region. *Transport Policy*, 127, 80-91. <https://doi.org/https://doi.org/10.1016/j.tranpol.2022.08.012>
- Xu, S., Liao, Q., & Saiers, J. E. (2008). Straining of Nonspherical Colloids in Saturated Porous Media. *Environmental Science & Technology*, 42(3), 771-778. <https://doi.org/10.1021/es071328w>
- Yahya, M. T., Galsomies, L., Gerba, C. P., & Bales, R. C. (1993). Survival of Bacteriophages MS-2 and PRD-1 in Ground Water. *Water Science and Technology*, 27(3-4), 409-412. <https://doi.org/10.2166/wst.1993.0382>
- Yan, X., Yang, X., Tang, Z., Fu, J., Chen, F., Zhao, Y., Ruan, L., & Yang, Y. (2020). Downward transport of naturally-aged light microplastics in natural loamy sand and the implication to the dissemination of antibiotic resistance genes. *Environmental Pollution*, 262, 114270. <https://doi.org/https://doi.org/10.1016/j.envpol.2020.114270>
- Yan, Z., Liu, Y., Zhang, T., Zhang, F., Ren, H., & Zhang, Y. (2022). Analysis of Microplastics in Human Feces Reveals a Correlation between Fecal Microplastics and Inflammatory Bowel Disease Status. *Environmental Science & Technology*, 56(1), 414-421. <https://doi.org/10.1021/acs.est.1c03924>
- Yang, D., Wu, L., Wang, S., Jia, H., Li, K. X., & Yang, D. (2019). How big data enriches maritime research – a critical review of Automatic Identification System (AIS) data applications How big data enriches maritime research – a critical review of. *Transport Reviews*, 39(6), 755-773. <https://doi.org/10.1080/01441647.2019.1649315>
- Yang, Y., Xie, E., Du, Z., Peng, Z., Han, Z., Li, L., Zhao, R., Qin, Y., Xue, M., Li, F., Hua, K., & Yang, X. (2023). Detection of Various Microplastics in Patients Undergoing Cardiac Surgery. *Environmental Science & Technology*, 57(30), 10911-10918. <https://doi.org/10.1021/acs.est.2c07179>
- Yates, M. V., Gerba, C. P., & Kelley, L. M. (1985). Virus persistence in groundwater. *Applied and Environmental Microbiology*, 49(4), 778-781. <https://doi.org/doi:10.1128/aem.49.4.778-781.1985>
- Zhai, X., Zhang, X.-H., & Yu, M. (2023). Microbial colonization and degradation of marine microplastics in the plastisphere: A review [Review]. *Frontiers in Microbiology*, 14. <https://doi.org/10.3389/fmicb.2023.1127308>
- Zhang, D., Chen, Q., Xu, T., & Yin, D. (2025). Current research status on the distribution and transport of micro(nano)plastics in hyporheic zones and groundwater. *Journal of Environmental Sciences*, 151, 387-409. <https://doi.org/https://doi.org/10.1016/j.jes.2024.03.042>
- Zhang, F., Wang, Z., Vijver, M. G., & Peijnenburg, W. J. G. M. (2022a). Theoretical investigation on the interactions of microplastics with a SARS-CoV-2 RNA fragment and their potential impacts on viral transport and exposure. *Science of The Total Environment*, 842, 156812. <https://doi.org/https://doi.org/10.1016/j.scitotenv.2022.156812>
- Zhang, W., Chai, J., Li, S., Wang, X., Wu, S., Liang, Z., Baloch, M. Y. J., Silva, L. F. O., & Zhang, D. (2022b). Physiological characteristics, geochemical properties and hydrological variables influencing pathogen migration in subsurface system: What we know or not? *Geoscience Frontiers*, 13(6), 101346. <https://doi.org/https://doi.org/10.1016/j.gsf.2021.101346>
- Zhang, X., Van Der A, R., Ding, J., Zhang, X., & Yin, Y. (2023). Significant contribution of inland ships to the total NOx emissions along the Yangtze River. *Atmospheric Chemistry and Physics*, 23(9), 5587-5604. <https://doi.org/10.5194/acp-23-5587-2023>
- Zhao, Q., Zhu, L., Weng, J., Jin, Z., Cao, Y., Jiang, H., & Zhang, Z. (2023). Detection and characterization of microplastics in the human testis and semen. *Science of The Total Environment*, 877, 162713. <https://doi.org/https://doi.org/10.1016/j.scitotenv.2023.162713>
- Zhao, W., Jiang, J., Liu, M., Tu, T., Wang, L., & Zhang, S. (2024). Exploring correlations between microplastics, microorganisms, and water quality in an urban drinking water source. *Ecotoxicology and Environmental Safety*, 275, 116249. <https://doi.org/https://doi.org/10.1016/j.ecoenv.2024.116249>

- Zhao, X., Korey, M., Li, K., Copenhaver, K., Tekinalp, H., Celik, S., Kalaitzidou, K., Ruan, R., Ragauskas, A. J., & Ozcan, S. (2022). Plastic waste upcycling toward a circular economy. *Chemical Engineering Journal*, 428, 131928. <https://doi.org/https://doi.org/10.1016/j.cej.2021.131928>
- Zhong, H., Wu, M., Sonne, C., Lam, S. S., Kwong, R. W. M., Jiang, Y., Zhao, X., Sun, X., Zhang, X., Li, C., Li, Y., Qu, G., Jiang, F., Shi, H., Ji, R., & Ren, H. (2023). The hidden risk of microplastic-associated pathogens in aquatic environments. *Eco-Environment & Health*, 2(3), 142-151. <https://doi.org/https://doi.org/10.1016/j.eehl.2023.07.004>
- Zhou, Y., He, G., Jiang, X., Yao, L., Ouyang, L., Liu, X., Liu, W., & Liu, Y. (2021). Microplastic contamination is ubiquitous in riparian soils and strongly related to elevation, precipitation and population density. *Journal of Hazardous Materials*, 411, 125178. <https://doi.org/https://doi.org/10.1016/j.jhazmat.2021.125178>
- Zhu, X. (2021). The Plastic Cycle – An Unknown Branch of the Carbon Cycle [Opinion]. *Frontiers in Marine Science*, 7. <https://doi.org/10.3389/fmars.2020.609243>
- Zhuang, J., Qi, J., & Jin, Y. (2005). Retention and transport of amphiphilic colloids under unsaturated flow conditions: Effect of particle size and surface property [Article]. *Environmental Science and Technology*, 39(20), 7853-7859. <https://doi.org/10.1021/es050265j>
- Ziajahromi, S., Neale, P. A., Rintoul, L., & Leusch, F. D. L. (2017). Wastewater treatment plants as a pathway for microplastics: Development of a new approach to sample wastewater-based microplastics. *Water Research*, 112, 93-99. <https://doi.org/https://doi.org/10.1016/j.watres.2017.01.042>

Appendix A: Supplementary material to Chapter 2

Table A1: Overview of the sampling dates at the respective transects, us...upstream, ds...downstream

Sampled transects												
Nr.	A	B+	B	C+	C	D+	D	E+	E	F	G	
transect	St.	us Melk	ds Melk	us	ds Dürnstein	us Krems	ds Krems	us Tulln	ds Tulln	Wien	Hainburg	
rkm	2108	2036.5	2035.6	Dürnstein	2009	2008	2003	2002	1964.4	1963.4	1915	1883
Sampling Dates	-	-	-	6.3.2019	6.3.2019	6.3.2019	6.3.2019	21.3.2019	21.3.2019	13.3.2019	13.3.2019	
	27.3.2019	27.3.2019	27.3.2019	3.4.2019	3.4.2019	3.4.2019	3.4.2019	17.4.2019	17.4.2019	10.4.2019	10.4.2019	
	13.5.2019	13.5.2019	13.5.2019	8.5.2019	8.5.2019	8.5.2019	8.5.2019	22.5.2019	22.5.2019	15.5.2019	15.5.2019	
	27.5.2019	27.5.2019	27.5.2019	5.6.2019	5.6.2019	5.6.2019	5.6.2019	17.6.2019	17.6.2019	12.6.2019	12.6.2019	
	1.7.2019	1.7.2019	1.7.2019	3.7.2019	3.7.2019	3.7.2019	3.7.2019	17.7.2019	17.7.2019	10.7.2019	10.7.2019	
	29.7.2019	29.7.2019	29.7.2019	31.7.2019	31.7.2019	31.7.2019	31.7.2019	12.8.2019	12.8.2019	7.8.2019	7.8.2019	
	26.8.2019	26.8.2019	26.8.2019	28.8.2019	28.8.2019	28.8.2019	28.8.2019	11.9.2019	11.9.2019	2.9.2019	2.9.2019	
	23.9.2019	23.9.2019	23.9.2019	2.10.2019	2.10.2019	2.10.2019	2.10.2019	16.10.2019	16.10.2019	9.10.2019	9.10.2019	
	23.10.2019	23.10.2019	23.10.2019	30.10.2019	30.10.2019	30.10.2019	30.10.2019	13.11.2019	13.11.2019	6.11.2019	6.11.2019	
	20.11.2019	20.11.2019	20.11.2019	25.11.2019	25.11.2019	25.11.2019	25.11.2019	11.12.2019	11.12.2019	4.12.2019	4.12.2019	
	18.12.2019	18.12.2019	18.12.2019	15.1.2020	15.1.2020	15.1.2020	15.1.2020	27.1.2020	27.1.2020	22.1.2020	22.1.2020	
	-	-	-	12.2.2020	12.2.2020	12.2.2020	12.2.2020	26.02.2020	26.02.2020	19.02.2020	19.02.2020	
04.03.2020	04.03.2020	04.03.2020	11.3.2020	11.3.2020	11.3.2020	11.3.2020	-	-	-	-		
n	11			13				12		12		

A1: Script for DoRIS ship data extraction

```
"# Python Libraries\n",  
"import pandas as pd\n",  
"from tabulate import tabulate\n",  
"import matplotlib.pyplot as plt\n",  
"import os\n",  
"import glob\n",  
"\n",  
"# Get the current working directory\n",  
"script_dir = os.getcwd()\n",  
"\n",  
"# Get the current working directory\n",  
"#script_dir = os.path.dirname(os.path.realpath(__file__))\n",  
"\n",  
"# Construct input file paths\n",  
"# Note: Schiffe0519 is the folder name where all the daily data folders are stored (e.g. 2019-  
05-01)\n",  
"ship_database_path = os.path.join(script_dir, 'ship_database', 'May2019') \n",  
"# input_date.txt is the file where all the user defined dates for analysis are stored\n",  
"input_date_path = os.path.join(script_dir, 'input_date.txt') \n",  
"\n",  
"# Construct output file paths\n",  
"output_extracted_path = os.path.join(script_dir, 'OutputFile_Extracted_Ship_Data.xlsx')\n",  
"output_categorized_path = os.path.join(script_dir,  
'OutputFile_Categorized_Ship_Data.xlsx')\n",  
"output_summary_path = os.path.join(script_dir, 'OutputFile_Summary.xlsx')\n",  
"\n",  
"# Reading ship database files \n",  
"# Important: input_date.txt is the file where all the user defined dates are stored in yyyy-  
mm-dd format (e.g. 2019-05-01)\n",  
"csv_file=[]\n",  
"with open(input_date_path, 'r') as x: #change it to your directory path\n",  
" for line in x:\n",  
" line = line.strip()\n",  
" newFolder = ship_database_path+'/'+line\n",  
" dirname = newFolder\n",  
" path = os.path.join(dirname, '**')\n",  
" for x in glob.glob(path):\n",  
" csv_file.append(x)\n",  
"print ("Total number of files:", len(csv_file)) \n",  
"\n",  
"##### Ship data extraction based on user inputs (Longitudnal river section and time interval)  
#####\n",  
"# Define river longitudnal section (only input values in the range: 1883 to 2223 km -  
Danube river in Austria)\n",  
"while True:\n",  
" try:\n",  
" a = float(input('Enter start point (choose value between 1883 and 2223): '))\n",
```

```
" b = float(input('Enter finish point (choose value between 1883 and 2223): '))\n",\n" if 1883 <= a <= 2223 and 1883 <= b <= 2223:\n",\n" break\n",\n" else:\n",\n" print("\\Invalid input. Please enter values in the range: 1883 to 2223 km.\\")\n",\n" except ValueError:\n",\n" print("\\Invalid input. Please enter a number.\\")\n",\n" print (\\\"River longitudinal section:\\\",a,\\\"to\\\",b,\\\"km\\\")\n",\n" \n",\n" # Define time interval in HH:MM:SS (e.g. 00:00:00 to 23:59:59)\n",\n" while True:\n",\n" try:\n",\n" c = str(input('Enter start time (choose between 00:00:00 to 23:59:59): '))\n",\n" d = str(input('Enter finish time (choose between 00:00:00 to 23:59:59): : '))\n",\n" pd.to_datetime(c, format='%H:%M:%S', errors='raise')\n",\n" pd.to_datetime(d, format='%H:%M:%S', errors='raise')\n",\n" break\n",\n" except ValueError:\n",\n" print("\\Invalid input. Please enter a time in the format HH:MM:SS.\\")\n",\n" print (\\\"Time interval:\\\",c,\\\"to\\\",d)\n",\n" \n",\n" # Analyze data files and extract ship data based on user inputs\n",\n" extracted_ship_data = pd.DataFrame()\n",\n" files = csv_file\n",\n" for f in files:\n",\n" try:\n",\n" data = pd.read_csv(f,index_col='timeStampLocal',delimiter=';', usecols=[0,6,13,14,15],\n",\n" parse_dates=['timeStampLocal'], dayfirst=True, decimal=',')\n",\n" except Exception as e:\n",\n" print(f\"Error reading file {f}: {e}\")\n",\n" continue\n",\n" \n",\n" # Check if necessary columns exist\n",\n" necessary_columns = ['riverkm', 'shipName']\n",\n" if not all(column in data.columns for column in necessary_columns):\n",\n" print(f\"File {f} is missing necessary columns\")\n",\n" continue\n",\n" \n",\n" data1 = data.loc[(data['riverkm']>=a) & (data['riverkm']<=b)]\n",\n" data2 = data1.between_time(c,d, include_start = True, include_end = True )\n",\n" data2 = data1.between_time(c,d, include_start = True, include_end = True ).copy() \n",\n" data2.drop_duplicates(subset = ['shipName'], keep = 'first' , inplace = True)\n",\n" \n",\n" if data2.empty: \n",\n" continue\n",\n" extracted_ship_data = extracted_ship_data.append(data2)\n",\n" extracted_ship_data.sort_values(\\\"riverkm\\\", inplace = True)\n",\n" \n",\n" #print (extracted_ship_data)\n",\n" \n",\n"
```

```

"# Save extracted ship data\n",
"extracted_ship_data.to_excel(output_extracted_path, header=True) #change it to your
directory path\n",
"\n",
"# Assign categories to ship types\n",
"df = pd.read_excel(output_extracted_path) #change it to your directory path\n",
"\n",
"# Function to map vessel type to ship category\n",
"def map_ship_type(vesselType):\n",
" if vesselType == 8440 or vesselType == 8443:\n",
" return \"Cruise Ship\"\n",
" elif vesselType == 8444 or vesselType == 1910 or vesselType == 1900:\n",
" return \"Passenger Ship\"\n",
" elif vesselType == 8510 or vesselType == 8450:\n",
" return \"Other Ship\"\n",
" else:\n",
" return \"Freight Ship\"\n",
"\n",
"# Applying the function to create a new column\n",
"df['ship_category'] = df['vesselType'].apply(map_ship_type)\n",
"\n",
"# Displaying the updated DataFrame\n",
"print(tabulate(df, headers='keys', tablefmt='fancy_grid'))\n",
"\n",
"# Save the categorized ship data\n",
"df.to_excel(output_categorized_path, header=True) # Change it to your directory path\n",
"\n",
"column_summary = df['ship_category'].value_counts()\n",
"#display(column_summary)\n",
"column_summary.to_excel(output_summary_path, header=True) # Change it to your
directory path\n",
"plt.figure(figsize=(10,5)) \n",
"column_summary.plot.bar()\n",
"plt.xlabel(\"Ship Category\")\n",
"plt.ylabel(\"Number of Ships\")\n",
"plt.title(\"Ship Category Summary\")\n",
"plt.show()
]

```

A2: Ship data assessment (SDA) using the DoRIS database

River Information Services (RIS) and inland Automated Identification System (AIS)

In Europe, standardized River Information Services (RIS) were implemented and harmonized to enable a reliable and efficient inland waterway transport via the EU Directive 2005/44/EC, (EUROPEAN PARLIAMENT, 2005). The RIS includes unified mandatory technical regulations for navigational equipment such as the inland Automated Identification System (AIS). Information transfer between ships and base-stations as well as from ships to ships is performed via radio signals received/transmitted by AIS transponders sending static, dynamic and trip-related data. Static data includes the official ship number, call sign, vessel name, type, length, and beam, all entered/updated by vessel operators. Dynamic and trip-related data includes ship position, time stamp, navigational status, destination, and estimated time of arrival and is updated automatically every 2-10 seconds while underway and every 3 minutes while at anchor (Commission et al., 2011; Vallant and Hofmann-Wellenhof, 2008; Zednicek et al., 2006).

Ship counting concepts

Pollution source profiling: Daily shipping activity was assessed for the entire investigated Danube River reach (river-km 2111 to 1873) as well as the sub-reaches: upstream of Vienna (river-km 2111 to 1937), Vienna (river-km 1937 to 1918) and downstream of Vienna (river-km 1918 to 1873). Number of ships per day with high season (HS-July/August 2019) and low season (LS-January/February 2020) differentiation was assessed using the SDA script and each ship being only counted once per day and reach.

Association analysis between general fecal pollution on the entire Danube River reach and ship numbers (regional): As water pollution is travelling with the river flow, a reverse ship traffic approximation (RSTA) concept was applied, enabling backtracking ships which passed the sampled water volume before it was sampled. The concept includes an extrapolation of river water/pollution flow by the formation of counting areas with the length, which the water travels within a specific time-frame depending on the flow velocity. Danube River flow lies between 1 m/s and 2 m/s, with both metrics being used for extrapolation. Extrapolation was started at the time-point and river-km of sampling for each individual sampling transect. The chosen time span was 1 h, which resulted in 3.6 river-km (1 m/s) or 7.2 river-km (2 m/s) in length of counting area, which was stepwise shifted upstream and back in time, assuming a constant river flow. The numbers of ships in the counting areas were assessed using the SDA script, with subsequent summarizing of ships for certain river flow time-spans/distances, allowing for association analysis with increasing time and distance metrics (see Figure S1). Selected river flow times until the water was sampled were 2 h, for short time/distance analysis, 8 h for medium time/distance analysis or 16 h for long time/distance analysis. As two different river flow velocities (1 or 2 m/s) were used for the ship traffic approximation, 6 different combinations for analysis from 3.6 river-km to a maximum of 115 river-km counting distance

upstream of the 7 sampled transects, without the upstream pairs were used for the correlation analysis (see Chapter 2, Figure 9).

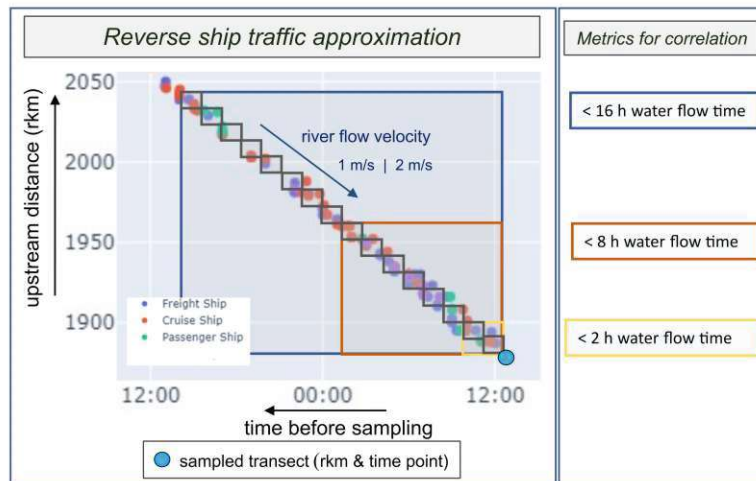


Figure A1: Scheme of the reverse ship traffic approximation: including the counting areas of 1h in time and 3.6 km or 7.2 km in length. Ships were summarized for short time/distance (< 2 h water flow time, yellow), medium time/distance (< 8 h water flow time, brown red) and long time/distance (< 16 h water flow time, blue) for the correlation analysis.

Association analysis at the ship dock areas (local)

For counting ships in the ship dock areas, the respective river kilometer of the upstream/downstream sampling transects (B⁺/B, C⁺/C, D⁺/D, E⁺/E) and the exact timespan for sampling (~30 minutes) was used as time and area input in the SDA script.

A3: Statistical analysis and data visualization

Used packages were mainly *ggplot2* (Wickham, 2016), *reshape* (Wickham, 2007) and *dplyr* (Wickham et al., 2021). Arrangement and drawing of schematic plots was performed using Inkscape (InkscapeProject, 2022) or created with BioRender.com.

For analysis of differences in the mean decadic logarithm of the *E.coli* concentrations of different groups (longitudinal, cross-sectional) analysis of variances ANOVA using the function *anova(lm())* with a level of significance of 0.05. For the post-hoc Tukey test the function *TukeyHSD()* was used. Spearman rank correlation analysis was performed using the functions *cor()*, *cor.mtest()*, *p.adjust()* with *method = "bonferroni"* for calculation in 3.3.1 water quality (n = 665) and *method = "fdr"* (false discovery rate, Benjamini and Hochberg, 1995) for calculations in main manuscript chapter 3.4.1 associations between ships and microbial faecal pollution (n = 84). Visualization of the correlation was performed using *corrplot()* function from the packages *stats* (R Core Team, 2022) and *corrplot* package (Wei and Simko, 2021). Rho values with a p-value higher than 0.05 (after adjustment) are given with n.s. (not significant) in correlation analysis plots. For scatterplots linear trend and Spearman rank correlation for local analysis were calculated using functions *ggpubr::stat_cor()*, *geom_smooth(method = MASS::rlm)*. For the multiple linear regression analysis at dock C+/C the function *lm()* was used.

The parameters for the regional association analysis *i.e.*, correlation of *E. coli* with environmental data, 3-day sum of precipitation (closest gauge), the average daily river discharge of the sampling day (closest gauge at the Danube River) and the sum tributary river discharges with a confluence point of 36 rkm upstream of the sampling transect were taken (<https://www.noel.gv.at/wasserstand/#!/de/Messstellen>, see **Table A2**). For WWTPs, a metric approach was performed for summing the discharge (data from the day of sampling) from different WWTPs with discharge point upstream of the sampled transect with i) up to 36 rkm, ii) from 36 rkm to 90 rkm upstream at Danube or iii) up to 90 rkm upstream at selected tributaries. Daily discharge data from 22 WWTPs in the catchment area with a population equivalent ranging from 14.000 – 4.000.000 was provided by the government of Lower Austria (**Table A3**). For the correlation with the number of ships, RSTA concept was applied as described in **Appendix A2**.

Table A2: Used gauges for precipitation data, selected rivers and their confluence points with the Danube River

Precipitation				River Discharge				
Nr.	Gauge Name	Gauge Nr.	Used Transect	Nr.	Rivers	rkm Danube confluence point	Gauge	Gauge Nr.
P1	Hollern	116350	G	R1	Schwechat	1914	Schwechat	208157
P2	Franzensdorf	108969	F	R2	Gr. Tulln	1965	Siegersdorf	208017
P3	Tulln (Bildeiche)	108779	E	R3	Perschling	1972	Atzenbrugg	208009
P4	Gedersdorf (Krems)	108761	C/D	R4	Krems	1978.5	Imbach	207878
P5	Melk	107284	B	R5	Kamp	1978.5	Stiefern	207993
P6	St. Pantaleon	108985	A	R6	Pielach	2034.5	Hofstetten (Bad)	207852
				R7	Melk	2036	Matzleinsdorf	207837
				R8	Weitenbach	2037	Weitenegg	207811
				R9	Erlauf	2047	Niederndorf	207803
				R10	Ybbs	2058	Greimpersdorf	207688
				R11	Enns	2112.5	Steyr (Ortskai)	205922

Table A3: Selected WWTP at the Danube River and selected tributaries

WWTP Danube				WWTP Tributary				
WWTP Danube Nr.	Population equivalent (PE)	rkm discharge point	receiving water	WWTP Tributary number	Population equivalent (PE)	km discharge points upstream of confluence	receiving water	
WWTP_D1	144 000	1906	Danube	WWTP_T1	130 000	24	Schwechat	R1
WWTP_D2	370 000	1914	Danube	WWTP_T2	27 000	25	Schwechat	R1
WWTP_D3	4 000 000	1921	Danube	WWTP_T3	45 000	33	Schwechat	R1
WWTP_D4	280 000	1980	Danube	WWTP_T4	34 000	6	Gr. Tulln	R2
WWTP_D5	255 000	1997	Danube	WWTP_T5	47 000	19	Gr. Tulln	R2
WWTP_D6	14 000	2035.5	Danube	WWTP_T6	70 000	22	Kamp	R5
WWTP_D7	25 000	2042	Danube	WWTP_T7	40 000	57	Kamp	R5
WWTP_D8	16 800	2043	Danube	WWTP_T8	35 000	17	Pielach	R6
WWTP_D9	20 000	2058	Danube	WWTP_T9	64 500	12	Erlauf	R9
WWTP_D10	950 000	2119	Danube	WWTP_T10	150 000	19	Ybbs	R10
				WWTP_T11	31 000	46	Ybbs	R11
				WWTP_T12	140 000	26	Enns	R11

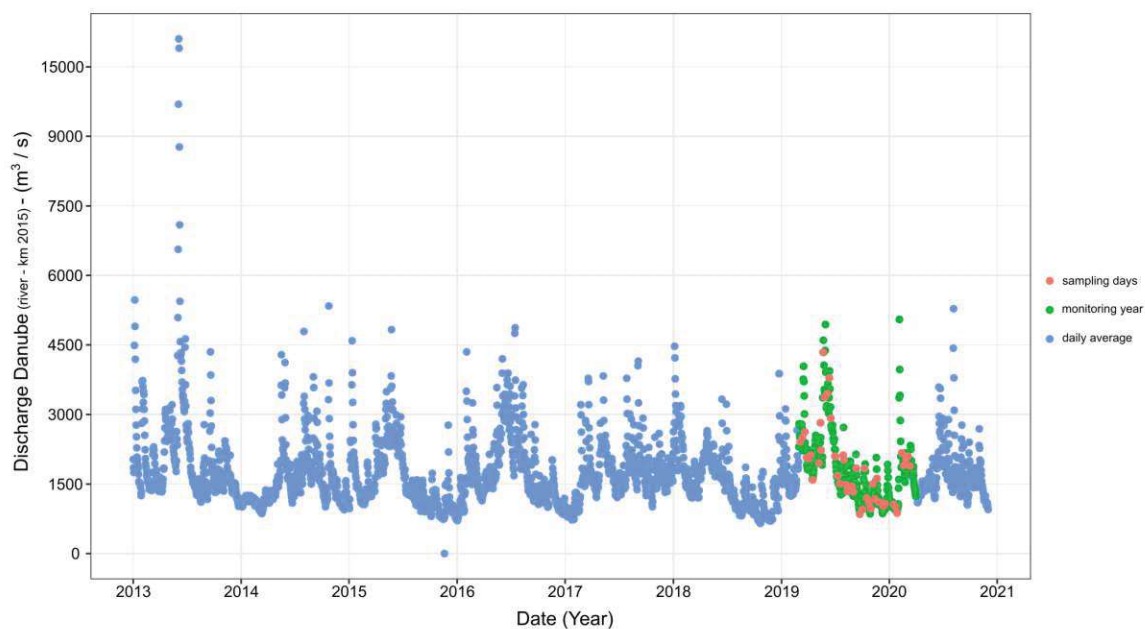


Figure A2: Danube River discharge at the gauge Kienstock (river-km 2015) for the years 2013 – 2021 (blue). Monitoring year given in green with sampling days given in red.

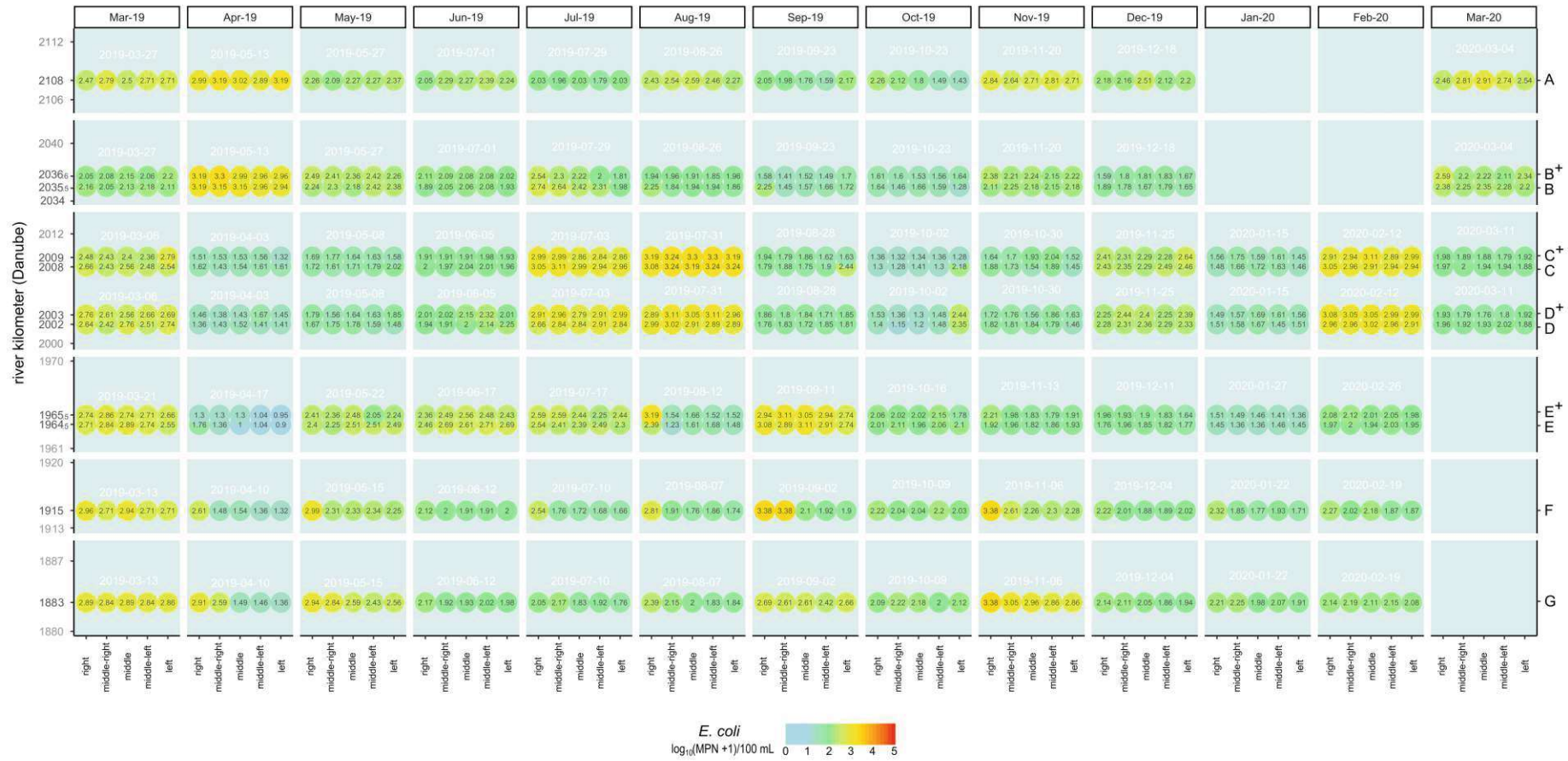


Figure A3: *E. coli* concentrations (log₁₀ (MPN+1) per 100 mL) of each individual sample (n = 655) visualized with respect to longitudinal as well as cross-sectional position and sampling month with specific days given above each sampling spot per transect.

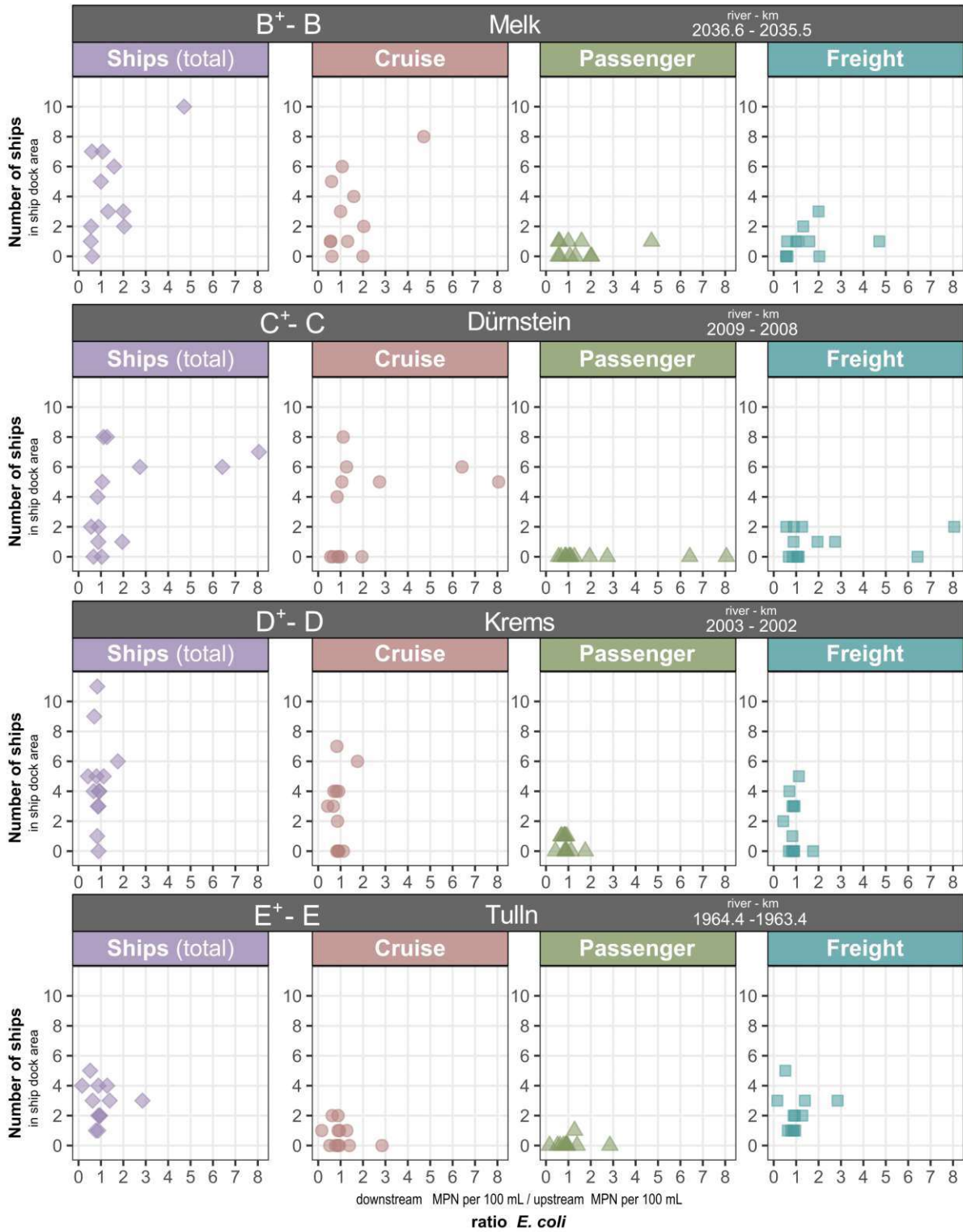


Figure A4: Scatterplot of the ratio of the *E. coli* concentration downstream/upstream ship docks (x axis) and the number of ships in the ship dock area (y axis) for all ships (Ship (total), cruise, passenger and freight vessels during sampling, for the four locations Melk, Dürnstein, Krems and Tulln

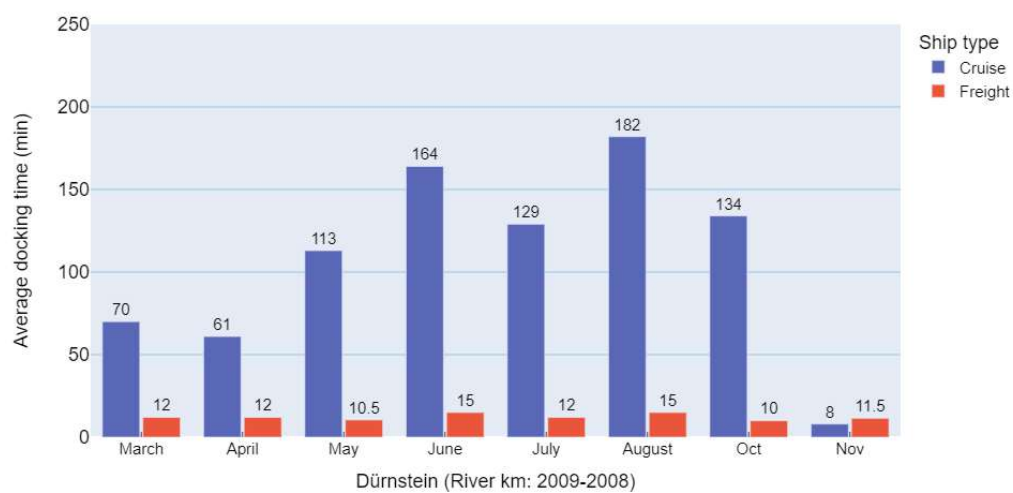


Figure A5: Average time of the ships at the ship dock Dürnstein at the day of sampling

Table A4: Descriptive statistics of the analyzed parameters for the single transects, us... upstream, ds...downstream

transect		code		river kilometer		
St Pantaleon		A		2108		
variable	n	median	mean (arithm.)	range (min-max)		unit
E. coli	55	2.29	2.37	1.43	3.19	log ₁₀ (MPN+1)/100 mL
temperature	55	13.3	12.8	4.4	21.4	°C
pH	55	8.10	8.09	7.00	8.30	-
conductivity	55	314	307	164	494	µS/cm
oxygen	55	10.5	10.7	8.6	13.6	mg/L
COD	55	3.0	4.7	1.0	11.0	mg/L
nitrogen (total)	55	3.0	3.0	1.0	6.0	mg/L
phosphorus (total)	55	1.0	1.1	1.0	3.0	mg/L
ammonium	55	5.0	4.8	1.0	9.0	mg/L
HF 183 II	26	3.47	3.45	2.40	4.83	log ₁₀ (ME+1)/100 mL
BacHum	27	3.92	4.00	3.10	5.34	log ₁₀ (ME+1)/100 mL
BacR	12	3.47	3.45	2.51	4.07	log ₁₀ (ME+1)/100 mL
Pig2Bac	1	2.08	2.08	2.08	2.08	log ₁₀ (ME+1)/100 mL
us Melk		B+		2036.6		
variable	n	median	mean (arithm.)	range (min-max)		unit
E. coli	55	2.08	2.10	1.41	3.30	log ₁₀ (MPN+1)/100 mL
temperature	55	13.1	12.8	4.6	21.4	°C
pH	55	8.10	8.07	7.70	8.30	-
conductivity	55	316	312	229	376	µS/cm
oxygen	55	10.7	10.6	8.5	14.7	mg/L
COD	55	2.0	4.7	1.0	11.0	mg/L
nitrogen (total)	55	3.0	3.0	1.0	5.0	mg/L
phosphorus (total)	55	1.0	1.1	1.0	3.0	mg/L
ammonium	55	5.0	4.9	1.0	11.0	mg/L

HF 183 II	0	-	-	-	-	\log_{10} (ME+1)/100 mL
BacHum	0	-	-	-	-	\log_{10} (ME+1)/100 mL
BacR	0	-	-	-	-	\log_{10} (ME+1)/100 mL
Pig2Bac	0	-	-	-	-	\log_{10} (ME+1)/100 mL
ds Melk B 2035.5						
variable	n	median	mean (arithm.)	range (min-max)		unit
E. coli	55	2.13	2.12	1.28	3.19	\log_{10} (MPN+1)/100 mL
temperature	55	13.1	12.8	4.6	21.4	°C
pH	55	8.10	7.98	6.80	8.30	-
conductivity	55	317	314	228	409	μ S/cm
oxygen	55	10.5	10.5	8.4	13.1	mg/L
COD	55	7.0	5.1	1.0	10.0	mg/L
nitrogen (total)	55	3.0	2.9	1.0	5.0	mg/L
phosphorus (total)	55	1.0	1.0	1.0	3.0	mg/L
ammonium	55	4.0	4.3	1.0	10.0	mg/L
HF 183 II	0	-	-	-	-	\log_{10} (ME+1)/100 mL
BacHum	0	-	-	-	-	\log_{10} (ME+1)/100 mL
BacR	0	-	-	-	-	\log_{10} (ME+1)/100 mL
Pig2Bac	0	-	-	-	-	\log_{10} (ME+1)/100 mL
us Dürnstein C+ 2009						
variable	n	median	mean (arithm.)	range (min-max)		unit
E. coli	65	1.91	2.11	1.28	3.30	\log_{10} (MPN+1)/100 mL
temperature	65	10.60	11.90	3.50	20.60	°C
pH	65	8.20	8.23	7.60	8.50	-
conductivity	65	338	321	232	393	μ S/cm
oxygen	65	10.9	10.9	8.3	14.2	mg/L
COD	65	8.0	6.1	1.0	11.0	mg/L
nitrogen (total)	65	3.0	2.8	1.0	5.0	mg/L

phosphorus (total)	65	1.0	1.4	1.0	5.0	mg/L
ammonium	65	5.0	4.8	1.0	11.0	mg/L
HF 183 II	0	-	-	-	-	log ₁₀ (ME+1)/100 mL
BacHum	0	-	-	-	-	log ₁₀ (ME+1)/100 mL
BacR	0	-	-	-	-	log ₁₀ (ME+1)/100 mL
Pig2Bac	0	-	-	-	-	log ₁₀ (ME+1)/100 mL
ds Dürnstein C 2008						
variable	n	median	mean (arithm.)	range (min-max)		unit
E. coli	65	1.97	2.16	1.28	3.24	log ₁₀ (MPN+1)/100 mL
temperature	65	10.70	11.86	3.50	21.00	°C
pH	65	8.30	8.26	7.80	8.50	-
conductivity	65	338	321	220	391	µS/cm
oxygen	65	11.0	10.9	8.6	13.6	mg/L
COD	65	8.0	5.6	1.0	11.0	mg/L
nitrogen (total)	65	3.0	2.9	1.0	5.0	mg/L
phosphorus (total)	65	1.0	1.4	1.0	6.0	mg/L
ammonium	65	4.0	4.4	1.0	11.0	mg/L
HF 183 II	0	-	-	-	-	log ₁₀ (ME+1)/100 mL
BacHum	0	-	-	-	-	log ₁₀ (ME+1)/100 mL
BacR	0	-	-	-	-	log ₁₀ (ME+1)/100 mL
Pig2Bac	0	-	-	-	-	log ₁₀ (ME+1)/100 mL
us Krems D+ 2003						
variable	n	median	mean (arithm.)	range (min-max)		unit
E. coli	65	1.92	2.14	1.30	3.11	log ₁₀ (MPN+1)/100 mL
temperature	65	10.80	11.80	3.50	20.70	°C
pH	65	8.30	8.26	7.80	8.50	-
conductivity	65	339	322	212	392	µS/cm
oxygen	65	11.0	10.9	8.5	13.5	mg/L
COD	65	8.0	6.3	1.0	11.0	mg/L

nitrogen (total)	65	3.0	2.8	1.0	5.0	mg/L
phosphorus (total)	65	1.0	1.3	1.0	4.0	mg/L
ammonium	65	4.0	4.5	1.0	11.0	mg/L
HF 183 II	0	-	-	-	-	\log_{10} (ME+1)/100 mL
BacHum	0	-	-	-	-	\log_{10} (ME+1)/100 mL
BacR	0	-	-	-	-	\log_{10} (ME+1)/100 mL
Pig2Bac	0	-	-	-	-	\log_{10} (ME+1)/100 mL
ds Krems D+ 2002						
variable	n	median	mean (arithm.)	range (min-max)		unit
E. coli	65	1.93	2.10	1.15	3.02	\log_{10} (MPN+1)/100 mL
temperature	65	10.8	11.9	3.5	21.9	°C
pH	65	8.30	8.22	7.60	8.50	-
conductivity	65	339	325	222	411	µS/cm
oxygen	65	10.9	11.0	8.2	14.4	mg/L
COD	65	8.0	5.6	1.0	11.0	mg/L
nitrogen (total)	65	3.0	2.8	1.0	5.0	mg/L
phosphorus (total)	65	1.0	1.3	1.0	5.0	mg/L
ammonium	65	4.0	4.6	1.0	12.0	mg/L
HF 183 II	16	3.3	3.5	2.9	4.6	\log_{10} (ME+1)/100 mL
BacHum	22	3.57	3.86	2.87	5.39	\log_{10} (ME+1)/100 mL
BacR	6	3.73	3.64	3.04	3.98	\log_{10} (ME+1)/100 mL
Pig2Bac	5	2.70	2.64	2.31	2.91	\log_{10} (ME+1)/100 mL
us Tulln E+ 1964.4						
variable	n	median	mean (arithm.)	range (min-max)		unit
E. coli	60	2.06	2.11	0.95	3.19	\log_{10} (MPN+1)/100 mL
temperature	60	11.45	11.53	3.40	20.90	°C
pH	60	8.30	8.27	7.40	8.70	-
conductivity	60	315	328	219	408	µS/cm

oxygen	60	10.9	11.0	8.1	14.5	mg/L
COD	60	8.0	5.5	1.0	11.0	mg/L
nitrogen (total)	60	3.0	2.8	1.0	4.0	mg/L
phosphorus (total)	60	1.0	1.2	1.0	4.0	mg/L
ammonium	60	5.0	4.6	1.0	13.0	mg/L
HF 183 II	0	-	-	-	-	log ₁₀ (ME+1)/100 mL
BacHum	0	-	-	-	-	log ₁₀ (ME+1)/100 mL
BacR	0	-	-	-	-	log ₁₀ (ME+1)/100 mL
Pig2Bac	0	-	-	-	-	log ₁₀ (ME+1)/100 mL
ds Tulln E 1963.4						
variable	n	median	mean (arithm.)	range (min-max)		unit
E. coli	60	2.02	2.10	0.90	3.11	log ₁₀ (MPN+1)/100 mL
temperature	60	11.40	11.49	3.30	20.30	°C
pH	60	8.30	8.30	8.10	8.60	-
conductivity	60	313	325	215	407	µS/cm
oxygen	60	10.9	10.9	8.3	15.0	mg/L
COD	60	8.0	6.4	1.0	11.0	mg/L
nitrogen (total)	60	3.0	2.7	1.0	4.0	mg/L
phosphorus (total)	60	1.0	1.1	1.0	4.0	mg/L
ammonium	60	5.0	4.7	1.0	9.0	mg/L
HF 183 II	0	-	-	-	-	log ₁₀ (ME+1)/100 mL
BacHum	0	-	-	-	-	log ₁₀ (ME+1)/100 mL
BacR	0	-	-	-	-	log ₁₀ (ME+1)/100 mL
Pig2Bac	0	-	-	-	-	log ₁₀ (ME+1)/100 mL
Wien F 1915						
variable	n	median	mean (arithm.)	range (min-max)		unit
E. coli	60	2.04	2.16	1.32	3.38	log ₁₀ (MPN+1)/100 mL
temperature	60	11.40	12.59	3.80	20.70	°C

pH	60	8.30	8.23	7.60	8.40	-
conductivity	60	296	292	226	379	µS/cm
oxygen	60	10.3	10.4	8.2	14.4	mg/L
COD	60	1.0	4.5	1.0	11.0	mg/L
nitrogen (total)	60	3.0	2.6	1.0	5.0	mg/L
phosphorus (total)	60	1.0	1.4	1.0	6.0	mg/L
ammonium	60	5.0	5.0	1.0	14.0	mg/L
HF 183 II	0	-	-	-	-	log ₁₀ (ME+1)/100 mL
BacHum	0	-	-	-	-	log ₁₀ (ME+1)/100 mL
BacR	0	-	-	-	-	log ₁₀ (ME+1)/100 mL
Pig2Bac	0	-	-	-	-	log ₁₀ (ME+1)/100 mL
Hainburg		G			1883	
variable	n	median	mean (arithm.))	range (min-max)		unit
E. coli	60	2.16	2.29	1.36	3.38	log ₁₀ (MPN+1)/100 mL
temperature	60	11.65	12.69	4.10	21.10	°C
pH	60	8.40	8.32	7.70	8.50	-
conductivity	60	285	289	222	390	µS/cm
oxygen	60	10.1	10.3	8.3	13.5	mg/L
COD	60	7.0	5.3	1.0	10.0	mg/L
nitrogen (total)	60	3.0	2.7	1.0	5.0	mg/L
phosphorus (total)	60	1.0	1.3	1.00	4.0	mg/L
ammonium	60	4.0	3.9	1.0	11.0	mg/L
HF 183 II	33	3.41	3.52	2.32	4.54	log ₁₀ (ME+1)/100 mL
BacHum	35	4.00	3.96	2.78	4.87	log ₁₀ (ME+1)/100 mL
BacR	5	2.53	2.64	2.44	2.99	log ₁₀ (ME+1)/100 mL
Pig2Bac	1	2.00	2.00	2.00	2.00	log ₁₀ (ME+1)/100 mL

Appendix B: Supplementary material to Chapter 3

Table B1: Chemical analysis of tap water.

Parameter	value
pH	8.0
Electrical Conductivity ($\mu\text{S cm}^{-1}$)	250
Temperature ($^{\circ}\text{C}$)	8.6–10
Dissolve Oxygen (mg L^{-1})	9.7–10.3
Total Organic Carbon (mg L^{-1})	0.4
Chloride (mg L^{-1})	2.6
Sodium (mg L^{-1})	1.2
Calcium (mg L^{-1})	46
Potassium (mg L^{-1})	<0.5
Magnesium (mg L^{-1})	9.3
Sulfate (mg L^{-1})	11
Nitrite (mg L^{-1})	<0.01
Nitrate (mg L^{-1})	4.9
Iron (mg L^{-1})	<0.05
Manganese (mg L^{-1})	<0.02

B1. Virus Enumeration

Polymerase chain reaction primers, standards and amplification

Quantification of PRD1 genome copies was performed as previously published (Sommer et al., 2021). The primers for PRD1 qPCR were used according to the protocol of Stevenson et al. (2015) using the non-specific DNA-dye EvaGreen® (Jena Bioscience GmbH, Jena, Germany). One qPCR reaction of 25 µL final volume contained 2.5 µL of 10 × reaction buffer (Biozym Scientific GmbH, Hessisch Oldendorf, Germany), 1.2 µM EvaGreen®, 200 µM of each dNTPs (dATP, dTTP, dGTP and dCTP), 120 nM of each PRD1 primer (Forward JSF1: AAACCTTGACCCGAAAACGT and Reverse JSR2: CGGTACGGCTGGTGAAGTAT) (Eurofins Genomics, Ebersberg, Germany) and 1 U of Taq DNA polymerase (Biozym Scientific GmbH, Hessisch Oldendorf, Germany). All qPCR assays were performed in an Mx3000 real-time PCR thermocycler (Stratagene, San Diego, CA, USA) with the following cycling conditions: 2 min 94 °C, 45 × (30 s 94 °C, 30 s 59 °C, 30 s 72 °C) (Fister et al., 2015). All qPCR experiments were performed in duplicate and included a standard series for calculation of a standard curve and a negative amplification control, whereas the standard curve was used for quantification of the viral nucleic acids expressed as phage genome numbers (PGN/mL).

Small-drop plaque assay method

The enumeration of infective virus titers of PRD1 was performed using a small-drop plaque assay (Mazzocco et al., 2009). All viruses were used at concentrations of approximately 10⁸–10⁹ plaque-forming units (PFU/mL). Initially, an overnight culture of *S. enterica* was diluted 10-fold in SM buffer (Kropinski et al., 2009; Mazzocco et al., 2009). A 10-fold serial dilution of the virus was prepared in the bacteria-containing buffer. Subsequently, 20 µL of each dilution was dropped onto a tryptone soya agar (TSA)-plate and incubated overnight at 37°C. Following overnight incubation, plaques were counted and compared with the untreated, positive controls. All plaque assay experiments were repeated at least twice as duplicates and the results are expressed as plaque-forming units (PFU/mL).

B2. Equations for Colloid Filtration Theory (CFT)

The following equations and parameters used for computing the collision coefficients (contact and attachment efficiencies) of PRD1 and MP-PRD1 (Tufenkji and Elimelech, 2004a):

The overall contact efficiency (equation 5) of colloids in a porous media medium can be decomposed into three primary components η_D (diffusion), η_I (interception), and η_G (settling or gravity). In equation 3.5, the contact efficiency due to diffusion (η_D) is described as:

$$\eta_D = 2.44A_s^{1/3} N_R^{-0.081} N_{Pe}^{-0.715} N_{vdw}^{0.052} \quad (\text{B1})$$

The governing parameters in equation SE1 are specific surface area of the colloid (A_s), aspect ratio (N_R), Peclet number (N_{Pe}) and Van der Waals number (N_{vdw}) and are given as follows:

$$N_R = \frac{d_p}{d_c} \quad (\text{B1.1})$$

$$N_{pe} = \frac{Ud_c}{D_\infty} \quad (\text{B1.2})$$

$$N_{vdw} = \frac{A}{kT} \quad (\text{B1.3})$$

In equation 5, the contact efficiency due to interception (η_I) is described as;

$$\eta_I = 0.55A_s N_R^{1.675} N_A^{0.125} \quad (\text{B2})$$

The governing parameters in the equation SE2 are specific surface area of the colloid (A_s), aspect ratio (N_R), and attraction number (N_A) and is given as follows:

$$N_A = \frac{A}{12 \pi \mu a_p^2 U} \quad (\text{B2.1})$$

In equation 5, the contact efficiency due to gravitational forces (η_G) is described as;

$$\eta_G = 0.22N_R^{-0.24} N_G^{1.11} N_{vdw}^{0.053} \quad (\text{B3})$$

The governing parameters in the equation SE3 is the gravity number (N_G), and is given as follows:

$$N_G = \frac{2 a_p^2 (\rho_p - \rho_f) g}{9 \mu U} \quad (\text{B3.1})$$

where d_p is the particle diameter (PRD1= 62nm and MP= 1 μ m), d_c is the quartz sand grain collector mean (d_{50}) diameter (0.95 mm), U is the influent solution velocity (2.89 x 10⁻⁵ m/s), D_∞ is the bulk diffusion coefficient, A is the Hamaker constant (PRD1: 7.0 x 10⁻²¹ J, MP: 6.78 x 10⁻²⁰ J), A_s is the Happel model parameter (31.71), k is the Boltzmann constant (1.38 x 10⁻²³

Joule/K), T is fluid absolute temperature (295 K), a_p is PRD1/MP particle radius, ρ_p is the PRD1/MP particle density (PRD1: 1349 kg/cm³, MP: 1050 kg/cm³), ρ_f is the fluid density (1000 kg/m³), μ is the absolute fluid viscosity (1.005 x 10⁻³ kg/m.s), and g is the gravitational acceleration (9.81 m²/s).

Table B2: Computation of single collector contact efficiency and contribution to various filtration mechanisms.

Experimental Scenario	N_R	N_{PE}	N_{vdW}	N_A	N_G	Single-collector contact efficiency			Overall η_o
						Diffusion η_D	Interception η_I	Gravity (settling) η_G	
Total Phages									
PRD1	6.53E-05	3.96E+03	1.72E+00	6.65E+00	6.13E-06	4.57E-02	2.16E-06	3.75E-06	0.046
PRD1 with MPs	1.05E-03	6.39E+04	1.67E+01	2.48E-01	9.38E-04	5.62E-03	1.51E-04	5.77E-04	0.006
Infectious Phages									
PRD1	6.53E-05	3.96E+03	1.72E+00	6.65E+00	6.13E-06	4.57E-02	2.16E-06	3.75E-06	0.046
PRD1 with MPs	1.05E-03	6.39E+04	1.67E+01	2.48E-01	9.38E-04	5.62E-03	1.51E-04	5.77E-04	0.006

B3. Equations for DLVO theory

We applied DLVO to calculate the potential energy between MPs and sand, PRD1 and sand, and PRD1-MP aggregates and sand under saturated conditions by treating as sphere-plate geometry according to the following equations (Wang et al., 2022b).

$$\varphi_{DLVO}(h) = \varphi_{vdw}(h) + \varphi_{edl}(h) \quad (B4)$$

$$\varphi_{vdw}(h) = \frac{-Ar_c}{6h \left[1 + \frac{14h}{\lambda}\right]} \quad (B5)$$

$$\varphi_{edl}(h) = \pi r_c \epsilon_r \epsilon_0 \left[2\psi_c \psi_s \ln \left(\frac{1 + \exp^{-\kappa h}}{1 - \exp^{-\kappa h}} \right) + (\psi_c^2 + \psi_s^2) \ln(1 - \exp^{-2\kappa h}) \right] \quad (B6)$$

$$\kappa = \left[\frac{2000 I_s N_A e^2}{\epsilon_r \epsilon_0 k_B T} \right]^{0.5} \quad (B7)$$

where φ_{DLVO} is the total interaction energy; φ_{vdw} is the gravitational potential energy corresponding to van der Waals force; φ_{edl} is the electrostatic potential energy; h represents the distance between the colloid and the medium (nm). Three different scenarios were applied to calculate Hamaker constants in water-mineral system: $A_{MP\text{-}quartz\text{-}water} = 4.25 \times 10^{-21}$ J (Wang et al., 2022b; Wu et al., 2020), $A_{PRD1\text{-}quartz\text{-}water} = 0.4 \times 10^{-20}$ J (Loveland et al., 1996), and $A_{(MP+PRD1)\text{-}quartz\text{-}water} = 1.49 \times 10^{-21}$ J computed by the formula given by (Elimelech et al., 1995; Gentile et al., 2021).

radius of colloid (r_c), $r_{MP} = 5 \times 10^{-7}$ m, $r_{PRD1} = 3.1 \times 10^{-8}$ m, $r_{PRD1+MP} = 5 \times 10^{-7}$ m; radius of soil grain (r_s) = 4.75×10^{-4} m; characteristic wavelength (λ) of the sphere-plate interactions = 10^{-7} m (Sotirelis and Chrysikopoulos, 2015); dielectric constant (ϵ_r) of water = 78.36 F m^{-1} at 25°C ; vacuum dielectric constant (ϵ_0) = $8.845 \times 10^{-12} \text{ F m}^{-1}$; ψ_c and ψ_s (V) are the surface potential of colloid and soil particles represented by zeta potential, $\psi_{MP} = -42 \times 10^{-3}$ V, $\psi_{PRD1} = -9 \times 10^{-3}$ V, $\psi_{(PRD1+MP)} = -17 \times 10^{-3}$ V, and $\psi_{quartz} = -43 \times 10^{-3}$ V.

κ represents the inverse of Debye-Hückel length (m^{-1}); where I_s is ionic strength = 3×10^{-3} M (tap water); Avogadro's constant (N_A) = $6.02 \times 10^{23} \text{ mol}^{-1}$; basic charge on the electron (e) = 1.602×10^{-19} C; Boltzmann constant (k_B) = $1.38 \times 10^{-23} \text{ J K}^{-1}$; absolute temperature (T) = 298.15 K.

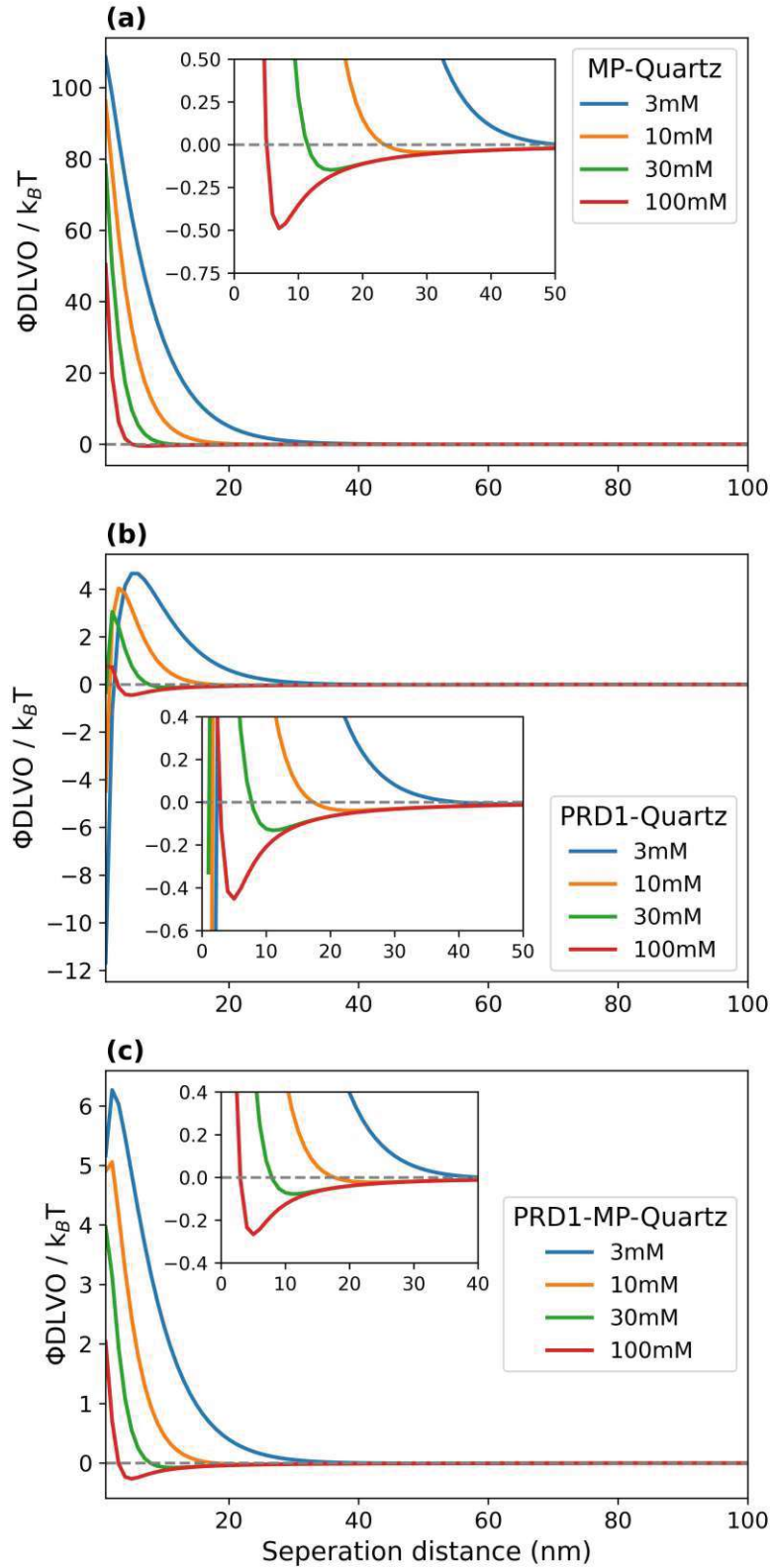


Figure B1: Plots of the DLVO potential energy profiles for colloid-mineral surface interactions corresponding to a minimum separation of 1 nm. (a) DLVO potential energy for MP-quartz. (b) DLVO potential energy for PRD1-Quartz. (c) DLVO potential energy for PRD1-MP-Quartz.

Table B3: Calculated Secondary Minimum Depth and Energy Barrier.

Scenario	Ionic Strength (mM)	Primary Minimum (kBT)	Secondary Minimum (kBT)	Energy Barrier (kBT)
MP-Quartz	3	-	-0.01	108.53
	10	-	-0.05	96.16
	30	-	-0.15	78.21
	100	-	-0.49	50.34
PRD1-Quartz	3	-11.66	-0.01	4.65
	10	-4.47	-0.04	4.03
	30	-0.33	-0.14	3.04
	100	-	-0.46	0.75
PRD1-MP-Quartz	3	-	-0.005	6.27
	10	-	-0.023	5.06
	30	-	-0.077	3.97
	100	-	-0.27	2.03

Appendix C: Supplementary material to Chapter 4

Table C1: Summary of column experiment parameters: soil median grain size (d_{50}), mean microplastic particle size (d_{MP}), and mean zeta potential of microplastics (ζ).

Porous media	Porosity θ	d_{50} (mm)	Column test	MP type	d_{MP} (μm)	ζ (mV)	Straining ratio d_{MP}/d_{50}	
Medium gravel (8.0 mm)	0.38	8	A1	FMPs	1.60	-21.19 ± 1.72	0.0002	
			B1	SMPs	20	-18.40 ± 0.89	0.0025	
			B2					
Fine gravel (4.0 mm)	0.36	4	C1	FMPs	1.80	-21.75 ± 3.79	0.0004	
			D1	SMPs	20	-18.22 ± 1.51	0.0050	
			D2					
Coarse quartz sand (0.6 – 1.3 mm)	0.41	0.95	E1	FMPs	1.40	-22.17 ± 2.05	0.0015	
			F1	SMPs	10	-19.39 ± 3.54	0.0105	
			F2					
			G1	SMPs	1	-21.05 ± 2.50	0.0011	
			G2					
Medium quartz sand (0.4 – 0.8 mm)	0.43	0.60	H1	FMPs	1.20	-21.48 ± 2.21	0.0020	
			I1	SMPs	10	-19.55 ± 3.61	0.0167	
			I2					

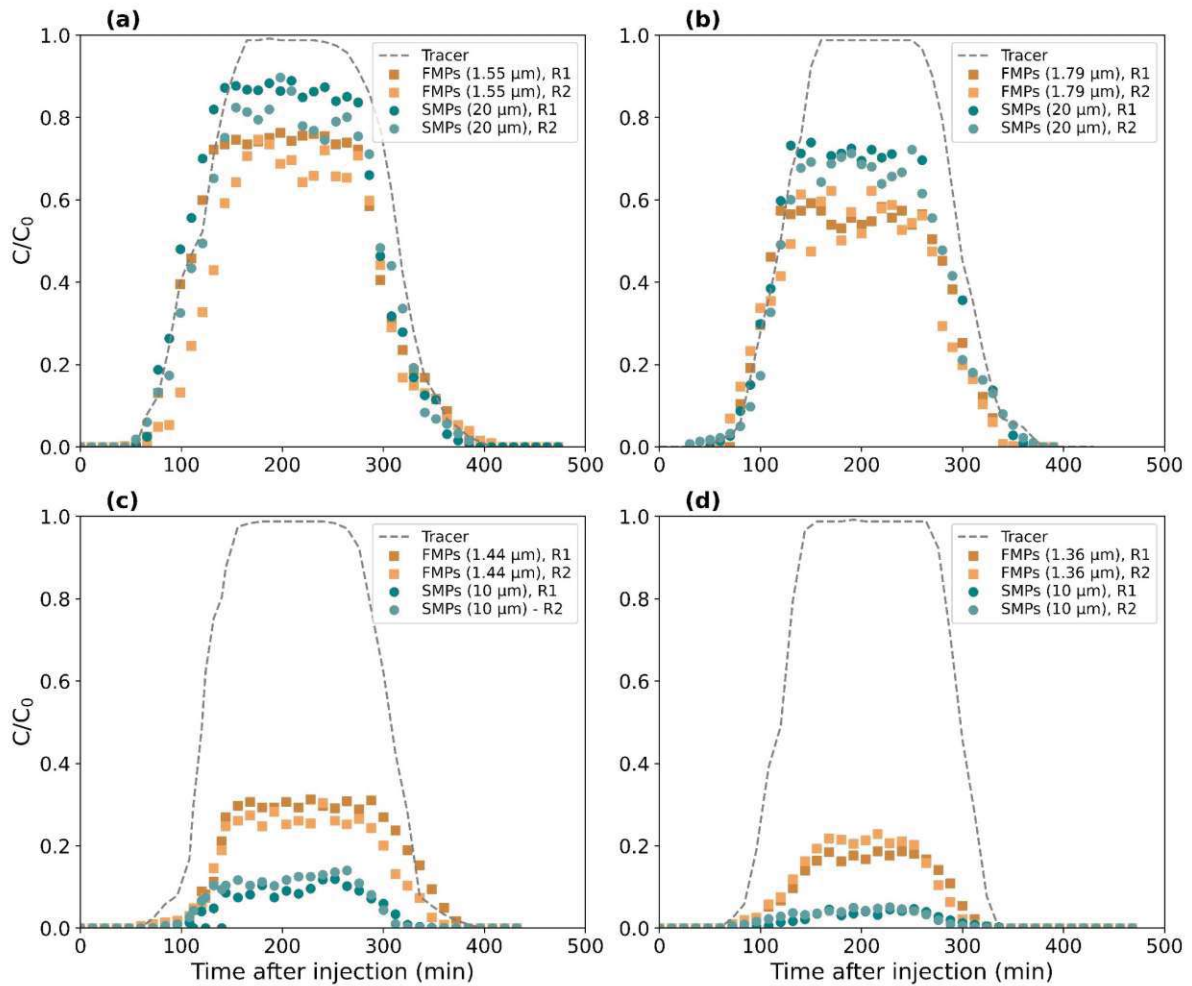


Figure C1: Observed BTCs of tracer (NaBr) and microplastics (SMPs and FMPs) in four different materials (a: medium gravel 8 mm; b: fine gravel 4 mm; c: coarse quartz sand 0.6–1.3 mm; d: medium quartz sand 0.4–0.8 mm). SMPs = spherical microplastics (10 and 20 μm only), FMPs = fragmented microplastics. Symbols (square and circle) represent experimental data. R1 and R2 are experimental runs 1 and 2 respectively. The column was packed with fresh material for each run. BTCs were plotted in the form of the normalized effluent concentration (C/C_0).

Table C2: Discriminant settings used for the ChemScan™ RDI (AES Chemunex, Ivry sur Seine, France). The settings are a version of the Beads.APP provided by the manufacturer.

Discriminant Settings	Minimum	Maximum
S/P Area Ratio	0	0.898
T/P Area Ratio	OFF	OFF
Single Line Samples	500	-
Samples	1	250
Lines	1	50
Peak Intensity	250	65536
Peaks Per Line	-	2.5
Wiggles Per Line	-	5
Half Width	-	15
Specific Intensity (AS)	10	-
Specific Intensity (HW)	35	-
2D Gaussian Fit	-	1800

Table C3: Summary of equations and dimensionless parameters governing microplastic filtration by Tufenkji and Elimelech (2004a):

Equation 2:
$$\eta_0 = \eta_D + \eta_I + \eta_G$$

Equation A:
$$\eta_D = 2.44A_s^{1/3} N_R^{-0.081} N_{Pe}^{-0.715} N_{vdw}^{0.052}$$

Equation B:
$$\eta_I = 0.55A_s N_R^{1.675} N_A^{0.125}$$

Equation C:
$$\eta_G = 0.22N_R^{-0.24} N_G^{1.11} N_{vdw}^{0.053}$$

Different parameters used in above equations:

$N_R = \frac{d_p}{d_c}$	Aspect ratio
$N_{pe} = \frac{Ud_c}{D_\infty}$	Peclet number
$N_{vdw} = \frac{A}{kT}$	Van der Waals number
$N_{gr} = \frac{4\pi a_p^4(\rho_p - \rho_f)g}{3kT}$	Gravitation force number
$N_A = \frac{A}{12\pi\mu a_p^2 U}$	Attraction number
$N_G = \frac{2a_p^2(\rho_p - \rho_f)g}{9\mu U}$	Gravity number

where d_p is the microplastic particle diameter, d_c is the grain collector diameter, U is the influent solution velocity, D_∞ is the bulk diffusion coefficient, A is the Hamaker constant (1.0×10^{-20} J), A_s is the Happel model parameter (31.70-49.10), k is the Boltzmann constant (1.38×10^{-23} Joule/K), T is fluid absolute temperature (295 K), a_p is microplastic particle radius, ρ_p is the microplastic particle density (1050 kg/cm^3), ρ_f is the fluid density (1000 kg/m^3), μ is the absolute fluid viscosity ($1.005 \times 10^{-3} \text{ kg/m.s}$), and g is the gravitational acceleration ($9.81 \text{ m}^2/\text{s}$).

Table C4: Computation of single collector contact efficiency and contribution to various filtration mechanisms.

Soil	MP type	d_{MP} (μm)	N_R	N_{PE}	N_{vdW}	N_A	N_G	Single collector contact efficiency			Overall η_o
								Diffusion η_D	Interception η_I	Gravity (settling) η_G	
Medium Gravel	SMP	20	2.50E-03	6.48E+06	2.46E+00	1.52E-04	6.23E-01	1.93E-04	3.46E-04	5.75E-01	0.58
	FMP	1.60	2.00E-04	5.18E+05	2.46E+00	2.37E-02	3.99E-03	1.44E-03	9.45E-06	3.87E-03	0.0053
Fine Gravel	SMP	20	5.00E-03	3.24E+06	2.46E+00	1.52E-04	6.23E-01	3.13E-04	1.26E-03	4.87E-01	0.49
	FMP	1.80	4.48E-04	2.90E+05	2.46E+00	1.89E-02	4.99E-03	2.14E-03	4.04E-05	4.09E-03	0.0063
Coarse Quartz Sand	SMP	10	1.05E-02	3.85E+05	2.46E+00	6.07E-04	1.56E-01	1.22E-03	3.79E-03	8.74E-02	0.092
	FMP	1.40	1.52E-03	5.54E+04	2.46E+00	2.93E-02	3.23E-03	5.69E-03	2.39E-04	1.88E-03	0.0078
	SMP	1	1.05E-03	3.85E+04	2.46E+00	6.07E-02	1.56E-03	7.60E-03	1.42E-04	9.15E-04	0.0087
Medium Quartz Sand	SMP	10	1.67E-02	2.43E+05	2.46E+00	6.07E-04	1.56E-01	1.56E-03	7.26E-03	7.83E-02	0.087
	FMP	1.20	2.00E-03	2.91E+04	2.46E+00	4.21E-02	2.24E-03	8.46E-03	3.54E-04	1.18E-03	0.010

Appendix D: Contributions of the Author

Chapter 2 of this thesis is based on

Steinbacher S.D.*, Ameen A.*, Demeter K., Lun D., Derox J., Lindner G., Sommer R., Linke R.B., Heckel M., Perschl A., Blöschl G., Blaschke A.P., Kirschner A.K.T., Farnleitner A.H. (2024). **Assessing the impact of inland navigation on the faecal pollution status of large rivers: A novel integrated field approach.** *Water Research*, 261, 122029. <https://doi.org/10.1016/j.watres.2024.122029>

*Shared first authors (contributed equally)

The contributions of Ahmad Ameen to this publication are:

- Contribution to the study design (research questions, focus)
- Developed programming framework for Danube River Information Services (DoRIS) database
- Developed python code for ship data extraction from more than 100,000 csv files
- Data analysis and interpretation of results
- Manuscript preparation together with Sophia Steinbacher

Chapter 3 of this thesis is based on

Ameen A., Mikuni-Mester P.J., Bromberger B., Kirschner A.K.T., Regina S., Blaschke A.P., Stevenson M.E. (2025). **Microplastics as vectors for virus transport in saturated porous media.** (*under review*).

The contributions of Ahmad Ameen to this publication are:

- Performed sample preparation for microplastic and PRD1 bacteriophages
- Performed batch and column experiments
- Enumeration of microplastics using microscopy and solid-phase cytometry
- Measurement of zeta potential of microplastics and PRD1 bacteriophages
- Interpretation of results by DLVO and colloid filtration theories
- Analysis and modelling of breakthrough curves using commercial software Hydrus 1D
- Data visualization and manuscript preparation

Chapter 4 of this thesis is based on

Ameen A., Stevenson M.E., Kirschner A.K.T., Jakwerth S., Derox J., Blaschke A.P. (2024). **Fate and transport of fragmented and spherical microplastics in saturated gravel and quartz sand.** *Journal of Environmental Quality*, 53, 727–742. <https://doi.org/10.1002/jeq2.20618>

The contributions of Ahmad Ameen to this publication are:

- Performing microplastic fragmentation in the laboratory
- Performing column experiments and preparation of influent solution
- Enumeration of microplastics using microscopy and solid-phase cytometry
- Measurements of zeta potential and microplastic size distribution of microplastics
- Interpretation of results by colloid filtration theory and analysis of breakthrough curves
- Modelling of breakthrough curves using commercial software Hydrus 1D
- Data visualization and manuscript preparation